The Relationship Between Variation in Genes, GABA, Structure and Gamma Oscillations in the Visual and Auditory System of Healthy Individuals and Psychiatric Disorder

By Jennifer Anne Brealy

A Thesis Submitted to the School of Graduate Studies

in Partial Fulfilment of the Requirements for the Degree

Doctor of Philosophy

School of Medicine

Cardiff University

Summary

Visual perception is highly variable across healthy individuals and increasing evidence suggests that this inter-individual variation could be due to differences at the genetic, neurochemical, structural and neurophysiological level. Specifically, variation in the *GAD1* gene (responsible for synthesising the majority of cortical GABA) has been associated with differences in the level of the inhibitory neurotransmitter GABA. In addition, differences in GABA and cortical structural parameters (surface area and thickness) have been shown to predict differences in neural gamma oscillations. However, these findings have not been replicated in large independent studies. Hence, Chapter 3 and 4 of this thesis combines the non-invasive neuroimaging tools MRI, MRS and MEG with genetic data to investigate the relationship between variations in genes, GABA, structure and gamma oscillations in the visual cortex of a large cohort of healthy individuals.

Group differences in GABA, structure and gamma oscillations have also been reported between psychiatric populations (schizophrenia and bipolar disorder) and healthy individuals. However, differences in the direction of effect (increase or decrease) and no group differences have been found. Thus, Chapter 5 aims to further study these inconsistent findings by exploring group differences in GABA, structure and gamma oscillations between a healthy group and a schizoaffective bipolar disorder group.

Lastly, inter- individual variation is also present in auditory perception but has received much less attention into the factors driving this variation. As in the visual system, similar links between neurochemical, structural and neurophysiological measures could be present in the auditory domain. Chapter 6 investigates the association between auditory gamma oscillations and auditory structural parameters in a healthy cohort.

Acknowledgements

First of all I would like to thank my two supervisors Dr. Paul Keedwell and Professor Krish Singh who have fully supported and guided me throughout my PhD. Special thanks to Krish Singh for happily taking over as main supervisor when Paul left CUBRIC during the second year of my PhD and for being fully interested and positive about combining neuroimaging and genetic data.

Thanks to the '100 Brains team' for aiding with the collection of large amounts of data. Within this team, special thanks go to Lisa Brindley for always being there to help and providing entertaining discussions during our many hours of MEG scanning. Also, thanks to Kathryn Tansey for helping with the genetic analysis and for highlighting the limitations of genetic imaging.

Many thanks must also go to everyone in CUBRIC who have provided such a friendly working environment and are always willing to listen and share their insightful opinions. Thanks to Dr. John Evans for sharing his knowledge and willingness to go through all the GABA spectra data with me.

Thanks to my family and friends who have always been so supportive and shown an interest in my PhD.

Lastly, thanks to Duncan McIntosh for your willingness to participate in many auditory pilot scans and your constant encouragement during my PhD. You have always been there to cheer me up and distract me with all your so-called policing knowledge, so thank you!

Impact of Thesis

Please note that Chapter 5 is based on the following publication:

Brealy, J.A., Shaw, A., Richardson, H., Singh, K.D., Muthukumaraswamy, S.D. and Keedwell, P.A. (2014). Increased visual gamma power in schizoaffective bipolar disorder. *Psychol Med*, 1-12.

Contents

Chapter 1 - General Introduction

1.1 Rationale

Vision and hearing are two of our most important senses, which enable us to perceive the environment and guide our behavioural responses. The visual and auditory system process relatively independent external stimuli and provide us with rich sources of information about objects in our surroundings. For example, the visual system processes *light waves*, so that we can perceive colour, depth, and motion and recognise familiar objects and faces. In contrast, the auditory system analyses the pattern of *sound waves* (changes in air pressure). This enables us to localise sound, recognise familiar sounds and voices, and to communicate via speech. The two systems can also work in conjunction with one another, such as in motion perception, which allows us to assess the speed of moving objects. In order to carry out these sensory functions, the visual and auditory systems are highly specialised and organised structures, showing both similarities and dissimilarities with one another. Small differences in the structure and chemical composition of these two systems may lead to subtle differences in visual and auditory perception in healthy individuals. Larger differences may lead to clinically measurable altered perception and behaviour. This thesis uses neuroimaging and genetic information to investigate individual differences in the visual and auditory cortex of healthy individuals and group differences between healthy individuals and a psychiatric population.

The introduction of modern brain imaging techniques has greatly improved our understanding of the structural and functional specialisation of the human brain *in vivo*. Different imaging techniques have particular methodological advantages that enable us to

build an intricate picture of the brain. The high field strength of magnetic resonance imaging (MRI) scanners allows detailed structural information to be obtained, while the high spatial resolution of functional magnetic resonance imaging (fMRI) means that the precise location of changes in regional blood flow (an indirect measure of neuronal activity) in response to stimulation can be identified. Electroencephalography (EEG) and magnetoencephalography (MEG) directly measure neural activity and have high temporal resolution, providing detailed information about the time course of neuronal activity, while magnetic resonance spectroscopy (MRS) can determine the concentration of specific brain metabolites. Importantly, different imaging modalities show correlational relationships between measures that can be translated to behavioural responses. This suggests that functionally relevant measures are being obtained. For example, in the visual cortex, a functional measure of neural inhibitory activity (gamma oscillations) correlates with an inhibitory chemical neurotransmitter measure (GABA concentration) (Muthukumaraswamy *et al.*, 2010) and behavioural measures of inhibition (Edden *et al.*, 2009, Yoon *et al.*, 2010).

Neuroimaging measures also show inter-individual variability, meaning that the measure obtained at a single time point is different between individuals. Little is known about the reasons for this variability and whether it has any perceptual consequences. Normally, studies consider this variability a confound and remove it by averaging participant data. However, increasing evidence suggests inter-individual variability may be of particular importance for explaining variability in our perception and behaviour. In particular, structural MRI studies have shown the importance of inter-individual differences in human brain structure in relation to behaviours. For example, differences in grey matter volume and the integrity of white matter have been shown to reflect differences in working memory, numerical processing and empathy (Banissy *et al.*, 2012, Krause *et al.*, 2014, Soto *et al.*, 2014). Thus, investigating

what underlies individual variability in our neuroimaging data is important, as it may help us explain differences in perception and behaviour in health and disease.

This thesis focuses on investigating inter-individual variability in gamma oscillatory activity (a functional imaging measure) in the human visual and auditory cortex. Several key studies have driven this context, as they have shown individual variability in gamma band oscillations in both the human visual (Hoogenboom *et al.*, 2006, Muthukumaraswamy *et al.*, 2010) and auditory cortex (Arrondo *et al.*, 2009, Artieda *et al.*, 2004). Gamma oscillations are high frequency oscillations (30-100Hz) and understanding their underlying driving factors is of particular interest as they have been implicated in cognitive and sensory processing (Ward, 2003). Importantly, gamma oscillations are thought to be generated via the balance of reciprocal connections between cortical inhibitory and excitatory neurons (Buzsaki and Wang, 2012). Given that these oscillations rely on the cortical inhibitory/excitatory balance of neuronal assemblies, it is reasonable to suggest that inter-individual differences in gamma measures may reflect underlying inter-individual differences in GABAergic and glutamatergic neurochemical measures and/or the cortical structural architecture. Indeed, in the visual cortex individual differences in gamma peak frequency have been found to positively correlate with baseline visual MRS GABA concentrations (Muthukumaraswamy *et al.*, 2009) and visual cortical surface area (Schwarzkopf *et al.*, 2012). However, these studies had small sample sizes and have failed to be replicated (Cousijn *et al.*, 2014, Perry *et al.*, 2013, Robson, 2012). Thus, one of the aims of this thesis is to investigate whether individual differences in visual gamma peak frequency measured using MEG can be explained by MRS measured occipital GABA concentration and/or structural properties of the visual cortex in a large independent sample. In contrast to the visual system, whether differences in structural or neurochemical properties of the auditory cortex can explain inter-individual variability in

auditory gamma oscillations is not clear, and to our knowledge has not been investigated. Therefore, this thesis also explores whether differences in the *structural properties* of the auditory cortex could explain inter-individual differences in auditory gamma oscillations.

Importantly, the non-invasive nature of neuroimaging allows us to explore the neurobiology of the human brain in both the healthy and diseased state. This has been particularly important in the field of psychiatry, as psychiatric disorders are poorly understood at the molecular and cellular level, which impedes the development of new drug targets. Currently, antipsychotics that primarily act through blockade of D2-type dopamine receptors are the only approved treatment for schizophrenia. However, many patients are unresponsive to these medications and they do not treat the negative and cognitive symptoms associated with the disorder (Miyamoto *et al.*, 2012). Similarly, in bipolar disorder no effective treatments are available for the cognitive symptoms and up to 37% of patients relapse within the first year even with mood stabilising treatment (Gitlin *et al.*, 1995). Thus, alternative neurochemical theories are needed as new drug targets to improve the treatment of these disorders.

Due to their implication in cognitive function, gamma oscillations have been studied in a range of psychiatric populations such as bipolar disorder and schizophrenia. Group differences between patient populations and healthy controls have been reported in a range of cortical areas (O'Donnell *et al.*, 2004, Williams and Boksa, 2010). Although the majority of studies report reductions in gamma band measures, the results have not been consistent, with increases and even no difference being reported (Riečanský *et al.*, 2010, Uhlhaas *et al.*, 2006). In conjunction, altered GABAergic function in schizophrenia and bipolar disorder has been supported via MRS measured *in vivo* GABA levels. However, these findings are also inconsistent across cortical regions, with increases (Brady *et al.*, 2013, Kegeles *et al.*, 2012)

decreases (Rowland *et al.*, 2013, Yoon *et al.*, 2010) and no group differences (Kaufman *et al.*, 2009, Tayoshi *et al.*, 2010) being reported. Therefore, another aim of this thesis is to build upon this literature by further investigating gamma oscillations and GABA levels in a psychiatric population that have both mood and psychotic episodes, known as schizoaffective bipolar disorder. Further understanding how gamma oscillations and GABA levels are perturbed in psychiatric disorders will help unravel the underlying neuronal networks and biology involved in these disorders.

One potential reason for confounding results may be that psychiatric populations are biologically heterogeneous groups, as they are classified into diagnostic categories based on their symptomology rather than their neurobiology. Hence, a psychiatric population may not be biologically specific enough, meaning that it is hard to identify reliable neuroimaging measures. In addition, imaging measures do not provide cellular resolution, such as differentiation between different types of neurons. This may be particularly relevant to help us understand the complex neurobiology of psychiatric disorders. Importantly, the new field of genetic imaging has allowed us to investigate more biologically specific pathways by grouping individuals based on their genetic make-up. This means that we can investigate how genes involved in a specific system such as enzymes, receptors or transporters influence downstream imaging measures and lead to the clinical and behavioural phenotype. Thus, differences in genetic make-up can also be applied to investigate specific individual differences in neuroimaging and behavioural data. For the context of this thesis, how genetic variants involved in cortical GABAergic signalling and schizophrenia risk-associated alleles influence downstream variation in neuroimaging measures of inhibition (gamma and GABA) was investigated. Overall, by linking imaging techniques with genetic information we can

learn more about individual and group differences in brain structure, chemical composition and function and relate these to behavioural changes in both health and disease.

This introductory chapter is divided into the following sections to provide a detailed background into the context and main components of this thesis:

1.2 The Anatomy and Microcircuitry of the Visual and Auditory System

The visual system is one of the most studied sensory modalities, with much of our knowledge of its anatomy and function originating from studies in the cat and macaque monkey (Hubel and Wiesel, 1962, Lund, 1988). The neural pathway of the visual system begins at the retinal ganglion cells that project from the retina, via the optic nerve to the optic chiasm and the optic tract. At the optic chiasm, the optic nerve from both eyes meet and cross over, meaning that the left visual field is viewed by the right hemisphere and the right visual field is viewed by the left hemisphere (Figure 1). The majority of optic tract axons form synaptic connections within the major relay station of the brain, at the lateral geniculate nucleus (LGN) of the thalamus. The LGN is made up of 6 layers and neurons from this nucleus project via the optic radiation to the primary visual cortex (V1, striate cortex) via two main pathways: the magnocellular and parvocellular pathway. The magnocellular pathway

originates from layers 1 and 2 of the LGN and projects to layer 4Cα of V1. The parvocellular pathway begins across layers 3, 4, 5 and 6 of the LGN and projects to layers 4A and 4Cβ of V1. V1 also provides strong feedback connections to the LGN.

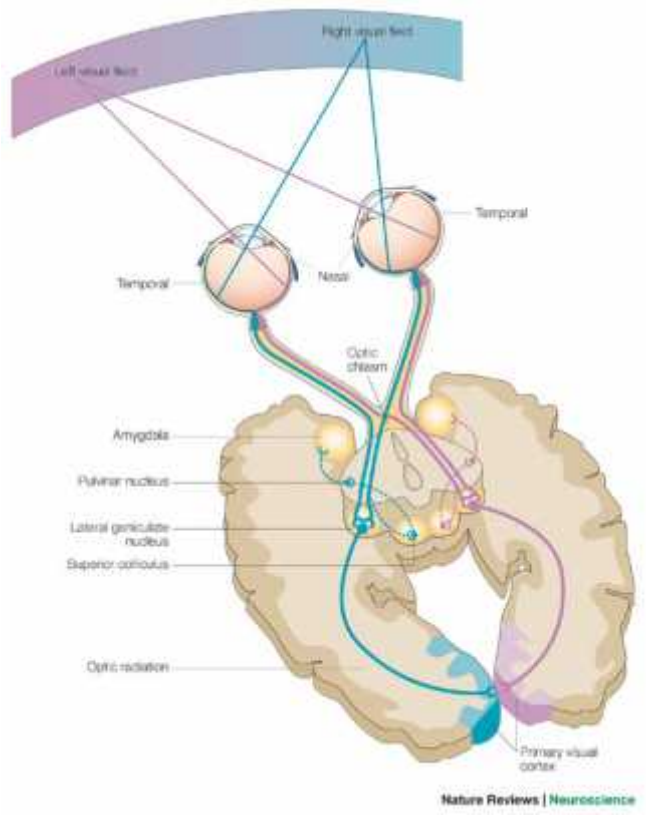

Figure 1.1: Illustration of the main pathways in the visual system. The left visual field (purple) is represented in the right hemisphere and the right visual field (blue) is represented in the left hemisphere. Image from (Hannula *et al.*, 2005).

As in the LGN, V1 is made up of 6 cortical layers, with layer 4 being split into 4A, 4B and 4C (4Cα and 4Cβ). Layer 1 lies under the pia matter and contains mainly axons and dendrites from cells in deeper layers. Interneurons make up about 15% of visual cortical neurons and make local connections within the cortex. Excitatory neurons (spiny stellate cells and pyramidal cells) make up 85% of visual cortical neurons; spiny stellate cells are found in layer 4C and make local connections whereas pyramidal cells are widespread in V1 and send axons within and outside of V1 (Callaway, 1998).

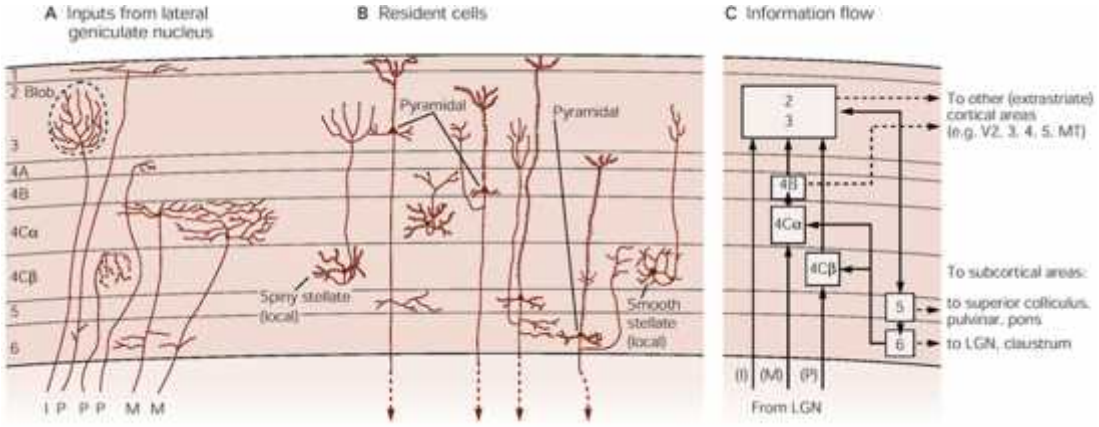

Figure 1.2: Laminar structure and cell types in the visual cortex. Image taken from "The Principles of Neuroscience" (Figure 27-10) (Kandel *et al.*, 2000).

The laminar and cell specific arrangement of V1 is a fundamental feature of the visual system that translates into functional organisation from the sensory periphery up to V1. This allows for topographic organisation, whereby neighbouring cells in V1 receive input from corresponding points of neighbouring cells in the LGN and retina. This provides V1 with a retinotopic map of the visual scene. In addition, functional specialisation can be found between the parvocellular and magnocellular pathways. The magnocellular pathway is involved in the perception of movement, depth and contrast whereas the parvocellular pathway is primarily involved in the perception of colour (Liu *et al.*, 2006). Within V1 itself, functional organisation is present horizontally and vertically, in which neurons with similar response properties are spatially grouped together. Neighbouring neurons have been found to have similar selectivity to the orientation and spatial frequency of a visual stimulus and a preferred eye input (ocular dominance) (Martinez *et al.*, 2005). Following considerable processing in V1, the visual signal is sent to subcortical areas and the extrastriate cortex, V2, V3, V4 and V5. These visual cortical areas are involved in higher level processing of the visual stimulus and are specialised for representing certain aspects of the visual stimulus: V2

for low level stimulus processing, V3 for depth perception, V4 for colour and V5 for motion (Grill-Spector and Malach, 2004).

In comparison, the auditory system is less well studied but shares corresponding components with the visual system. Sound waves are transduced to neural signals by hair cells in the cochlea, and sent along the auditory nerve via spiral ganglion cells to the ventral cochlear nucleus and dorsal cochlear nucleus in the medulla. Multiple efferent pathways are present from these nuclei but the main pathway continues to the superior olive on both sides of the brainstem. This bilateral innervation enables sound to be heard in both ears. Projections from the superior olive ascend to the inferior colliculus in the midbrain and synapse on the medial geniculate nucleus (MGN) of the thalamus. Lastly, afferent neurons from the MGN project to the primary auditory cortex (A1), located on the superior temporal gyrus in the temporal lobe. Information from A1 is then sent to the association area, located adjacently to A1, for processing of the more complex parameters of the stimulus.

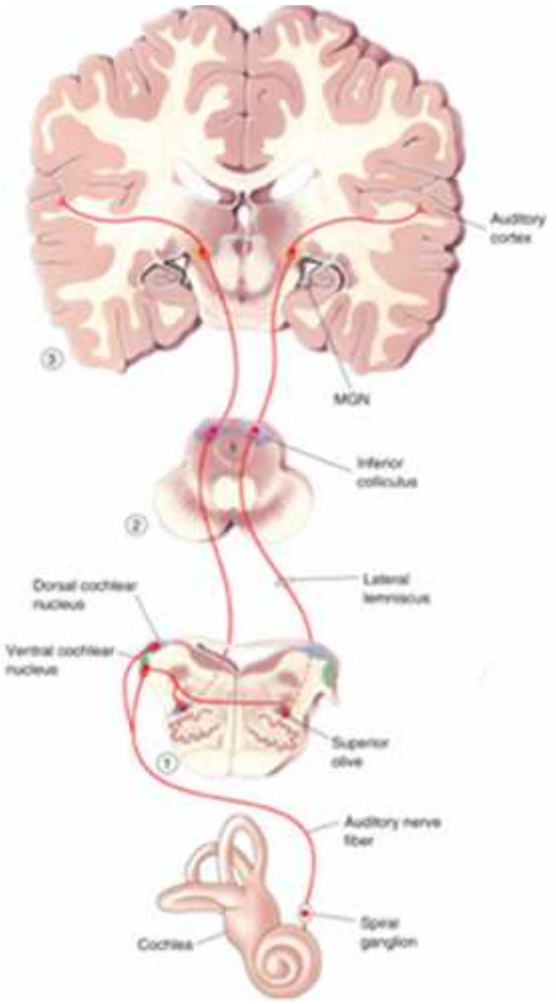

Figure 1.3: The main pathways in the auditory system. Image taken from "Neuroscience: Exploring the Brain" (Figure 11.18) (Bear *et al.*, 2007).

Thus, both sensory systems share analogous anatomic components; a receptor organ, sensory receptors, ganglion projection cells, thalamic relay station, primary sensory cortex and association areas. However, the auditory modality contains many more cortico-thalamic pathways, suggesting that processing in the midbrain is an important part of auditory perception.

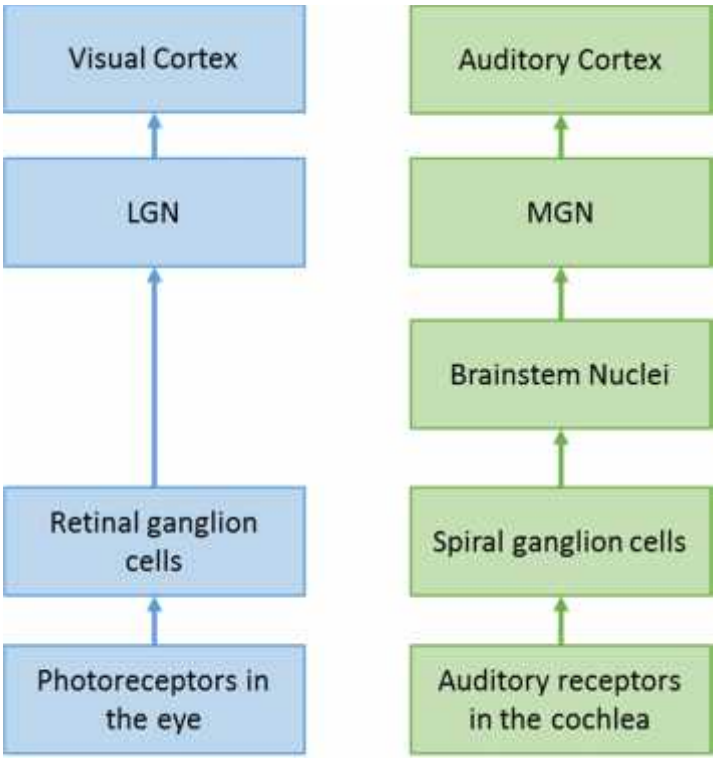

Figure 1.4: The main components of the visual and auditory cortex.

The microcircuitry of A1 is also similar to that of V1, with 6 cortical layers and local connections between layers formed by interneurons and cortico-cortical connections from pyramidal cells (Winer and JA, 1992). One of the main differences between the two sensory cortices is the different functional organisation of A1. The auditory system does have a topographic map, in which hair cells along the cochlear respond to different sound frequencies that is maintained across subthalamic nuclei. However, this frequency representation (tonotopy) does not seem to be as well defined in A1 (Castro and Kandler, 2010). In addition, the response properties of A1 neurons to certain parameters of acoustic stimuli (frequency, duration and amplitude) are not as straightforward. Although clusters of neurons do show sensitivity to a particular frequency, the response properties are generally less sharply tuned and not spatially organised. It has been hypothesised that this difference may be due to the increased processing at lower levels, such as in the inferior colliculus and

that A1 may be involved in more complex processing. For example, A1 neurons are preferentially driven by stimuli with spectral and temporal complexity rather than simple pure tones (Wang *et al.*, 2005). Thus, the auditory cortex is not a simple translation from the visual cortex. Auditory processing involves more processing at lower levels and A1 may in fact, not be organised for simple sound parameters but for higher order parameters comparable to the inferior temporal cortex of the visual system (King and Nelken, 2009).

1.3 Gamma Oscillations in the Visual and Auditory System

EEG and MEG are widely used to noninvasively measure cortical neural oscillations (synchronous activity of large groups of neurons). Importantly, two main types of oscillatory activity can be measured: evoked and induced. Evoked activity is time and phase-locked to the stimulus, occurring about 70-120ms after stimulus onset. Induced activity is time-locked but not phase-locked to the stimulus and occurs 200ms onwards from stimulus onset (Pantev, 1995). Another type of activity, called the steady-state response (SSR), which is considered an evoked response can also be measured via EEG and MEG. The SSR is produced in response to a repeated sensory stimulus in which populations of neurons are entrained to the stimulus at the frequency of stimulation (Herrmann, 2001).

As well as being classed into evoked or induced activity, neural oscillations are divided into several categories, based on their frequency bands; delta (1-4Hz), theta (4-8Hz) alpha (8-12Hz), beta (12-30Hz) and gamma (30-100Hz). Each frequency band has their own specialised function and are differentially modulated (Pfurtscheller and Lopes da Silva, 1999). Oscillations in the lower frequency bands are thought to reflect long-range synchronisation across brain areas whereas higher frequency oscillations reflect synchronisation in local networks (Schnitzler and Gross, 2005). Gamma oscillations can be

measured from a wide range of brain regions, including the prefrontal cortex and sensory regions.

Modelling and neurophysiological studies have shown that gamma oscillations are generated via reciprocally connected interneuron and pyramidal cell assemblies (Buzsaki and Wang, 2012, Whittington *et al.*, 2011). Interneurons can be classed into three main types of GABAergic neurons: parvalbumin, calretinin and somatostatin (Gonchar *et al.*, 2007). Parvalbumin (PV) expressing interneurons make up half of the GABAergic interneurons in the cortex and it is these neurons that are specifically essential for the generation of gamma oscillations. The main model to explain gamma oscillatory generation and maintenance is the pyramidal-interneuron network gamma (PING) model (Gonzalez-Burgos and Lewis, 2012). In this model, parvalbumin expressing interneurons are recruited by phasic glutamatergic input from pyramidal cells (primarily via NMDA receptors) and provide fast-spiking feedback inhibition to pyramidal cells (primarily via $GABA_A$ receptors).

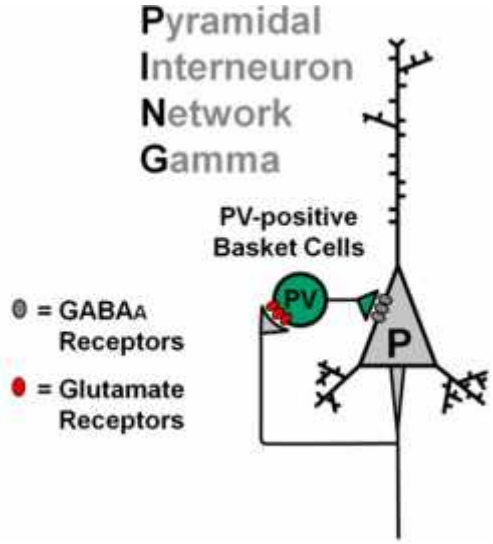

Figure 1.5: The PING model showing the reciprocal connectivity between pyramidal and parvalbumin positive cells. Image taken from (Gonzalez-Burgos and Lewis, 2012).

Optogenetic studies in mice support the model and have shown that *in vivo*, PV positive interneurons are essential for driving cortical gamma oscillations (Cardin *et al.*, 2009, Sohal *et al.*, 2009). Computational models have been used to manipulate the parameters of the PING model and have shown that gamma oscillations are intricately modulated, both excitatory and inhibitory input and output can alter the response (Spencer, 2009).

Gamma oscillations are significantly enhanced by sensory input and are modality specific; visual stimuli create large increases in the primary visual cortex and auditory stimuli generate increases in the temporal cortex (Jefferys *et al.*, 1996). In the human visual cortex, gamma oscillations can be optimally induced using square-wave, high-contrast gratings (Adjamian *et al.*, 2004, Hoogenboom *et al.*, 2006, Muthukumaraswamy *et al.*, 2010) that closely resemble those measured invasively in the macaque (Hall *et al.*, 2005). Thus, a square-wave, high contrast grating is used in this thesis to induce visual gamma activity. This type of visual stimulus produces both an early evoked and a later sustained response, which have been localised to V1 (Hoogenboom *et al.*, 2006, Perry *et al.*, 2011).

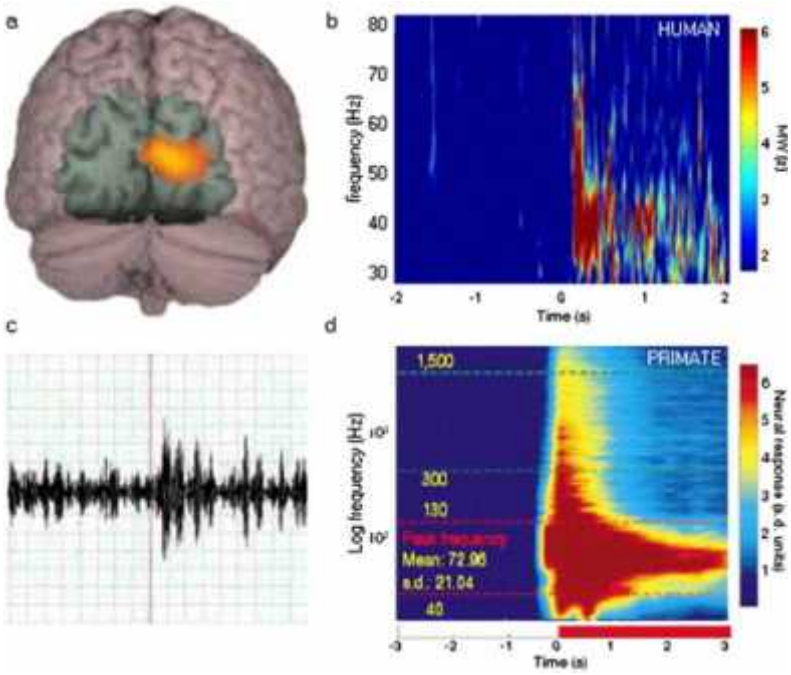

Figure 1.6: Visually induced gamma oscillations located to the primary visual cortex in the human (a+b) which are comparable to the local field potential obtained from the macaque monkey (c+d). Image taken from (Hall *et al.*, 2005).

Within the sustained response, two main measures are typically extracted from the above time-frequency spectra; peak gamma frequency and power. These two measures can be modulated by stimulus parameters including contrast (Ray and Maunsell, 2010), orientation (Koelewijn *et al.*, 2011), spatial frequency (Adjamian *et al.*, 2004), motion (Swettenham *et al.*, 2009) and size (Perry *et al.*, 2013). These findings imply that sustained visual gamma oscillatory activity has a role in encoding the stimulus properties of a visual stimulus to aid perception. An important aspect of visually induced gamma oscillations is that individuals show inter-individual variability in peak gamma frequency and power that is stable over time (Muthukumaraswamy *et al.*, 2010). The factors underlying this variability are unknown, but may represent underlying differences in the chemical or structural properties of V1. Peak gamma frequency has been shown to positively correlate with resting occipital GABA concentration (Muthukumaraswamy *et al.*, 2009), V1 surface area (Schwarzkopf *et al.*, 2012)

and V1 thickness (Gaetz *et al.*, 2012, Muthukumaraswamy *et al.*, 2010). Similarly, the exact significance of the variability is also unknown but may translate to differences in behavioural measures of the visual system (Edden *et al.*, 2009). Pharmaco-MEG work further supports the involvement of GABAergic signalling in visually induced gamma measures, as modulation of $GABA_A$ receptors alters gamma responses (Campbell *et al.*, 2014, Saxena *et al.*, 2013). However, recent work in a larger cohort suggests that these quantitative inhibitory measures are not correlated and that the main driving factor between the previously correlated occipital GABA and gamma peak frequency is age (Robson, 2012). Hence, this thesis aimed to explore this finding in a large homogeneous cohort.

In the auditory cortex, steady-state responses (SSRs) can be obtained with trains of clicks (Galambos *et al.*, 1981) or amplitude-modulated tones (Picton *et al.*, 1987). Interestingly, if the auditory cortex is driven with auditory stimuli over a range of frequencies, SSRs show a main peak at 40Hz and a secondary peak between 80 to 120Hz (Galambos *et al.*, 1981, Lins *et al.*, 1995), while higher or lower frequencies produce smaller amplitudes. The cause of this specific increased response around 40Hz is still debated; one theory suggests they are the result of phase summation from middle latency responses whereas others believe it is due to the preferential working frequency of the auditory network (Pastor *et al.*, 2002). Support for the latter theory has recently been shown, whereby following delivery of click trains at various frequencies, 40Hz produces the largest increase in regional cerebral blood flow in auditory areas (Pastor *et al.*, 2002), suggesting increased cortical synaptic activity at 40Hz. Using MEG and fMRI, ASSRs have been localised to the superior temporal gyrus of the auditory cortex (Herdman *et al.*, 2003). Significantly, not only is A1 activated to 40Hz auditory stimuli but a network of regions involving a cortico-cerebellar-thalamic loop are

specifically activated at 40Hz (Pastor *et al.*, 2008). These findings further enforce the importance of cortico-thalamic processing in auditory processing.

The majority of auditory SSRs studies specifically drive the cortex at 40Hz as they are interested in the power of the response at that frequency. However, one study has shown the importance of using a stimulus that drives the auditory cortex simultaneously over a range of frequencies. This method has identified inter-individual differences in gamma oscillations in the human auditory cortex (Artieda *et al.*, 2004). Using an amplitude-modulated tone, which increased in frequency from 1 to 120Hz (chirp), individuals were found to have two peak frequency responses. The strongest peak response across individuals ranged between 20 to 65Hz and the second weaker peak response ranged between 80 to 120Hz (Figure 1.7).

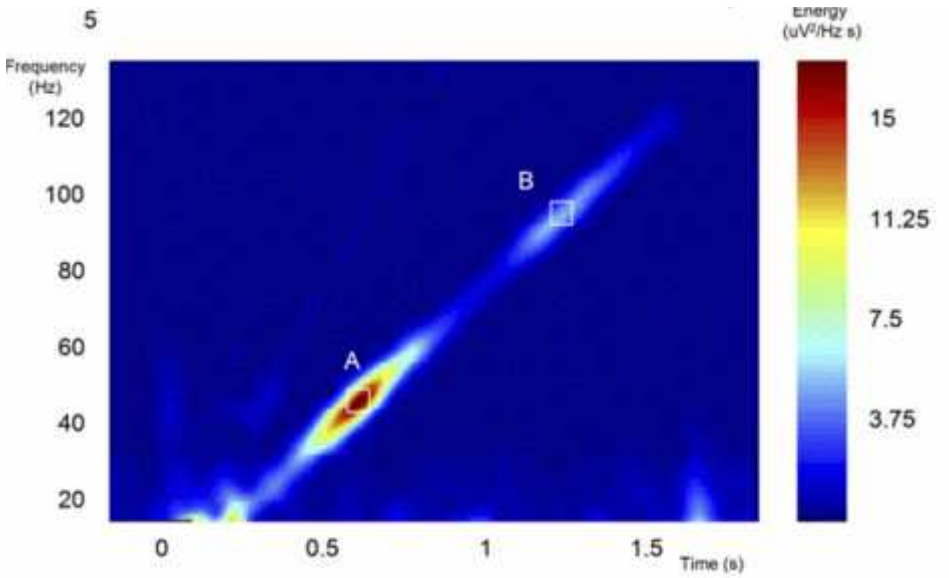

Figure 1.7: The auditory steady-state response obtained from an amplitude-modulated tone that increases in frequency from 1 to 120Hz. Image taken from (Artieda *et al.*, 2004).

As in the visual modality, the factors underlying the auditory individual differences are still unknown. The chemical composition of A1 may play an important part, as increasing inhibition with a $GABA_AR$ agonist increases the amplitude of the ASSR in rats (Vohs *et al.*,

2010). Interestingly, the peak gamma frequency has also been related to behavioural responses. Lower peak frequencies to the amplitude-modulated tone were associated with multiple sclerosis (MS) patients with a cognitive impairment compared to MS patients with higher cognitive abilities or healthy controls (Arrondo *et al.*, 2009).

This thesis aims to increase our understanding of individual gamma differences in the auditory response by using an auditory chirp in a healthy population and seeing if they can be explained by structural properties of the primary auditory cortex. In addition, peak gamma frequencies in the auditory cortex will be compared with peak frequencies obtained from the visual cortex to determine if there is a relationship between the two measures.

1.4 Gamma Oscillations and GABA in Psychiatric Disorders

Schizophrenia and bipolar disorder are two of the most common and debilitating psychiatric disorders, with prevalence rates of about 1% (Regier *et al.*, 1993) and 3.5% (Merikangas *et al.*, 2007) respectively. These psychiatric disorders have been classed as separate diseases since the 19th century, known as the Kraepelin dichotomy. This dichotomy distinguishes between the two disorders based on their differential symptom patterns. Schizophrenia individuals show positive symptoms (hallucinations, delusions, and disordered thoughts), negative symptoms (lack of interest and emotional flatness) and cognitive symptoms (problems with attention, working memory and executive functioning). Bipolar disorder is characterised by extreme mood changes, including manic (e.g. feeling euphoric, restlessness, racing thoughts) and depressive episodes (e.g. feeling worthless, lack of interest, fatigue). Bipolar individuals can also show symptoms of psychosis (hallucinations and delusions) and cognitive difficulties that are similar to those experienced by schizophrenia individuals.

Initially, sensory processing deficits were not considered a major clinical feature of schizophrenia or bipolar disorder. This is due to the more evident presentation of thought disorder, delusions and/or mood episodes. However, following substantial evidence, disturbances in visual and auditory processing are now accepted as core deficits in schizophrenia (Iliadou *et al.*, 2013, Javitt, 2009) and are increasingly being recognised as deficits associated with bipolar disorder (O'Bryan *et al.*, 2014). In terms of visual processing, behavioural deficits are evident in the discrimination of orientation, motion, contrast and object size (Chen, 2011, Chen *et al.*, 2006, O'Bryan *et al.*, 2014). In auditory processing, deficits can be found in the ability to discriminate tones by pitch (Javitt *et al.*, 2000) and duration (Todd *et al.*, 2003). Importantly, these low level processing deficits may lead to higher level cognitive impairments.

Neuroimaging studies have further added to the importance of these sensory two systems in psychiatric disorders, by identifying structural and neurophysiological abnormalities (Hirayasu *et al.*, 2000). Due to their implication in cognition and sensory perception, gamma band oscillatory measures have been studied in a range of cortical regions in schizophrenia and bipolar disorder (O'Donnell *et al.*, 2004, Williams and Boksa, 2010). Studies investigating group differences in the gamma band can compare several different measures including evoked power, induced power, phase locking and peak frequency. The methods of analysis for these measures are explained in the methods section (Chapter 2) of this thesis. Both disorders show alterations in evoked, induced and steady-state gamma band activity compared to healthy individuals in response to a variety of tasks (Uhlhaas and Singer, 2010). In schizophrenia individuals, gamma oscillatory activity is often reduced in response to basic sensory stimuli using EEG and MEG. For example, in the visual domain an oddball task using letters as stimuli (individuals have to count rare target stimuli) found no evoked gamma

power (25-45Hz) or reduced gamma phase locking over the occipital cortex in schizophrenia patients (Spencer *et al.*, 2008a). Similarly, using an illusory square (individuals identify if an illusory square is present or absent) schizophrenia individuals show reduced visual evoked gamma phase locking (Spencer *et al.*, 2003) and reduced gamma frequency (Spencer *et al.*, 2004). Evoked visual gamma activity is also altered in more demanding visual tasks such as a backward masking task, where reduced gamma power (30-40Hz) has been found across EEG electrodes (Wynn *et al.*, 2005). In addition, *induced* visual high gamma frequency oscillations (60-120Hz) in response to mooney faces are reduced in schizophrenia (Grützner *et al.*, 2013). In the auditory domain, most studies have investigated auditory gamma steady-state responses in schizophrenia and have identified decreases in power and frequency in the gamma range (O'Donnell *et al.*, 2013).

In contrast, gamma measures in bipolar disorder have been less extensively studied but disturbances have also been identified. Bipolar individuals show reduced gamma power at both high and low gamma frequencies and reduced phase locking in auditory steady-state responses (O'Donnell *et al.*, 2004, Oda *et al.*, 2012, Rass *et al.*, 2010). Altered higher level processing in the visual domain has also been identified in response to an implicit emotional face task (identify gender) (Liu *et al.*, 2014).

Importantly, these disturbances in gamma oscillatory activity suggest an altered excitatory/ inhibitory cortical balance. This coincides with the wealth of evidence implicating altered GABAergic and glutamatergic dysfunction in schizophrenia and bipolar disorder. One of the most widely replicated findings of altered GABAergic function in schizophrenia and bipolar disorder originate from post-mortem studies, in which *glutamic acid decarboxylase 1* (*GAD1*) mRNA levels are decreased across multiple cortical regions, including sensory areas

(Gonzalez-Burgos *et al.*, 2010, Hashimoto *et al.*, 2008, Thompson *et al.*, 2009). The *GAD1* gene encodes the GAD67 enzyme, which is responsible for the majority of GABA synthesis via the catalysis of glutamate (Asada *et al.*, 1997). Significantly, *GAD1* mRNA reductions have primarily been found in the subclass of parvalbumin expressing interneurons, which are critical for producing gamma oscillations. Further evidence for altered GABAergic signalling in major mental disorders has been shown by MRS GABA imaging studies (Brady *et al.*, 2013, Yoon *et al.*, 2010). One specific theory suggests that dysfunction of parvalbumin neurons is due to a hypofunction of N-methyl-D-aspartate (NMDA) receptors (Nakazawa *et al.*, 2012). NMDA receptor hypofunction has been a major hypothesis in the pathophysiology of schizophrenia (Poels *et al.*, 2014) and is supported by genetic evidence showing lowered expression of NMDA receptor subunit mRNA (Weickert *et al.*, 2013). Also, NMDA receptor blockade via ketamine administration induces the positive, negative and cognitive symptoms observed in schizophrenia (Krystal *et al.*, 1994, Lahti *et al.*, 2001). Therefore, disrupted GABAergic and glutamatergic signalling may lead to an inability to synchronise cortical activity such as gamma oscillations, leading to the symptoms observed in schizophrenia and bipolar disorder.

Although the majority of studies demonstrate reduced gamma oscillatory activity in schizophrenia and bipolar disorder, which is supported by reduced *in vivo* GABA levels, increases and/or no group differences in these measures have also been reported (Kegeles *et al.*, 2012, Spencer *et al.*, 2008a, Uhlhaas *et al.*, 2006). These findings could be due to a number of reasons including different regions studied, different stimuli and the heterogeneity of psychiatric populations. This thesis aims to explore gamma oscillatory activity and GABA concentration in the visual cortex of a subgroup of bipolar individuals, known as schizoaffective bipolar disorder (SABP). SABP individuals display episodes of mania and

depression but also psychotic symptoms. Hence, exploring the neurophysiology and neurobiology in this subtype may help us learn about specific alterations in psychosis and aid us to differentiate between schizophrenia and bipolar disorder. In addition, genetic evidence implies a specific influence of $GABA_AR$ genes in the SABP phenotype that is not applicable to the wider bipolar phenotype (Craddock *et al.*, 2010). The SABP group may therefore also present a more biologically homogenous group in which to investigate how altered $GABA_AR$ function affects gamma oscillations.

1.5 Genetic Imaging

A gene is a stretch of deoxyribonucleic acid (DNA) that codes proteins. Proteins carry out most processes in cells and affect how a cell processes and responds to stimuli. This means that variations in our DNA may affect the expression or function of a protein, leading to downstream functional changes in a single cell or cell assembly. In order for DNA to work efficiently it has a specific structure, consisting of nucleotides, which they themselves are made up of a phosphate, a sugar (deoxyribose) and one of four chemical bases: adenine (A), guanine (G), cytosine (C) and thymine (T). These chemical bases pair up in a particular way, so that A is always paired with T and C is always paired with G.

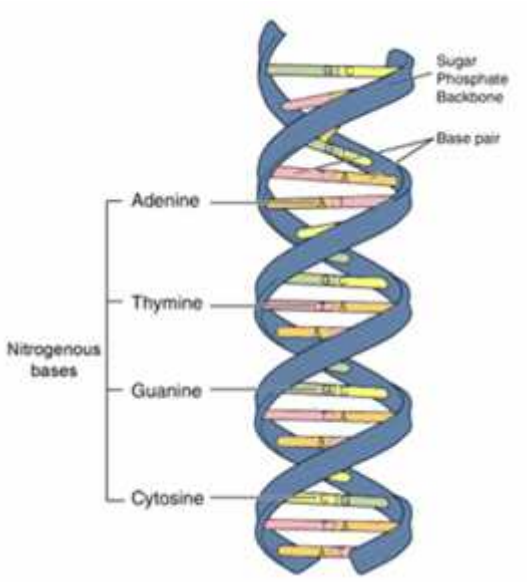

Figure 1.8: The structure of DNA. Image taken from the National Human Genome Research Institute: http://www.genome.gov/.

Variations in chemical base pairs are common and include insertions, deletions, duplications and single nucleotide polymorphisms (SNPs). SNPs are the most common type of genetic variation (~10 million SNPs in the human genome) and to be classified as a SNP, must occur in at least 1% of the population. They are defined as a change in a single base pair (e.g. a C base substituted for a T base) and may have protective effects or be associated with risk for certain disorders.

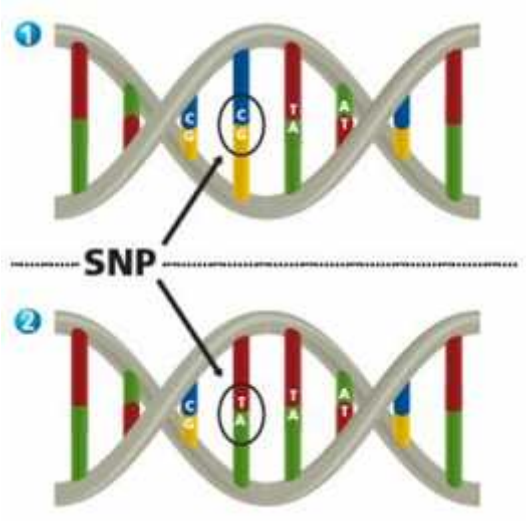

Figure 1.9: An example of a SNP in a region of DNA. Image taken from http://www.farma.ku.dk/index.php/Personlig-medicinering-af-type/11444/0/.

Genetics has been a major research area in neuropsychiatric illness, as genes are thought to play a major role in the predisposition of schizophrenia and bipolar disorder. This is primarily due to twin studies that have shown high heritability estimates of 81% and 75% in these disorders respectively (Sullivan *et al.*, 2012). These twin studies estimate heritability based on the idea that monozygotic twins share 100% of their genes and dizygotic twins share 50% of their genes. Therefore, differences between monozygotic and dizygotic twin pairs are interpreted as being due to genetic differences. To identify the particular genes associated with these disorders, genome-wide association studies (GWAS) have been employed, in which genetic variation is compared between cases with the disease and matched controls. A GWAS can provide large amounts of genetic information as they can analyse the entire genome (more than 500,000 SNPs) using chip-based genotyping (Lawrence *et al.*, 2005). These large studies have revealed that schizophrenia and bipolar disorder are complex genetic disorders, with a considerable genetic overlap (Cardno and Owen, 2014). Importantly, not only one but multiple genetic variants, together with environmental interactions predispose individuals to these disorders (Purcell *et al.*, 2009). Thus, schizophrenia and bipolar disorder are known as polygenic illnesses, with each 'risk' SNP increasing the susceptibility to a disorder by a small fraction. To date, variants involved in calcium neuronal signalling, neuronal development and signal transduction have been implicated (Consortium, 2011, Group, 2011, Ripke *et al.*, 2013).

The new field of genetic imaging has rapidly expanded over the past decade and is being used to understand how these genetic variants are influencing downstream biological functions, which may lead to clinical phenotypes. In psychiatric genetic imaging, genetic and brain imaging data are combined to study psychiatric illness. The approach aims to understand more about the biological effects of genes by using a quantitative imaging measure as an

intermediate phenotype (endophenotype) that lies in between the genetic and clinical phenotype pathway (Flint and Munafò, 2007). Although the imaging endophenotype cannot explain the effects of variants at a cellular level it can identify effects at a functional circuit level. The idea is that the endophenotype lies closer to the genetic variant, so is more sensitive to the consequential biological effects than the clinical phenotype. In principle, the endophenotype is also less genetically complex than the clinical phenotype and so should reduce the sample size needed to identify specific genetic effects. In order to be accepted as an endophenotype, the measure must meet certain criteria: be stable over time, heritable and occur in the patient and unaffected family member more frequently than in the general population (Gottesman and Gould, 2003).

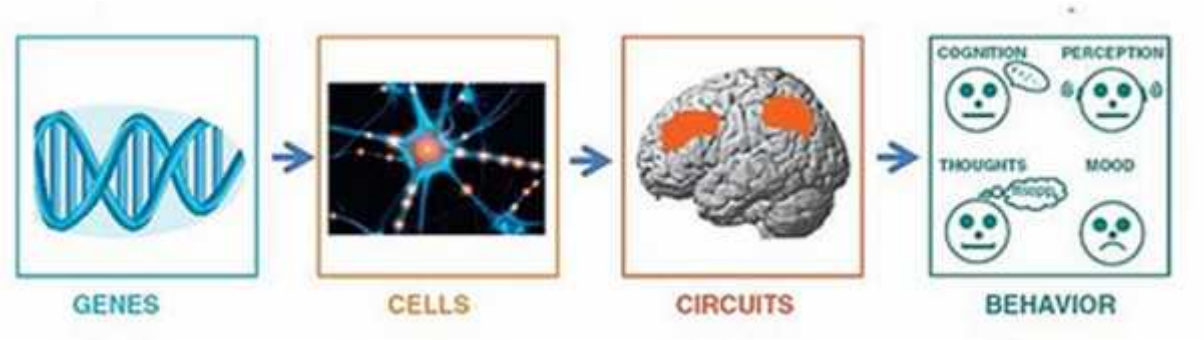

Figure 1.10: The concept of genetic imaging to help link genes with microcircuitry and behaviour.

At present, two main genetic imaging approaches that use endophenotypes exist: a candidate gene approach and a GWAS approach (Amos *et al.*, 2011). A candidate gene approach investigates the effect of a specific SNP on an imaging measure and the SNP is chosen based on a biological hypothesis from prior knowledge. The advantage of this approach is that it has high statistical power but it does not discover new genes that may be involved in the disorder and is vulnerable to false positive findings. In comparison, a GWAS approach is unbiased and investigates the influence of the entire genome on the imaging measure. A GWAS can

identify new genes that may be implicated in the disease even if their function is unknown. However, this method has low statistical power due to the number of independent tests and requires large sample sizes. To combat the issue of low statistical power in GWAS but still test the effect of multiple SNPs, a new approach using polygenic risk scores has been implemented. This method pools together the effects of common genetic risk variants with small effects and weights them by their effect size (Dudbridge, 2013).

So far, candidate gene approaches have been the main method used in genetic imaging and have produced some promising results implicating variants in the COMT, BDNF, CACNA1C gene on functional measures (Prathikanti and Weinberger, 2005). For example, individuals with a risk variant in the CACNA1C gene (important for calcium signalling) which has been strongly associated with bipolar disorder, schizophrenia and unipolar depression through GWAS, show reduced hippocampal and subgenual cingulate gyrus activation during an episodic memory task (Erk *et al.*, 2010). Importantly, these findings have recently been independently replicated (Erk *et al.*, 2014) and suggest that the CACNA1C risk variant has functional effects in the hippocampus and prefrontal cortex that may explain symptoms shared across psychosis-affective disorders. This means that following further understanding and specifics, CACNA1C could be a potential new drug target.

1.5.1 Impact of Genetic Variation on Gamma Frequency and GABA

Brain oscillations across all the main frequency bands have been proposed as potential endophenotypes, as they are highly heritable and are altered in psychiatric disorders (van Beijsterveldt *et al.*, 1996, van Beijsterveldt and van Baal, 2002). For the context of this thesis, studies have shown that gamma oscillations in both the auditory and visual domain could be useful endophenotypes (Hall *et al.*, 2011b, Hong *et al.*, 2004, van Pelt *et al.*, 2012).

Essentially, these studies have shown that gamma oscillations present biologically relevant and stable measures and that dysfunctions in these measures are present in both patients and their relatives. A vital study has recently shown that the peak frequency of visual gamma oscillations is highly heritable (van Pelt *et al.*, 2012). This suggests that individual variation in peak gamma frequency has a strong underlying genetic component and has been the main driving factor to investigate the effect of genetic variation on visual peak gamma frequency in this thesis. Coinciding with this, GABA concentration has also been proposed as a potential endophenotype (Hasler and Northoff, 2011) and individual differences in GABA may also be primarily genetically determined. Thus, another aim of this thesis was to use a candidate and whole gene approach to explore if genetic variation in GABAergic genes could explain individual differences in visual gamma peak frequency and occipital GABA levels in a large group of healthy controls. In addition, the association between schizophrenia polygenic risk scores and gamma peak frequency and GABA were investigated. Understanding which genetic variants underlie individual differences in visual gamma frequency and GABA could help explain more specifically which components of the biological pathway are involved in these measures and the consequential behavioural differences they influence.

1.6 Outline of Thesis Chapters

This thesis uses structural MRI, MRS and MEG information, as well as genetic data to answer several important questions explained above. Chapter 2 provides details on these imaging methods and the data analysis used in this thesis. Chapter 3 is the first experimental chapter and explores the relationship between visual gamma oscillations, occipital GABA and V1 structural properties in a cohort of 100 healthy individuals. Specifically, individual differences in occipital GABA, V1 thickness and surface area are used to explain individual differences in visual gamma peak frequency. This cohort was part of a large genetic imaging

study, named ‘100 Brains’, in which individuals were ‘GWASed’, giving us a wealth of genetic data to relate to our imaging phenotypes. Hence, Chapter 4 looks at the effect of genetic variants known to be involved in GABAergic pathways on occipital GABA and visual gamma peak frequency. Chapter 5 investigates group differences between healthy controls and SABP individuals in visual gamma oscillatory measures, occipital GABA and V1 structural measures. Chapter 6 investigates individual differences in auditory peak gamma responses and whether these can be explained by individual differences in the structural properties of the auditory cortex. This chapter also determines if peak gamma responses obtained in the auditory cortex share a relationship with visual peak gamma responses. Lastly, Chapter 7 discusses the experimental findings of Chapters 3 to 6 and their implications.

Chapter 2 - Methods

This chapter describes the main principles behind the three imaging modalities MRI, MRS and MEG. In addition, the analysis methods used in this thesis to obtain quantitative imaging data from these imaging modalities are described.

2.1 Magnetic Resonance Imaging

The concept of Magnetic Resonance Imaging (MRI) originated over 35 years ago (Lauterbur, 1989, Mansfield and Maudsley, 1977) and since its discovery, this *in vivo* imaging technique has been widely applied in the clinic for diagnosis and research purposes (Symms *et al.*, 2004). MRI can be divided into two fundamental types, known as structural MRI and functional MRI. Structural MRI provides static anatomical information whereas functional MRI provides physiological information based on cerebral blood flow. This section focuses on the principles behind MRI and its application for acquiring structural MRI data.

An MRI image is essentially based on information about protons, which are highly abundant in the human body. These protons have a positive electrical charge that is constantly moving because they possess a spin. The moving electrical charge (electrical current) induces a magnetic field, meaning that each proton has its own magnetic field. Normally, protons within the body are randomly spinning (precessing) on their axis but when an individual is placed in the magnetic field of the MRI scanner (an external magnetic field), the protons align themselves to the field in a parallel or anti-parallel direction. This results in protons precessing around the direction of the magnetic field, either pointing with or against the external field. The speed at which the protons are precessing (precession frequency) is an

important component that is calculated using the Larmor equation and is a product of the strength of the external magnetic field (B_0) and the gyromagnetic ratio (g) (Storey, 2006).

The parallel and anti-parallel alignments that protons take once placed in the MRI field have different energy levels and more protons go to the lower energy level that is parallel to the external magnetic field (Figure 2.1A). This results in the individual having a sum magnetisation that is longitudinal to the external magnetic field (Figure 2.1B). However, as this longitudinal magnetisation is in the same direction as the external magnetic field, its strength cannot be measured directly and so magnetisation at an angle perpendicular to the external magnetic field is required, known as transverse magnetisation. To induce transverse magnetisation a radio frequency (RF) pulse that is at the same frequency as the precession frequency of the protons is sent to the body. This has two resulting effects on the protons: firstly, some protons gain energy and move into the higher energy level that is antiparallel to the external field. This decreases longitudinal magnetisation. Secondly, the protons precess in phase (in the same direction and at the same time) in the transverse plane, which establishes a new transverse magnetisation (Figure 2.1C). A radiofrequency pulse that causes the magnetisation to move 90^0 (from longitudinal to transversal) is known as a 90^0 RF pulse. Importantly, it is this sum of transverse magnetisation that is detected by the receiver coil of the MRI and forms the basis of the MRI signal.

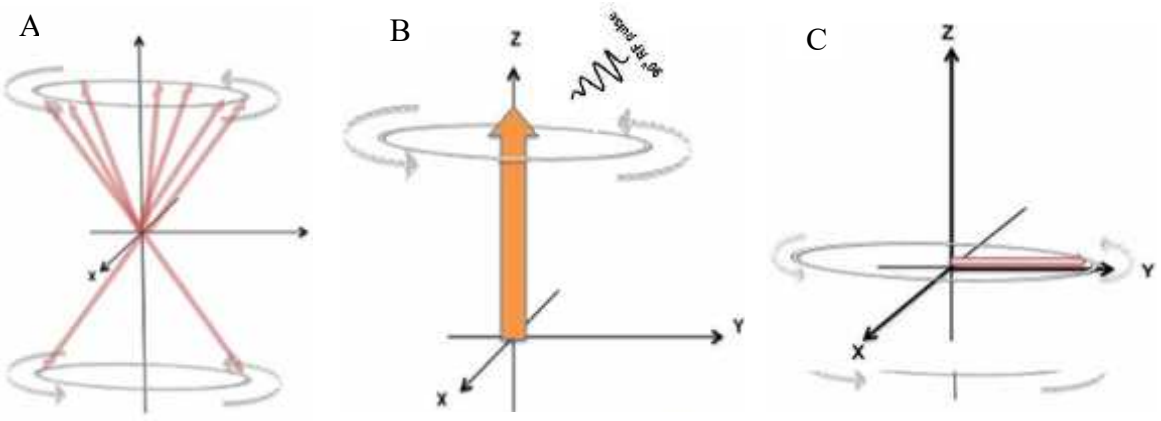

Figure 2.1 A) Shows the typical parallel and antiparallel alignment taken by protons once they are placed in the external magnetic field. As more protons go to the parallel direction, this results in bulk magnetisation in the longitudinal direction (B). Once the 90^0RF pulse is added, longitudinal magnetisation decreases and the protons are in phase, causing transversal magnetisation (C). Image adapted from http://www.medscape.com/viewarticle/780917_3.

Once the RF pulse is switched off protons gradually lose their energy to the surrounding tissue (lattice) and return to the parallel alignment, causing longitudinal magnetisation to go back to its original strength. This longitudinal relaxation time is described by the time constant T1, which is the time it takes for 63% of the original longitudinal magnetisation to be reached. Importantly, T1 is affected by the composition of the lattice, so that surroundings with high water content/liquids have a longer T1 compared to surroundings with a higher fat content. This difference in T1 based on tissue composition arises because water molecules have a high Larmor frequency, making it difficult for protons to transfer their energy to the lattice. The loss of the RF pulse also causes protons to dephase, meaning that the transversal magnetisation is lost (transversal relaxation). Transversal relaxation is described by the time constant T2, when transversal magnetisation decreases to 37% of its original value. In comparison to T1, T2 is primarily affected by variations in the magnetic fields of

neighbouring protons (spin-spin interactions). Tissues with a high amount of water molecules/liquids have fast local magnetic fields and no large net differences in magnetic fields, meaning that protons stay in phase for longer and thus have a long T2. In comparison, tissues with larger fatty molecules have bigger magnetic fields causing differences in local magnetic fields and results in a short T2. Therefore, a key aspect of T1 and T2 is that they allow us to differentiate between tissues, based on their molecular content and surroundings. This means that in the brain we can differentiate between white matter, grey matter and CSF using T1 and T2 data. An image that contrasts between tissues based on T1 data is a T1-weighted image whereas one that distinguishes between tissues based on T2 data is T2-weighted.

As well as being affected by spin-spin interactions T2 can be affected by inhomogeneities in the external magnetic field. The combination of these two inhomogeneities (T2* effects) causes a gradual decrease in the transverse magnetic field and the corresponding signal is known as free induction decay (FID). Thus, a typical FID signal initially has a large increase in signal due to the transverse magnetic field and an associated decrease by T2* that shapes the signal sent to the receiving coil of the MRI. To combat the loss of signal caused by the inhomogeneity in the external magnetic field, a certain amount of time after the 90^0 pulse (TE/2), a 180^0 pulse is applied to the protons. The pulse results in an increase in signal due to rephasing of the protons and is called a spin echo.

Ultimately, MRI protocols use spin-echo sequences that consist of repeated 90^0 and 180^0 RF pulses. During MRI acquisition, certain parameters of the sequence are modified in order to produce the required signal and desired image. For example, changing the time in between the 90^0 pulse and the echo (TE) can increase or decrease the difference in signal due to

differences in the T2 of tissues. Having a long TE means that differences in amplitude between tissues can be detected as they will have had enough time to develop differences in T2*. This long TE creates a good contrast between tissues and a more T2-weighted image. However, the TE must not be too long otherwise the amplitude of the signal will be too low, creating a 'noisy' image.

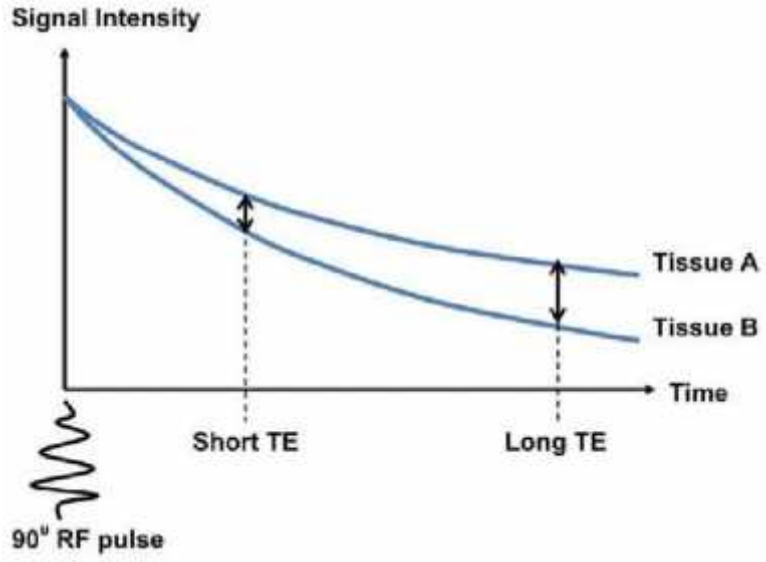

Figure 2.2: A plot showing that tissue B has a shorter T2 time than tissue A. Using a long TE time allows this difference in T2 to be more distinct by allowing enough time for a larger contrast in signal intensity to be measured. Image adapted from http://www.medscape.com/viewarticle/780917_3.

In contrast, if a more T1-weighted image is required then the parameter TR (time to repeat the 90^0 pulses) is altered. Having a short TR means that differences in T1 between tissues can be detected as both tissues will not have had enough time to fully recover to their original longitudinal magnetisation.

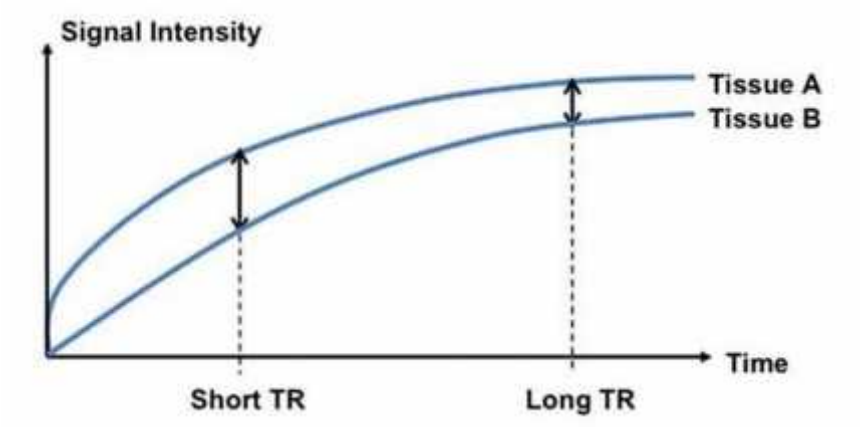

Figure 2.3: A plot showing the advantage of using a short TR for distinguishing between two tissues that differ in T1 time. Image adapted from http://www.medscape.com/viewarticle/780917_3.

Another concept of MRI image acquisition is the need of spatial information in order to examine a particular slice and then locate where the signals are arising from within that slice. To locate a particular slice a gradient magnetic field is applied via gradient coils. This induces a linear gradient of Larmor frequencies across the individual's body in the applied direction. Next, a RF pulse with the same frequency as that of the Larmor frequency within the slice of interest is applied. This results in an MRI signal only being created from this specific section. The thickness of the slice can also be selected by varying the steepness of the gradient field or the bandwidth of the RF pulse.

Subsequently, to determine where the signals are originating from within the slice of interest two more gradient fields are applied, called a frequency encoding and phase encoding gradient. The phase encoding gradient is applied first and this causes protons within a row or column (depending on the selected gradient direction) to have a frequency gradient varying from low to high. Once the gradient is turned off the protons return to the base frequency and spin at the same rate but they are now out of phase with one another. Next, the frequency

encoding gradient is applied orthogonally to the phase encoding gradient and induces a range of Larmor frequencies within protons across columns or rows depending on the selected gradient direction. Overall, the two types of gradient result in a range of signals that have a unique characteristic based on their phase or frequency that can be localised in space. The phase and frequency data is stored as a data matrix called K-space which is then converted into an image using the Fourier transform (Gallagher *et al.*, 2008). Thus, obtaining an MRI image is a complex process that requires a combination of precisely timed RF pulses and gradients to induce a set of characteristic signals that are interpreted mathematically to construct a 2D or 3D image.

In this thesis optimised parameters using spin echo sequences, RF pulses and gradients as described above are used to obtain T1-weighted images for three main purposes. One purpose is to obtain structural properties of the primary visual cortex and auditory cortex including surface area and thickness using FreeSurfer (Hinds *et al.*, 2008). Secondly, the structural image is used for locating a region of interest (occipital cortex) in which to measure GABA levels using MRS. Thirdly, for co-registration purposes between MRI and MEG data, which is detailed later in this methods chapter.

2.2 Magnetic Resonance Spectroscopy

The application of *in vivo* magnetic resonance spectroscopy (MRS) began in the early 1980s, in parallel to the introduction of MRI (Bertholdo *et al.*, 2013). MRS is based on similar principles as MRI but instead of producing structural images provides physiological information, by quantifying chemical metabolites. The particular usefulness of this biochemical information has meant that MRS and MRI are commonly used in conjunction with one another, such as for monitoring brain tumours and metabolic diseases. Importantly,

MRS can detect subtle biochemical changes that may not be visible using structural MRI. This has led to MRS being used in psychiatry research with the aim of further identifying clinically relevant group differences in biochemical metabolites (Frangou and Williams, 1996, Stanley, 2002).

Proton MRS (^{1}H-MRS) is the most commonly used technique as hydrogen has a high magnetic sensitivity and is highly abundant in most metabolites. The main concept in MRS is that of chemical shift, which relies on how protons act in their chemical environment within the magnetic field of the MR scanner. As noted above, protons precess at a Larmor frequency that is mainly dependent on the strength of the external magnetic field. Due to the relative homogeneity of the external field the protons precess at relatively similar rates. However, the protons do precess at slightly different rates due to differences in the surrounding local magnetic fields that are produced by electrons. If the protons have a high electron density around them, they resonate at a lower frequency as the electrons shield the proton from the external magnetic field. This means that protons in different molecules and protons in the same molecule but at different positions will have slightly different Larmor frequencies. Essentially, it is the chemical structure of the molecule that determines the shift in frequency and it is these chemical shifts that are plotted in a MRS spectra and allow us to identify and quantify molecules. In a typical MRS plot, the horizontal axis shows the Larmor frequencies (or chemical shift) in parts per million and the vertical axis shows the relative signal amplitude in arbitrary units.

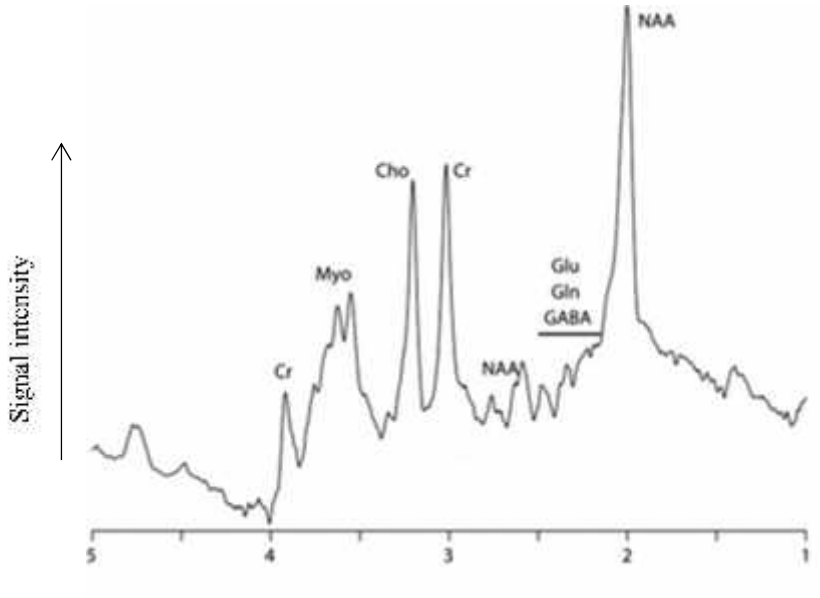

Figure 2.4: A typical MRS spectrum showing the brain metabolites that can be detected and their chemical shift frequencies. Image adapted from (Puts and Edden, 2012).

Although the human brain contains hundreds of metabolites, a typical MRS spectrum only displays the amounts of certain brain metabolites (Figure 2.4). This is because MRS can only detect a few of them as they need to be in at least milli-molar concentrations in order to be detected. This means that many neurotransmitters cannot be detected. The major brain metabolites that are detected are N-acetyl aspartate (NAA), creatine (Cr), choline (Cho), myo-inositol (Myo), glutamate (Glu), glutamine (Gln) and GABA. Another feature of the MR spectrum is that some metabolites have several peaks instead of one single peak. This is due to the phenomenon of J-coupling or spin-spin coupling. J-coupling arises when protons within a metabolite are found in different chemical groups, meaning that they have slightly different local magnetic fields and resulting spin frequencies.

Typically, MRS data is collected following the acquisition of anatomical images so that a region of interest can be selected. The spectrum can either be obtained from a single voxel

(SVS) or multiple voxels, known as magnetic resonance spectroscopic imaging (MRSI). Normally, a single voxel is used as this is a more robust technique that provides a better signal to noise ratio. This means that placing the voxel of interest is a crucial step as only one spectrum is obtained using SVS. To obtain ^{1}H-MR SVS data, two types of pulse sequences can be used: a Point Resolved Excitation Spin echo sequence (PRESS) or a stimulated echo acquisition mode (STEAM) (Storey, 2006, van der Graaf, 2010). PRESS uses sequences of one 90^0 excitatory RF pulse followed by two 180^0 refocusing pulses, with the spectral data being obtained from the spin echo after the second 180^0 pulse (see figure below). In contrast, STEAM uses sequences of three consecutive 90^0 RF pulses and the spectral data is obtained from a stimulated echo. The stimulated echo has a lower amplitude than the spin echo, meaning that the PRESS method has a better signal to noise ratio. For both methods, each pulse is delivered across a different plane (x, y or z) so that spatial selectivity is acquired in each direction (Figure 2.5)

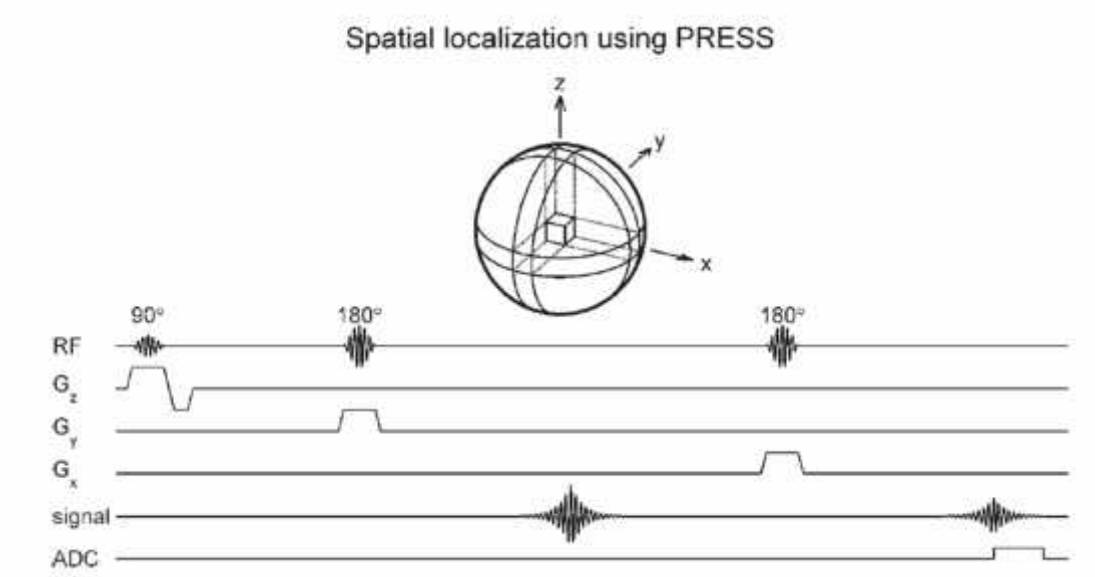

Figure 2.5: Outline of the acquisition method for PRESS. The 90^0-180^0-180^0 RF pulse is delivered with each RF in a separate orthogonal direction to obtain a 3D voxel in the region of interest. ADC denotes when the spectral data is acquired. Image taken from (Storey, 2006).

To make sure that the acquired signal is specific to the voxel of interest, spoiler gradients are added to dephase protons and reduce the signal from areas surrounding the region of interest. In addition, the large water signal is suppressed to enable the smaller signals from metabolites of interest to be detected. Lastly, the resulting signals are analysed by Fourier transform to obtain the frequency data and plot the spectrum.

2.2.1 GABA Acquired MRS

Measuring *in vivo* GABA levels via MRS is more difficult than measuring conventional metabolites such as NAA and Cr. Even so, studies measuring MRS GABA are steadily increasing as more accurate and reliable methods are being developed (Puts and Edden, 2012). GABA is particularly difficult to measure due to three main reasons. Firstly, it is found at a relatively low concentration of 1mM/mm³ in the human brain, compared to concentrations of about 10mM/mm³ for NAA and 7mM/mm³ for Cr (Henriksen, 1995, Puts and Edden, 2012). Secondly, the chemical structure of GABA means that it produces signals between 1.8-3.1ppm, which are overlapped by the stronger signals originating from NAA, Cr and Glx (glutamate and glutamine) (Figure 2.6). Lastly, J-coupling is present between spins at 3ppm and 1.9ppm, causing a smaller signal and a broader frequency shift.

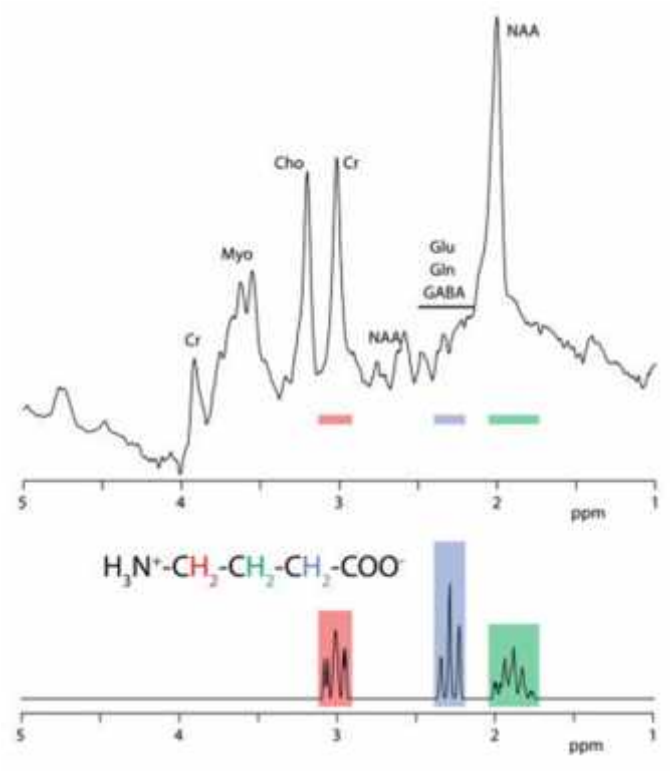

Figure 2.6: The chemical structure of GABA and its MR spectrum. GABA produces three separate signals along the frequency spectrum due to its three methylene groups. The large Cr signal at 3ppm overlays that of the GABA signal at 3ppm. Image taken from (Puts and Edden, 2012).

To overcome problems of specificity and sensitivity of GABA measures, particular spectral editing methods can be applied. The most common spectral editing method used for detecting GABA uses a pulse sequence called MEGA-PRESS (Mescher *et al.*, 1998, Mullins *et al.*, 2014). This method separates GABA signals at 3ppm from overlying Cr signals based on the J coupling between signals at 3ppm and 1.9ppm. Two distinct spectra are measured. For acquiring the first spectrum, a frequency-selective pulse that directly affects signals at 1.9ppm is applied (known as 'ON' spectrum). The pulse also has an indirect effect on signals at 3ppm due to coupling. As signals from other metabolites at 3ppm are not coupled to those at 1.9ppm the pulse only affects GABA signals at 3ppm. The second spectrum is collected

using a normal PRESS sequence, without the editing pulse (known as 'OFF' spectrum) and is subtracted from the ON spectrum. The resulting difference spectrum allows the residual GABA signals at 3ppm to be quantified. This MEGA-PRESS technique has been used for measuring GABA levels in a number of brain areas, including occipital, motor, temporal and frontal regions (O'Gorman *et al.*, 2011, Puts *et al.*, 2011, Shaw *et al.*, 2013). In the visual and sensorimotor cortex, GABA measurements using MEGA-PRESS have been shown to be highly repeatable and sensitive enough to detect inter-individual variation (Evans *et al.*, 2010). Therefore, experiments in Chapter 3, 4 and 5 of this thesis used the MEGA-PRESS sequence to accurately measure GABA levels in a single voxel of the occipital cortex.

To quantify the GABA peak at 3ppm from the edited spectra, the CUBRIC Gannet analysis pipeline was used (www.gabamrs.blogspot.co.uk). This fits the GABA peak with a single Gaussian model to estimate the area under the peak. This raw GABA measure is an arbitrary value that depends on several factors such as the distance between the coils and the head, and the temperature of the scanner. To remove these factors, the GABA value is calculated relative to a known concentration reference, such as Cr or water. Cr has the advantage of being acquired during the MEGA-PRESS scan whereas the water measurement is normally acquired at the end of the scan and so is more susceptible to motion effects. However, water has a higher signal to noise ratio. Thus, both references are commonly used in experiments. The benefit of using the Gannet pipeline is that GABA values are reported using both Cr and water as references. One last factor that must be taken into consideration is that GABA concentration differs depending on the tissue type; CSF has low GABA concentrations in comparison to tissue. Similarly, water visibility in H20, grey matter and white matter also differ. Thus, GABA estimates need to account for differences in voxel composition. In this

thesis, MRS GABA values were corrected for tissue composition using estimates of grey matter, white matter and CSF from the FSL tool, FAST (Zhang *et al.*, 2001).

Although the MRS-GABA methods described above have been dramatically improved since being first implemented, several limitations must also be pointed out. For example, MRS GABA spectra are acquired from relatively large voxels (3cm x 3cm x 3cm) due to GABA's low SNR. This means that MRS measures 'bulk' GABA concentration as it cannot distinguish between different pools of GABA, such as vesicular, cytoplasmic or extracellular GABA (Stagg *et al.*, 2011b). Therefore, how MRS GABA levels relate to these individual pools is still unknown. In addition, the GABA signal at 3ppm is also made up of signals from macromolecules. This is because j-editing also picks up the macromolecule spins that are coupled to spins at 1.7ppm. These macromolecules make up around 50% of the GABA signal and so GABA is often described as GABA+. Even though these limitations are present, MRS GABA levels have been shown to correlate with behaviourally relevant measures that are functionally specific to the cortical region studied (Boy *et al.*, 2010, Stagg *et al.*, 2011a, Sumner *et al.*, 2010). These findings suggest that MRS is obtaining measures that are relevant to the effects produced by the synaptic activity of GABA.

2.3 Magnetoencephalography

Magnetoencephalography (MEG) is also a relatively recent non-invasive imaging modality, with the first magnetic signals being measured from the human brain in 1968 (Cohen, 1968). The advantage of using MEG is that it measures direct neural activity with a high temporal resolution. The neural activity arises from the summation of postsynaptic currents in the dendrites of pyramidal cells and it is these postsynaptic currents that produce measurable magnetic fields outside the brain (Okada, 1989). The magnetic fields are generated by

pyramidal cells in layers 3, 4, 5 and 6 of the cortex and are extremely small. However, as pyramidal cells are orientated in the same way, this allows the fields to summate in the same direction. Even so, simultaneous activity from at least 100,000 cells needs to occur in order to detect a measurable signal. As the magnetic fields are so small, the MEG system is also placed in a magnetically shielded room to avoid the signals being contaminated with the stronger environmental magnetic noise.

Special sensors called magnetometers and gradiometers are used to measure the amount of magnetic field passing through their conducting coil, known as the magnetic flux. Magnetometers measure the magnetic flux through a single coil whereas gradiometers measure the difference in magnetic flux between at least two coils. Using this set up of two coils means that gradiometers are efficient at suppressing environmental noise. As both coils equally pick up environmental noise (as they are relatively at the same distance from the noise) the unwanted noise is removed when the difference in magnetic flux is measured between the two coils. Due to this efficient environmental suppression, MEG systems are typically made up of gradiometers. Gradiometers can also be subdivided into axial and planar based on their orientation with the scalp. Axial gradiometers are aligned orthogonally to the scalp (one above the other), while planar gradiometers have two pick up coils in the same plane (next to each other). Magnetic fields described in this thesis were obtained using a CTF 275-channel axial gradiometer system.

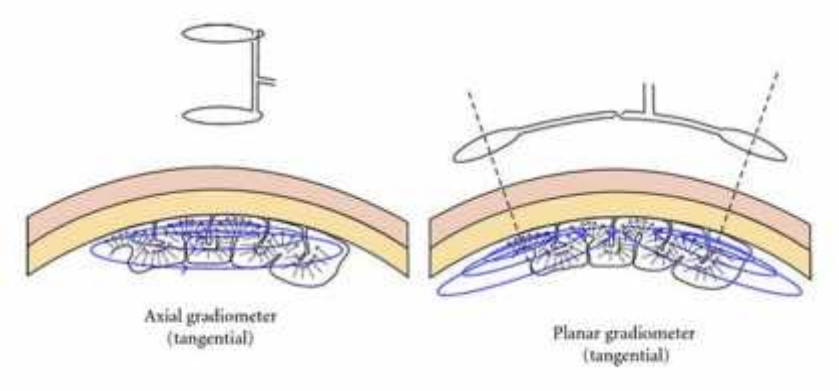

Figure 2.7: Orientation of axial and planar gradiometers to measure the magnetic fields produced by synchronised post synaptic currents in pyramidal cells. Image taken from http://www.hindawi.com/journals/cin/2009/656092/fig3/.

Importantly, the magnetic flux induces electrical currents in the coils of the gradiometers which are transferred to super conducting quantum interface device (SQUIDS) to further amplify the signal (Vrba and Robinson, 2001). The signals are then digitised and analysed by computer systems. Once these signals have been detected externally (in sensor-space), the source producing the signals in the brain needs to be identified (in source-space) – this is known as the *inverse problem*. Although the magnetic field generated by a known configuration of sources within the head can easily be calculated – the so-called *forward problem* - there is insufficient information in the external MEG measurements to uniquely solve the inverse problem. As an infinite number of different sources could explain the observed magnetic fields, the inverse problem is known as an ill-posed problem. In order to solve the inverse problem, different kinds of a prior information can be used and thus different solutions (Barnes *et al.*, 2006). Although several methods are available for solving the inverse problem, two main methods known as equivalent current dipole (ECD) modelling and beamforming will be described.

ECD modelling is one of the most common and simple source estimation techniques. The technique assumes that the magnetic fields measured by the MEG sensors can be explained by a single dipole (small patch of activated cortex). An initial guess about the location, orientation and amplitude of the dipole is made and then these parameters are adjusted until the magnetic field generated by this simulated dipole best fits the measured magnetic fields. If the single dipole does not fit the data well then multiple dipoles can be used, with each dipole having their parameters needing adjusting. ECD modelling is typically used for estimating the source of evoked responses. As this thesis is primarily focused on oscillatory activity from induced responses, another technique called beamforming was used.

Beamforming does not manipulate parameters of the source (location, orientation and amplitude) in order to explain the measured field. Instead, the technique estimates the output of a source at a particular location in the voxel of the brain. This is known as spatial filtering, in which the signal at a particular source is measured, while signals from other locations are suppressed. The spatial filtering is achieved by selectively weighting how much each sensor contributes to the overall beamformer output. These weights are estimated using an analysis of the data covariance matrix (Hillebrand and Barnes, 2005).

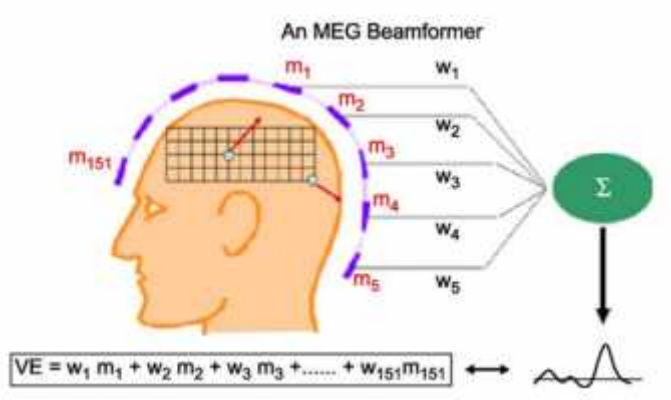

Figure 2.8: Concept of beamforming in MEG. The signal at a particular location is calculated by multiplying the signal from a particular MEG sensor (m_1) by a weighting factor (w_1). This

means that only the signal from the location of interest will contribute to the beamformer output while signals from other unwanted areas will be attenuated. Image taken from (Hillebrand and Barnes, 2005).

Synthetic aperture magnetometry (SAM) is a novel beamforming approach that assumes the signal is produced from several distinct dipoles and that these sources are uncorrelated in time (Robinson and Vrba, 1999). A major advantage of using SAM is that it can be performed on selected time windows and frequency bands of interest. Thus, at a particular location of interest, responses to a stimulus can be identified at a specific moment in time and across a particular frequency band. This has led to SAM being widely adopted in the MEG community and has proven successful for analysing MEG data in sensory domains such as the visual, auditory and motor cortex (Brookes *et al.*, 2011, Fawcett *et al.*, 2004, Gaetz *et al.*, 2009, Herdman *et al.*, 2003). Due to the ease and efficiency of SAM this approach was used in this thesis to obtain the time and frequency profiles of the evoked and induced activity from the visual cortex.

Due to the latter assumption of SAM, in which sources are presumed uncorrelated in time, it cannot accurately detect temporally correlated sources (such as bilateral auditory sources) as the signals cancel each other out. This is why evoked responses which have very short durations and are therefore more likely to be correlated in time are not usually localised using SAM. Therefore, to measure the auditory evoked steady-state responses in this thesis, rather than using a source space analysis, a sensor space approach was used. For sensor space analysis, the sensor that elicited the strongest response following presentation of the auditory response was selected and subsequent time-frequency analysis was performed on the data acquired from this single sensor.

It is usually desirable to map source-localised MEG activity onto the individual's anatomical MRI scan. This is done by placing three electromagnetic head coils at the nasion and left and right preauricular points on the individual (fiducial markers). This enables the location of the coils, and thus the location of the participant's head, inside the dewar to be determined. The locations of the fiducial points are then marked onto the MRI image to enable coregistration between the MEG data and MRI image. Once SAM has been performed on the selected time window and frequency band and has been coregistered with the structural brain scan, an activity map across different voxels can be seen. From this map the voxel with the 'peak response' across these parameters can be selected so that a 'virtual sensor' is placed at this location.

2.3.1 Analysis of Induced, Evoked and Steady-State Activity

To view the response profile of the electrophysiological signal at the virtual sensor from source space or the real sensor from sensor space, time-frequency analysis is performed. This results in a time-frequency spectra in which amplitude changes (increases or decreases) across the selected time and frequency domains can be viewed (Figure 2.9). Within the time-frequency spectra, three main types of activity can be measured; evoked, induced and steady-state responses. Evoked responses are phase-and time-locked to the stimulus. They are detected by averaging the signal across a number of individual trials. This analysis produces an event-related potential or event-related field potential (ERP/ERF). If desired, this average response can be taken forward for time-frequency analysis of the evoked oscillatory response. Induced responses are not phase locked to the stimulus and so time-frequency analysis needs to be performed on a single trial basis. This is because averaging across trials would cancel out the induced responses as they have essentially random phase on each trial. The time-frequency representation of each individual trial is then averaged to reveal the induced

oscillatory responses. Steady-state responses are produced following presentation of a repeated stimulus, in which the frequency of the response is the same as that of the stimulus. These responses are normally analysed in the same way as evoked responses by averaging across trials as they are deemed to be phase locked to the repetitive stimulus.

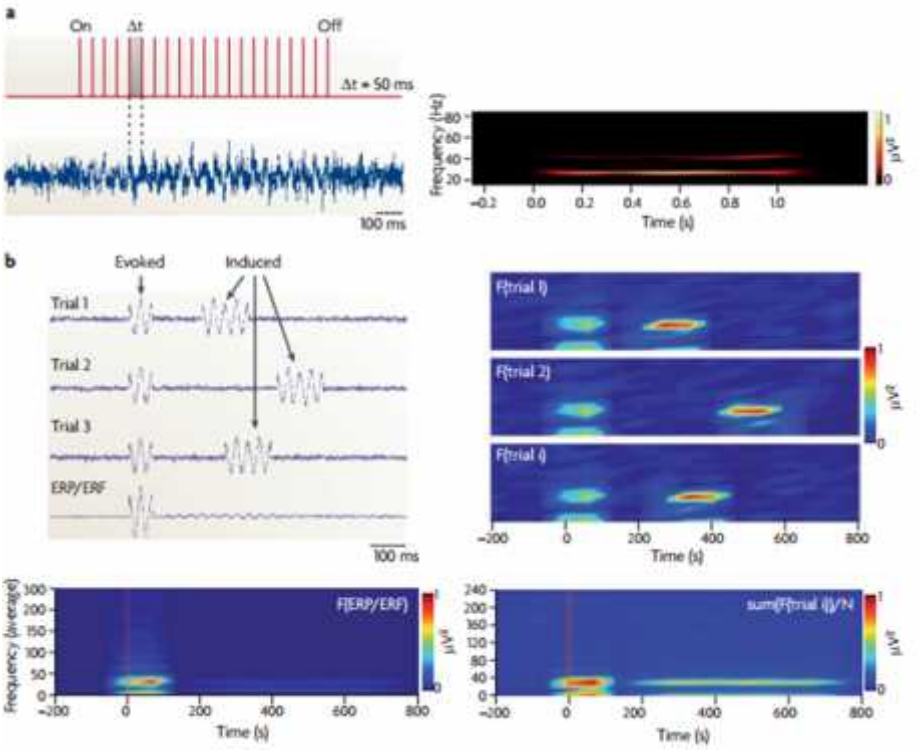

Figure 2.9: Spectra acquired from a time-frequency analysis of evoked, induced and steady-state responses. a) shows a continuous steady-state stimulus at a frequency of 20Hz and the resulting continuous 20Hz response in a MEG recording and in a time-frequency spectra. b) shows the phase locking in evoked and non-phase locking from induced responses in individual trials and their amplitudes in the time-frequency spectra. Image taken from (Uhlhaas and Singer, 2010).

Different components of the evoked, induced and steady-state response can be analysed. The most common parameter studied for all three types is the amplitude of the response. Experiments in this thesis looked at the amplitude of the induced and evoked response to a visual stimulus (Chapter 3 and 5) and the amplitude of the steady-state potential in response

to a repetitive auditory stimulus (Chapter 6). Another measure is the degree of phase locking, known as the phase locking factor (PLF). PLF measures the variance of phase across single trials and ranges from 0 (random distribution) to 1 (perfect phase locking). Lastly, the peak frequency (the frequency at which the largest amplitude is recorded) can be analysed. This thesis measures the peak frequency of the induced response following a visual stimulus and the peak frequency of an auditory steady-state response (Chapter 3, 5 and 6). Given the different profiles of evoked and induced activity they are thought to reflect different aspects of information processing. Evoked responses are thought to reflect bottom up sensory processing whereas induced oscillations may be involved in higher cognitive functions. However, these presumptions must be interpreted with caution as many different measures (such as those described above) within the response itself can be obtained.

Chapter 3 - Investigating the Influence of GABA and the Structural Properties of V1 on Inter-individual Variability in Peak Gamma Frequency

3.1 Abstract

Background: Determining the factors driving individual variability in visual gamma peak frequency will ultimately help us understand differences in visual perception in both health and disease. Previous studies have indicated that the neurochemical MRS GABA measure and the structural measures of the thickness and surface area of the primary visual cortex (V1) may influence individual variability in visual gamma frequency. However, these findings have not been replicated in larger independent studies. Hence, this study aims to investigate the influence of these structural and neurochemical measures on visual gamma peak frequency in a large homogenous cohort.

Methods: Visual gamma peak frequency, GABA+, V1 surface area and V1 thickness measures were obtained from a homogenous group of 100 healthy individuals who participated in a genetic imaging study, called '100 Brains'.

Results: Correlational analyses revealed no significant associations between any of the variables studied (GABA+, V1 surface area, V1 thickness) with peak gamma frequency ($p=0.690$, $p=0.640$,$p=0.108$, respectively).

Conclusion: These findings contradict previous studies that have found positive associations between GABA+, V1 surface area and V1 thickness on peak gamma frequency. As these variables are influenced by age, previous positive associations may have been driven by a mutual influence of age. This is supported by other independent studies in which once the effect of age is removed, the variables no longer correlate and further highlights the importance of using large homogenous cohorts. Further investigation using large sample sizes is needed to determine the factor(s) driving individual variability in visual gamma frequency.

3.2 Introduction

The structural and neurochemical properties of the visual system are known to vary widely across individuals (Dougherty *et al.*, 2003, Puts and Edden, 2012). The exact significance of this variation is unknown but emerging research suggests that inter-individual differences in the visual system are functionally important and may shape our visual perception (Edden *et al.*, 2009, Kanai and Rees, 2011, Schwarzkopf *et al.*, 2011, Song *et al.*, 2013). For example, Schwarzkopf et al. (2011) found that variation in the effective connectivity of the human primary visual cortex determines variability in orientation perception (Schwarzkopf *et al.*, 2011). Thus, further understanding the factors that determine functional variation may help us explain individual differences in the perception of our environment.

Investigating the factors underlying individual differences in gamma oscillations (30-100Hz) has been of particular interest in the physiology research field. This is because these high frequency oscillations are found in many cortical areas, have been implicated in sensory and cognitive processing (Başar, 2013, Engel *et al.*, 2001, Ward, 2003) and are altered in disease (Başar and Güntekin, 2008, Uhlhaas and Singer, 2010). In the visual cortex, sustained narrow-band gamma oscillations (30-80Hz) can be elicited using visual gratings (Adjamian *et al.*, 2004, Hoogenboom *et al.*, 2006, Muthukumaraswamy *et al.*, 2010, Swettenham *et al.*, 2009) and have been implicated in the encoding of stimulus features as they are modulated by stimulus orientation (Koelewijn *et al.*, 2011), size , contrast (Hall *et al.*, 2005) and eccentricity (van Pelt and Fries, 2013). Importantly, the two main parameters of the visual gamma response, peak gamma frequency and peak gamma power show inter-individual variation that is stable and repeatable over time (Adjamian *et al.*, 2004, Hoogenboom *et al.*, 2006, Muthukumaraswamy *et al.*, 2010, Swettenham *et al.*, 2009). Although the majority of studies have investigated the amplitude/power of visual gamma oscillations, peak frequency

is an equally important measure and has been shown to be functionally important as it is negatively correlated with orientation discrimination thresholds (Edden *et al.*, 2009). The exact factor/s driving the inter-individual variability in peak gamma frequency are unknown but recent evidence suggests that these factors are under genetic control (van Pelt *et al.*, 2012).

Neurophysiological studies and computational models suggest that gamma oscillations are generated via reciprocally connected interneuron and pyramidal cell assemblies (Buzsaki and Wang, 2012, Traub *et al.*, 1997, Whittington *et al.*, 2011). In particular, the inhibitory drive from parvalbumin containing fast-spiking basket cells in layers 2-6 appears to be vital for generating cortical gamma oscillations (Cardin *et al.*, 2009). In support of this, the visual gamma measures peak power and peak frequency are modulated by the balance between this inhibitory and excitatory network and are affected by parameters such as its excitation/inhibition ratio, strength and time constants (Brunel and Wang, 2003). The dependency of visual gamma parameters on the cortical excitatory and inhibitory balance led to the investigation of the influence of the inhibitory neurotransmitter GABA on visual gamma parameters using neuroimaging. This provided *in vivo* evidence for the primary involvement of GABAergic transmission in gamma generation, as visual gamma peak frequency measured using MEG was shown to positively correlate with MRS resting occipital GABA+ (Muthukumaraswamy *et al.*, 2009). This finding was explained as those individuals with higher levels of GABA+ having increased inhibition, which decreases the excitation/inhibition ratio, resulting in higher peak frequencies. Following this, the structural parameters of V1, cortical thickness (Gaetz *et al.*, 2012, Muthukumaraswamy *et al.*, 2010) and V1 surface area (Schwarzkopf *et al.*, 2012) were also shown to positively correlate with peak gamma frequency.

The positive association between cortical thickness and gamma frequency can be explained by the possible effect of thickness on the excitatory/inhibitory balance. Cortical thickness is thought to reflect the density of neuronal and glial cells within the radial columns of the cortex (Rakic, 1988). This density of neurons is determined during development and depends on the number of neurogenic progenitors in these units that proliferate or generate neurons (Pontious *et al.*, 2008). Therefore, variability in cortical thickness may have downstream effects on the number of neurons and hence the excitatory/inhibitory balance. For example, if an individual has a thicker cortex, this may be due to a larger number of neurons and as V1 has a high number of GABAergic inhibitory neurons (Hendry *et al.*, 1987) this could potentially lead to increased GABA levels and hence a higher peak gamma frequency.

In comparison, the positive correlation between V1 surface area and visual gamma frequency was proposed to be due to the homogeneity of factors such as the cytoarchitecture and receptor density within the V1 radial columns (Schwarzkopf *et al.*, 2012). Participants with a larger V1 were proposed to have a more homogenous functional architecture, where the local connections travel shorter distances, leading to local pools oscillating at similar frequencies and hence a higher peak frequency. These differences in lateral connectivity could also alter gamma frequency indirectly by affecting the GABAergic/glutamatergic balance of the cortex.

Overall, these studies suggest that variability in occipital GABA+, V1 cortical thickness and V1 surface area may influence variability in visual gamma peak frequency. However, as cortical thickness and surface area may not influence peak gamma directly but indirectly via GABAergic transmission, the effect of these variables must be interpreted with caution as they may be mutually correlated and not entirely independent. Furthermore, these correlations have been demonstrated in small sample sizes and have failed to be replicated in

independent studies (Perry *et al.*, 2013, Shaw *et al.*, 2013) or in a larger sample size (Cousijn *et al.*, 2014). Using a retrospective, pooled analysis of data from CUBRIC (n=46), Robson et al. (2012) found cortical thickness and GABA+ to weakly positively correlate with peak frequency. However, when age was accounted for these correlations were no longer significant and age was left as the only determinate factor of peak frequency, explaining 13% of the variance (Robson, 2012). As cortical thickness (Salat *et al.*, 2004), surface area (Hogstrom *et al.*, 2013), GABA+ (Bigal *et al.*, 2008) and peak gamma frequency (Gaetz *et al.*, 2012) are found to decrease with age it was suggested that previous correlations between these measures may have been driven by their mutual relationship with age. Thus, age is an important factor that should be taken into account when assessing the effect of these variables on gamma measures.

However, a potential weakness of this pooled study was that not all MEG and MRS data was collected using identical experimental/acquisition parameters. To further investigate the relationship between visual gamma peak frequency, GABA+, thickness and surface area, these measures were therefore obtained in a large homogeneous cohort of 100 healthy individuals that were part of a large genetic imaging study called '100 Brains'. Identical experimental protocols were used for each individual. The aim was to keep the sample homogenous in order to reduce potential confounds such as age. This allowed us to determine whether inter-individual differences in visual gamma peak frequency are influenced by inter-individual differences in occipital GABA+, V1 cortical thickness and/or V1 surface area.

3.3 Methods

3.3.1 Participants

100 healthy individuals with normal or corrected vision (with MRI/MEG compatible lenses) took part in the study. As this study was part of a large genetic imaging project (called 100 Brains), variance from non-genetic factors needed to be minimised so a group homogenous in age, ethnicity, education and handedness were required. This led to nine participants being excluded; one due to not fully completing the study, another due to previously undocumented medication, another due to left-handedness, four that were genetically identified as population outliers (non-Caucasian) and two that were identified as age outliers. This meant we had a homogenous group of 91 individuals (33 males and 58 females) aged between 19-34 (mean 23.5, SD 3.4) that were healthy, right-handed, Caucasian and had all completed or were currently completing a degree. Right-handedness was determined by the Edinburgh Inventory (Oldfield, 1971). Mental well-being was screened using the 12-Item General Health Questionnaire (GHQ-12), with additional questions including a history of excessive drug or alcohol use and any regular medications. All participants gave written informed consent to participate.

3.3.2 MEG Stimulus

The visual task was one of six MEG paradigms that all participants completed. The visual stimulus consisted of a stationary, vertical, square-wave grating with maximum contrast, and a spatial frequency of 3 cycles per degree. Stimuli were presented on a mean luminance background with a red central fixation point (Figure 1), using a Mitsubishi Diamond Pro 2070 monitor (1,024 × 768 pixels and 100Hz frame rate). Participants were instructed to fixate on the central fixation point and to press a button once the grating disappeared. The grating was presented for 1.5-2s and participants were given 0.75s for their button press

response. If a response was late or no response was obtained a warning would be presented. Following the response period, only the red fixation point was presented for 2s. The visual session contained 100 trials and took ~10 minutes to complete.

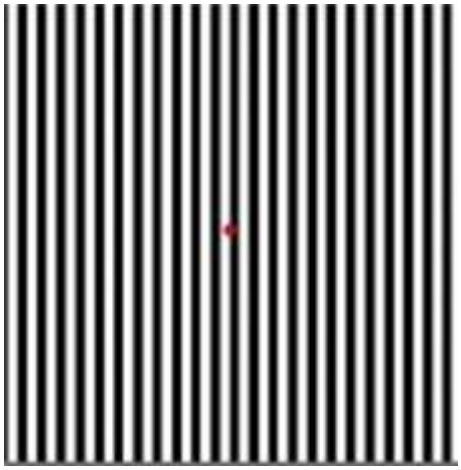

Figure 1: The visual grating stimulus used in the study

3.3.3 MEG Acquisition

Whole-head MEG data was acquired on a CTF 275-channel radial gradiometer system. Three of the 275 channels were turned off due to excessive sensor noise. An additional 29 reference channels were recorded for noise cancellation purposes and the primary sensors were analysed as third-order gradients (Vrba and Robinson, 2001). Three electromagnetic head coils were placed onto participants at fixed distances from their anatomical landmarks (nasion and pre-auriculars) and were localised relative to the MEG system before and after each session to localise the head. Subjects were seated upright in the magnetically shielded room.

Each dataset was epoched offline -2 to 2s around stimulus onset. Individual trials were visually inspected for data quality and those with large signal artefacts such as head movements, muscle clenching and eye blinks were removed from further analysis. From the 91 datasets, on average 10.4% (SD 10.9, range 0-51%) of the 100 trials were removed. Source localisation was calculated using synthetic aperture magnetometry (SAM) (Robinson

and Vrba, 1999). For each participant, a global covariance matrix was calculated for the gamma band (30-70Hz) and beamformer weights were computed for the entire brain at 4mm isotropic voxel resolution (Robinson and Vrba, 1999).

Student-t images to reveal source increases were calculated using a baseline period of -1.5s to 0s and a stimulation period of 0 to 1.5s. Using these images, for each participant, their strongest increase in the gamma band was located and a virtual sensor was placed at this location. To reveal the time-frequency response at this location, the virtual sensor was repeatedly band-pass filtered between 1 and 100Hz at 0.5Hz frequency step intervals with an 8Hz bandpass, 3rd order Butterworth filter (Le Van Quyen *et al.*, 2001). The Hilbert transform was used to obtain the amplitude envelope at each frequency step, resulting in time-frequency spectra. Spectra were computed as a percentage change from the mean baseline amplitude. From these spectra the peak amplitude and peak frequency were extracted in the sustained (0.3 to 1.5s) response (Swettenham *et al.*, 2009).

3.3.4 MRI Acquisition

Magnetic Resonance (MR) data was acquired on a 3T General Electric HDx MRI scanner with an 8-channel receive-only head coil. A high resolution T_1-weighted anatomical image (FSPGR) with 1-mm isotropic resolution (TE/TR/inversion time = 2.98/7.8/450msec, flip angle =20^0) was obtained for each participant. Using these anatomical images, the occipital voxel (3cm x 3cm x 3cm) was placed in each subject (Figure 3A and 3B). The voxel was placed bilaterally in the occipital cortex to include both hemispheres with the lower edge of the voxel aligned to the superior border of the cerebellum and the anterior edge aligned with the parieto-occipital sulcus. GABA spectra were acquired using a MEGA-PRESS sequence (TE=68ms, TR=18s, 332 transients of 4096 datapoints and 16msec editing pulses applied at

1.9 parts/million (ppm) (ON) and 7.5 ppm (OFF). In addition, 8 transients were acquired without water suppression. The acquisition time for the T1 weighted scan took ~9 minutes and the GABA spectrum acquisition took ~12 minutes. MEG and MRI/MRS data were usually collected on different days.

GABA analysis was carried out with the in-house software Gannet, a batch-analysis tool for GABA-edited MRS data (http://gabamrs.blogspot.co.uk/). The GABA peak at 3.0ppm in the difference edited spectrum was fitted with a single Gaussian model. GABA values obtained from the Gaussian model fit are described as GABA+, as the GABA signal at 3ppm is likely to contain a co-edited macromolecular signal (Henry *et al.*, 2001). GABA+ concentrations were quantified using both creatine (GABA+/Cr) and water (GABA+/H_20) as an internal concentration reference. For the reported GABA+/H_20 values, the ratio of GABA+ to water was converted to institutional units (IU) by correcting for the voxel tissue fraction (grey matter and white matter) and the effective visibility of water. Grey matter, white matter and CSF fraction were determined using FAST (Zhang *et al.*, 2001). Both creatine and water were used as reference molecules to ensure the reliability of the findings and that they were not due to using a particular reference molecule.

3.3.5 V1 Structural Properties

FreeSurfer was used to estimate the cortical thickness and surface area of V1 for each participant from their 3D FSPGR scan. FreeSurfer is an automated technique and identifies the calcarine sulcus and curvature heuristics to estimate the location of V1 and is a validated technique (Hinds *et al.*, 2008). As the visual stimulus was presented on the full visual field, estimates of V1 surface area and thickness were calculated by averaging the right and left hemisphere.

3.3.6 Statistical Analysis

Correlations between GABA+ concentration, peak gamma frequency and V1 structural parameters (surface area and thickness) were carried out using the Pearson correlation coefficients (r) in SPSS 20.

3.4 Results

3.4.1 Visual Gamma Responses

Following presentation of the visual grating, all except one of the participants showed a clear source increase in the visual gamma band (30-70Hz) that was localised to the primary visual cortex (Figure 2 (A)). This participant was excluded from further analysis. Figure 2B displays the grand-averaged time-frequency analysis of the virtual sensor at the group and individual level. The time-frequency spectra reveal the typical response morphology that is obtained using this type of visual stimulus (Swettenham *et al.*, 2009). Initially, a transient broadband gamma response (0-0.3s) occurs, followed by a sustained narrow gamma band response (0.3-1.5s) that remains for the duration of the stimulus. In the lower frequency bands, there is an early evoked response and a reduction of power in the alpha band. The main variable of interest for this study, *peak gamma frequency* (30-70Hz) was extracted from the sustained response (0.3-1.5s). Upon visual inspection of the time-frequency analysis, 13 of the 90 individuals displayed no clear gamma peak and were excluded from further analysis. Many of these 13 participants were excluded because they displayed 2 peaks within the 30-70Hz range and this made it difficult to distinguish a single peak. Thus, a total of 78 participants are included in the data analyses. Peak gamma frequency in the 78 participants ranged from 41.5-64.5Hz (mean 53.2 (SD=4.8)) which is consistent with previous studies (Muthukumaraswamy *et al.*, 2010). The variability in peak gamma frequency between

individuals can be seen in Figure 2B and 2C; participant 1 has a low gamma band frequency (48.5Hz) compared to participant 2 with a high gamma band frequency (61.5Hz).

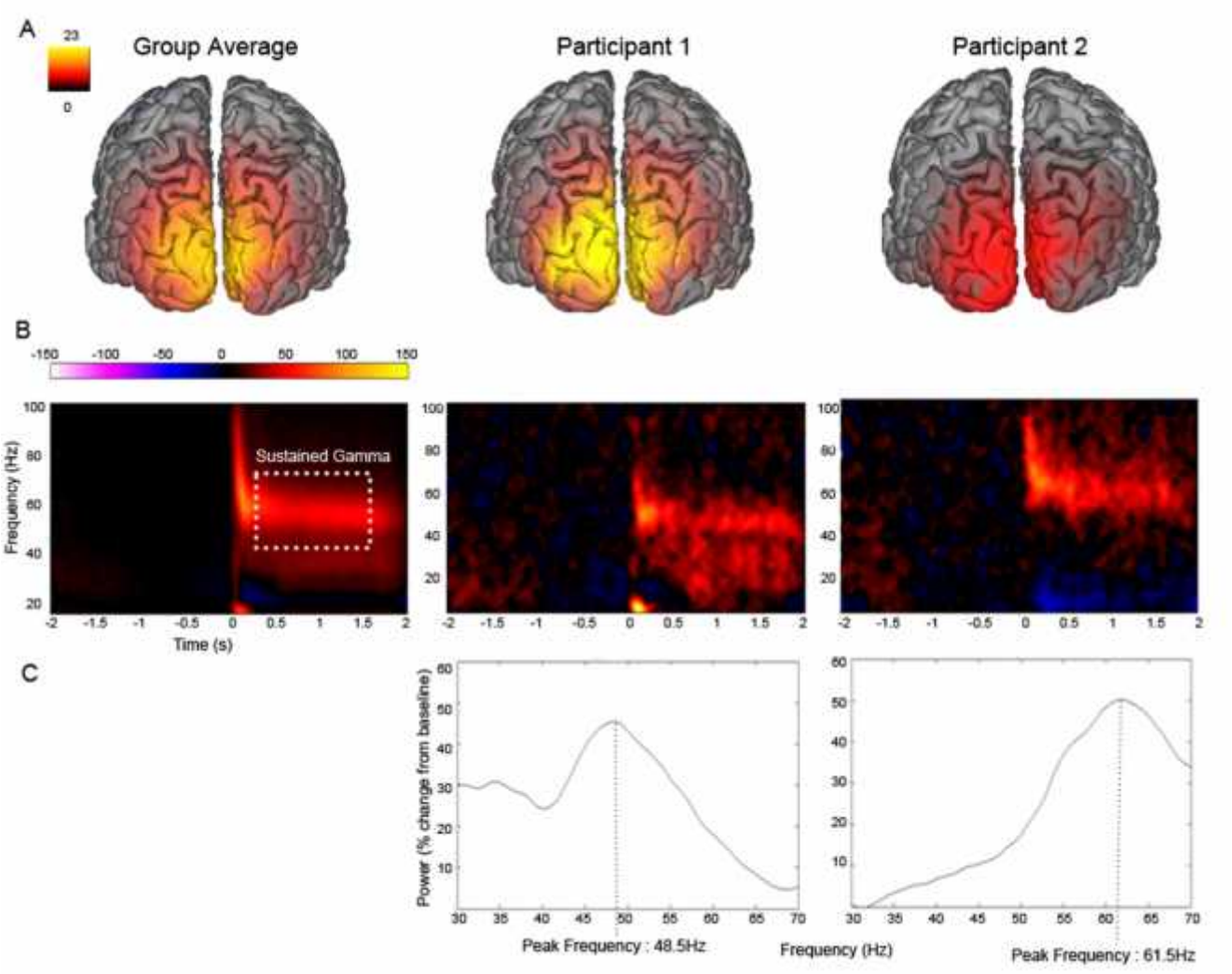

Figure 2: (A) Source localisation maps for increases in the gamma band (30-70Hz) for the group average (n=78) and 2 single participants. Images share the same scaling and units are student *t* values. (B) Grand-averaged time-frequency spectra for the group average and 2 individual participants. Spectra share the same scaling and units are % change from baseline. (C) Power-frequency plots showing the peak gamma frequency obtained from the sustained time window (0.3-1.5s).

3.4.2 Occipital GABA+ Quantification

From the 91 participants, four participants were excluded; 2 had no data available, 1 had bad quality spectra upon visual inspection and 1 was identified as an outlier (1 for GABA+/Cr and 1 different participant for GABA+/H_20). Thus, 87 participants are included in the data for both GABA+/Cr and GABA+/H_20 values. All 87 participants showed a clear resolved GABA peak at 3ppm that was well modelled by a Gaussian fit. Figure 3C shows the edited MRS spectra for 2 single participants.

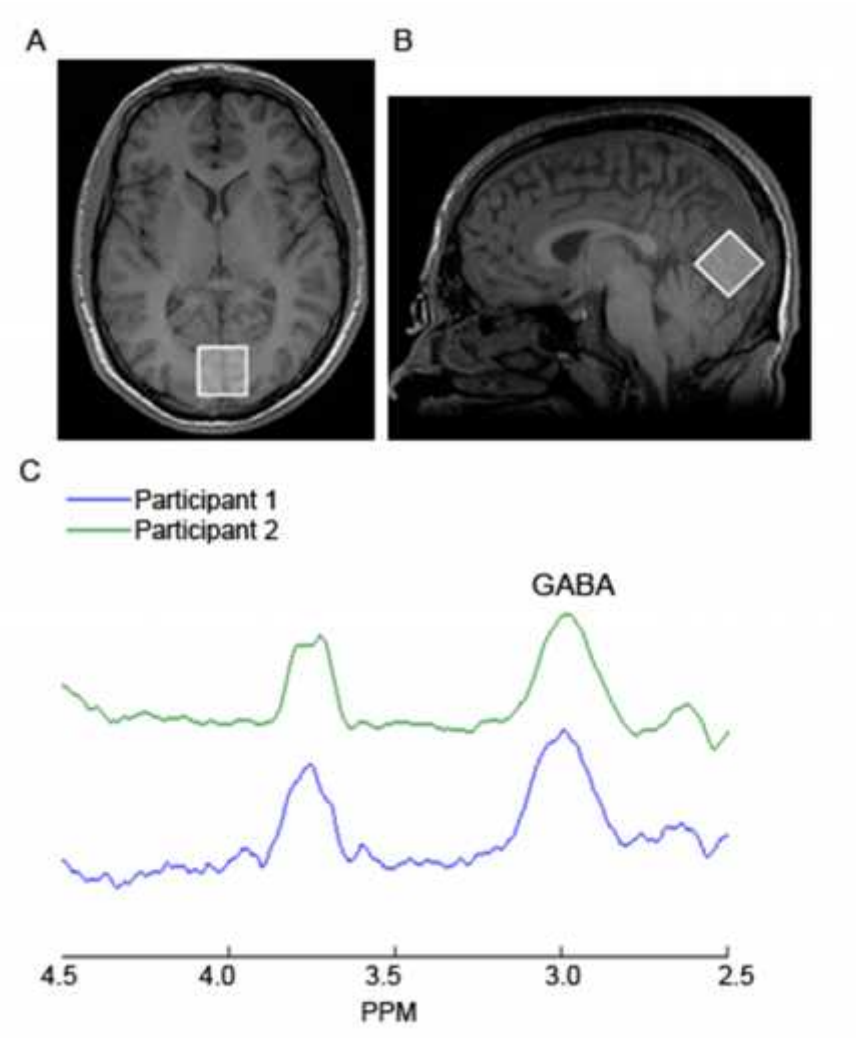

Figure 3: (A+B) Representative occipital voxel locations from 1 participant in (A) the horizontal plane and (B) the sagittal plane. (C) Representative edited MRS spectra for 2 single participants. The Gaussian-shaped GABA signal is visible at 3ppm and a co-edited Glx (glutamate and glutamine) peak is visible at 3.75ppm.

3.4.3 V1 Structural Parameters

FreeSurfer analysis of V1 calculated surface areas and cortical thickness for all participants. One participant had a cortical thickness measure that was identified as an outlier, and so was excluded from further analysis.

3.4.4 Descriptive Statistics

The descriptive statistics for the variables of interest are shown in Table 1. The variables were normally distributed apart from age which was positively skewed (+1.03).

Table 1: Descriptive statistics for the main variables of interest

	Number of participants	Minimum-Maximum	Mean	SD
Sustained Peak Gamma Frequency (0.3 to 1.5s) (Hz)	78	41.5-64.5	53.2	4.8
Age (years)	91	19-34	23.5	3.4
V1 Cortical Thickness (mm)	90	1.65-2.26	1.93	0.14
V1 Surface Area (cm^2)	91	1697.5-3318.0	2406.6	360.3
Occipital GABA+/Cr	87	0.10-0.22	0.16	0.02
Occipital GABA+/H20 (IU)	87	1.18-2.44	1.75	0.24

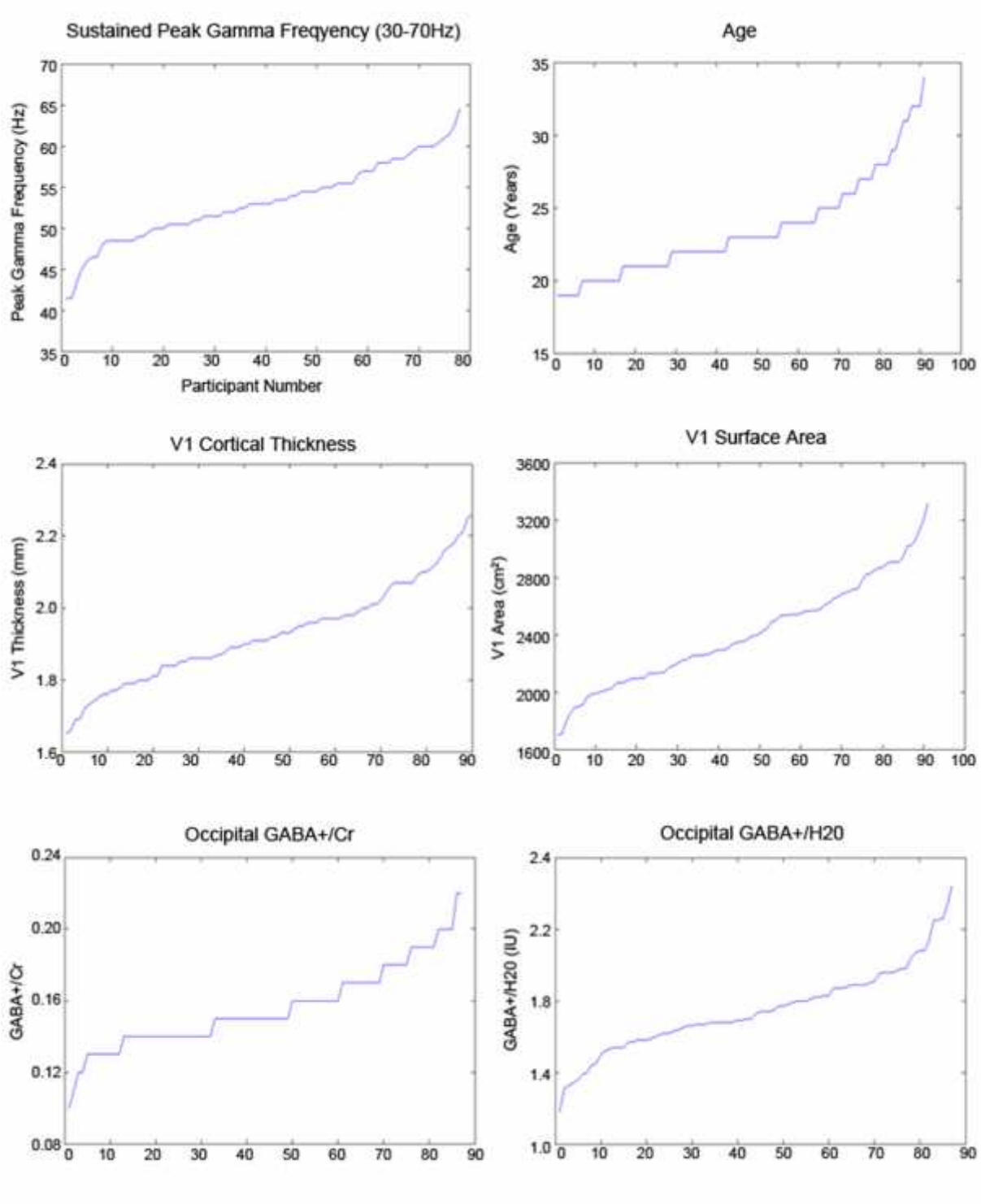

Figure 4: Sorted plots to show the distribution of the variables of interest.

3.4.5 Correlational Analysis

Table 2: Correlations between peak gamma frequency and the structural measures: cortical thickness and surface area and the neurochemical measure: GABA+.

	Peak Gamma Frequency	Age	Cortical Thickness	Surface Area	GABA+/Cr	GABA+/H_20 (IU)
Peak Gamma Frequency	1					
Age	n = 78 R = -0.115 p = 0.317	1				
Cortical Thickness	n = 78 R = -0.183 p = 0.108	n = 90 R = -0.014 p = 0.898	1			
Surface Area	n = 78 R = -0.054 p = 0.640	n = 91 R = -0.246 p = 0.019		1		
GABA+/Cr	n = 74 R = -0.047 p = 0.690	n = 87 R = -0.020 p = 0.857			1	
GABA+/H_20 (IU)	n=74 R=0.023 p=0.847	n=87 R=0.053 p=0.625				1

No significant correlations were found between peak gamma frequency and the structural parameters of V1 (cortical thickness and surface area) or the neurochemical measure, GABA+ (Table 2 and Figure 5A). To ensure that the lack of correlation between gamma frequency and GABA+/Cr was not due to using creatine as a reference, a correlational analysis was carried out using H_20 as a reference but this also produced no significant association (R=0.023, p=0.847). As age has previously been found to be a determining factor of peak gamma frequency (Gaetz *et al.*, 2012) correlational analysis was performed on these two variables but no such correlation was found in this dataset (Figure 5B). Age also showed no association with cortical thickness or GABA+ as previously reported but did negatively correlate with surface area (Figure 5B). As age was negatively correlated with surface area a

partial correlation between gamma frequency and surface area (accounting for age) was performed, to ensure that a possible correlation between gamma frequency and surface area was not masked by the age effects on surface area. Gamma frequency still showed no association with V1 surface area (R=-0.86, p = 0.458). Peak gamma power (% change from baseline) was also not associated with any of the four parameters tested (cortical thickness R=-0.011, p =0.927; surface area R=-0.060, p=0.612; GABA+/Cr R=0.150, p=0.212; GABA+/H_20 R=0.063, p =0.599).

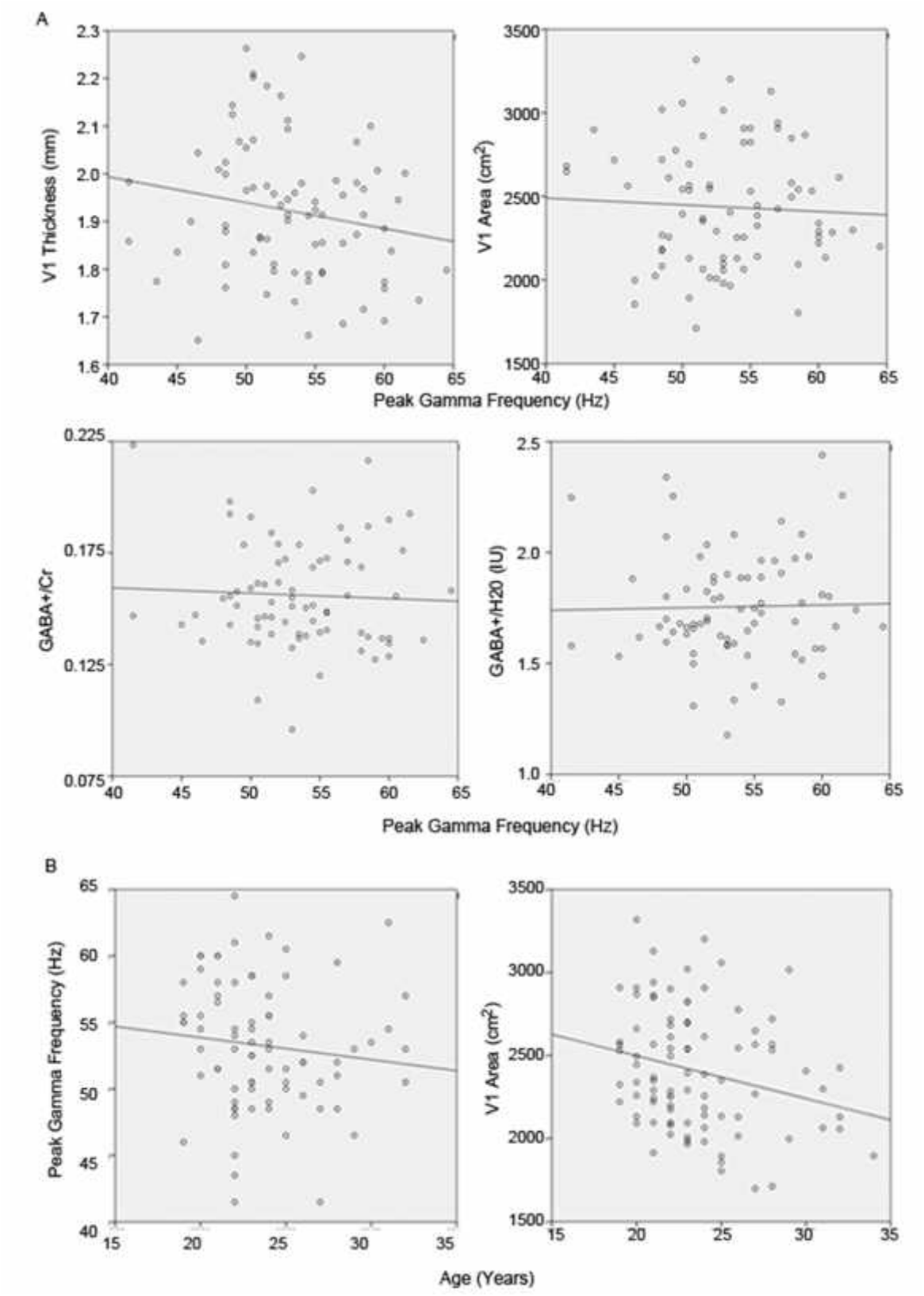

Figure 5: Scatterplots with best fit linear regression lines to investigate associations between (A) peak gamma frequency with V1 thickness, V1 area and GABA+ (B) Age and peak gamma frequency and V1 area.

3.5 Discussion

Aiming to build upon previous studies indicating that inter-individual variability in peak gamma frequency is determined by variability in the structural parameters of V1 (Muthukumaraswamy *et al.*, 2010, Schwarzkopf *et al.*, 2012) and occipital GABA+ (Muthukumaraswamy *et al.*, 2009), we investigated these associations in a large sample size of 100 healthy individuals. No correlations were found between peak gamma frequency and any of the three imaging parameters: V1 thickness, V1 surface area or GABA+ (using either creatine or water as a reference). This null finding between peak gamma frequency and GABA+ is contrary to Muthukumaraswamy et al. (2009), who found that in 12 healthy male subjects, peak gamma frequency was positively correlated with GABA+ ($R=0.68$, $p<0.02$). These opposing findings should not be due to differences in acquisition, as both used similar stimuli and analysis methods to quantify gamma and GABA+. The only two main methodological differences between the studies are the difference in size of the visual grating and the difference in gender ratio of participants. A full field grating stimulus (4 quadrants) was used in this study rather than a single quadrant grating in the lower left visual field. However, this should not have affected the results as the size of the grating has not been found to affect peak gamma frequency (Perry *et al.*, 2013). In fact, using a full field stimulus is more optimal as it produces a larger gamma response, which makes the peak gamma frequency measure more easily identifiable and robust. In terms of possible gender effects, this study had a gender ratio of 33 males: 58 females compared to all male participants. However, partial correlations (accounting for gender) also revealed no associations between gamma frequency and GABA+ or V1 structural measures. Thus, using the results from this study with a larger sample size would suggest that with the current imaging methods, peak gamma frequency and GABA+ do not correlate. This null finding is also supported by recent studies in our group and others that have used larger sample sizes (Cousijn *et al.*, 2014,

Robson, 2012, Shaw *et al.*, 2013). Together, these findings highlight the importance of using large sample sizes and identical experimental parameters.

Given the experimental and modelling evidence supporting the dependence of gamma frequency on inhibitory transmission (Sohal *et al.*, 2009), the lack of correlation between peak gamma frequency and GABA+ may depend on several factors. Firstly, the exact inhibitory components that GABA+ measurements reflect are not clear. As MRS GABA+ is quantified from a relatively large voxel size (3cm x 3cm x 3cm) the measure is likely to be combining GABA from different pools, including cytoplasmic GABA, vesicular GABA and free extracellular GABA (Stagg *et al.*, 2011b). In addition, GABA+ typically contains a 50% macromolecule contribution, making the measure less specific to GABA (Near *et al.*, 2011). Therefore, the resting MRS GABA+ quantification in this study is unlikely to reflect the specific GABAergic activity that may be most relevant to the generation of gamma oscillations such as that of parvalbumin cells. This lack of specificity may account for the lack of replication between GABA+ and gamma frequency and may need to be improved before consistent findings are reported.

Secondly, gamma frequency is determined not only by inhibitory transmission but by the balance between excitatory and inhibitory transmission in a complex neuronal and glial network (Buzsaki and Wang, 2012). However, measures of excitatory transmission through MRS Glx (a combined measure of glutamate and glutamine) have failed to find an association with gamma frequency or gamma power (Cousijn *et al.*, 2014, Muthukumaraswamy *et al.*, 2009). Thus, individual measures of GABA+ and Glx may not be reflecting the overall balance of the neural network and so measures that take into account

both excitatory and inhibitory transmission may be more appropriate to investigate their effect on gamma frequency.

The complex relationship between gamma band activity and GABA/glutamate is supported by MEG pharmacological studies that modulate GABAergic and glutamatergic transmission. Increasing endogenous GABA levels with tiagabine (blocks the GABA transporter 1 (GAT-1)) does not affect gamma frequency or the power of the response (Muthukumaraswamy *et al.*, 2013). In contrast, decreasing the excitability but increasing the inhibition of the visual cortex with alcohol (blocks the NMDAR and is a $GABA_AR$ agonist) decreases the peak frequency of the response but increases the power of the response (Campbell *et al.*, 2014). Furthermore, propofol (a $GABA_AR$ agonist) had no effect on frequency but increased the power of the response (Saxena *et al.*, 2013). These findings suggest that in the visual cortex, peak gamma frequency is more sensitive to modifications of specific components of the GABAergic and glutamatergic network. Further pharmacological studies are needed in order to identify the specific components of the GABAergic and glutamatergic system that influence the generation and maintenance of gamma oscillations.

In addition, no correlation was found between peak gamma frequency and the structural parameters of V1: thickness and surface area. This null finding between V1 surface area and peak gamma frequency contradicts that of Schwarzkopf et al. (2012) who found a positive correlation between peak gamma frequency and V1 surface area in a small cohort of 16 healthy participants (Spearman's p: R_s=0.63, p= 0.011). A possible explanation for this discrepancy could be due to the different methods used to delineate V1. In this study FreeSurfer was used to estimate the *whole* surface area of V1 whereas Schwarzkopf et al. (2012) determined the *central* surface area of V1 (includes about 50% of V1) using

functional retinotopic mapping. Therefore, the two methods may not be representing the same proportions of V1 surface area, accounting for the different results. In support of the null finding in this study, other studies using the same FreeSurfer analysis to estimate V1 surface area have found no associations between peak gamma frequency and V1 surface area (Muthukumaraswamy *et al.*, 2010, Perry *et al.*, 2013). Further independent studies using functional retinotopic mapping to define V1 will need to be conducted in order to verify the findings of Schwarzkopf et al. (2012) and determine whether this functional method is more applicable.

No relationship between peak gamma frequency and V1 thickness was found, inconsistent with a previous study reporting a positive correlation between the two variables (Muthukumaraswamy *et al.*, 2010). However, this previously reported correlation was weak ($R=0.392$, $p =<0.05$) and supporting the finding from this study, has failed to be replicated in other studies (Perry *et al.*, 2013).

Importantly, age did not correlate with peak gamma frequency, GABA+ or V1 thickness. Although age was significantly negatively correlated with surface area, this association was relatively weak. A moderately narrow age range was chosen for this study (19-34 years) in order to reduce the effects of age on the variables of interest as they are affected by age and thus the true relationship between the variables could be confounded by age. Interestingly, by reducing possible age effects the findings of the lack of correlation between the three variables surface area, thickness and GABA+ with gamma frequency coincide with the overall conclusion of other studies. Using collective data from CUBRIC with an age range of 19-45 years, Robson et al. (2012) initially found GABA+ and V1 thickness to be associated with peak gamma frequency. However, once age was accounted for, these associations no

longer remained significant. Similarly, in a separate study, V1 thickness and peak frequency have been found to correlate (R^2=0.06,p=0.06) but after accounting for age, was no longer associated (Gaetz *et al.*, 2012). Therefore, previous correlations between GABA+ and gamma frequency may have been driven by age rather than a true relationship with the two variables.

Overall, the structural and neurochemical measures investigated did not predict peak gamma frequency. This finding is supported by recent studies (Cousijn *et al.*, 2014, Shaw *et al.*, 2013). Even though none of the variables studied were found to influence peak gamma frequency, the factors driving inter-individual variability in peak gamma frequency warrant further investigation as they may help explain behavioural differences and differences in health and disease. The recent finding that peak gamma frequency is strongly genetically determined (van Pelt *et al.*, 2012) suggests that factors which are genetically controlled (such as structural and neurochemical parameters) present themselves as suitable factors to be investigated.

Chapter 4 - Effect of Genetic Variation in GAD1, the $GABA_AR$ and Schizophrenia Polygenic Risk Scores on GABA+ and Gamma Frequency

4.1 Abstract

Background: Combining genetic and neuroimaging information provides novel insights into the link between genes, neurobiology and behaviour, in both healthy and disease states. The neuroimaging measures occipital GABA+ and visual gamma peak frequency show inter-individual variation that is behaviourally and clinically important but the factors driving this variation are not clear. This study investigates the impact of genetic variants on GABA+ and gamma frequency with the aim of further understanding the biological pathways involved in these two measures and their implication in schizophrenia.

Methods: Neuroimaging data (occipital GABA+ and visual gamma frequency) and genome-wide genotype data was obtained from a group of 100 healthy individuals who participated in a large genetic imaging study. The effect of genetic variation on GABA+ and gamma frequency was assessed in three ways: (1) testing the association between eight candidate *GAD1* SNPs with GABA+ and gamma frequency (2) testing the association between ten candidate SNPs in genes encoding $GABA_AR$ subunits with GABA+ and gamma frequency and (3) testing the association of schizophrenia polygenic risk scores with occipital GABA+ and gamma frequency.

Results: Three of the eight *GAD1* SNPs (rs10432420, rs3749034 and rs2241165) showed an association with occipital GABA+/Cr, in which individuals with the schizophrenia risk associated SNP had lower GABA+/Cr levels. None of the eight *GAD1* SNPs significantly impacted gamma frequency and none of the $GABA_AR$ genes or polygenic risk scores showed an association with either the GABA+ or gamma frequency measure.

Conclusion: This study adds further support for the involvement of genetic variants within *GAD1* and *in vivo* GABA levels. Studies using larger sample sizes are needed to reinforce these findings and to determine the genetic variants driving variability in visual gamma peak frequency.

4.2 Introduction

Genetic imaging is an encouraging research field that studies how individual genetic differences lead to differences in brain structure/function and behaviour (Linden, 2012). This is providing novel insights into the biological mechanisms underlying neuroimaging measures and how these are linked to behaviour and/or disease. Genetic imaging has been widely applied in psychiatry, as psychiatric disorders have a strong genetic basis and the neural mechanisms underlying these disorders are still poorly understood (Sullivan *et al.*, 2012). Most of these studies have employed a candidate approach, in which the impact of a single genetic variant from a biologically relevant system is assessed (Meyer-Lindenberg, 2010b). While providing insights into the downstream effects of the genetic variant, the usefulness of the single candidate approach for understanding psychiatric disorders as a whole is not clear. This is because the combined effect from thousands of common genetic variants, rather than from one single variant are thought to predispose individuals to psychiatric disorders (Purcell *et al.*, 2009). Thus, with the advent of efficient genome-wide genotyping, the genome-wide association study (GWAS) approach is also being used. This hypothesis-free method tests the impact of the entire genome on the neuroimaging measure and has the potential for implicating new genetic variants and thus new biological pathways (Potkin *et al.*, 2009a). However, this method is limited by the need to correct for multiple comparisons and so to reduce the problem of multiple testing but still incorporate the effects of multiple genes, a new polygenic risk score approach has been devised (Purcell *et al.*,

2009). The polygenic risk score reflects an aggregate measure of common variants that are associated with the disorder of interest and tests for the effects of these risk alleles on the imaging measure.

In the candidate gene, GWAS and polygenic risk score imaging approach, the structural or functional brain imaging measure is used as an intermediate phenotype (endophenotype) (Gottesman and Gould, 2003). The imaging phenotype is proposed to be closer to the underlying biological etiology than the heterogeneous diagnosis of a psychiatric disorder. This means that it should be easier to identify the genes underlying the disorder and the method will have greater statistical power, so a smaller sample size is needed (Potkin *et al.*, 2009b).

The neuroimaging measures occipital GABA+ and visual gamma peak frequency are valid endophenotypes in which to investigate how genetic variation influences their individual variability. Visual gamma peak frequency is a stable and repeatable measure (Muthukumaraswamy *et al.*, 2010) that has recently been shown to be highly heritable via a twin study (van Pelt *et al.*, 2012) and visual gamma oscillations are often perturbed in schizophrenia (Grützner *et al.*, 2013, Sun *et al.*, 2013, Tan *et al.*, 2013). Similarly, occipital MRS GABA+ is a measure that is repeatable over time (Near *et al.*, 2014), under genetic control (Hasler and Northoff, 2011) and altered in schizophrenia (Yoon *et al.*, 2010). Thus, assessing the impact of genetic variants on these two measures, will determine whether genetic variants may be implicated in the downstream effects of individual variability in GABA+ and gamma oscillatory activity, which may subsequently be important biomarkers for schizophrenia. This study will also allow us to further disentangle the relationship between these two neuroimaging measures by determining whether similar genetic variants

produce similar effects on both. Three different approaches were used to test the impact of genetic variation on individual differences in GABA+ and gamma peak frequency, two of which are candidate gene approaches - investigating single nucleotide polymorphism (SNP) and a gene-wide approach, and the third was a schizophrenia polygenic risk score approach.

The first approach assesses the impact of SNPs in *glutamic acid decarboxylase 1 (GAD1)* on occipital GABA+ and visual gamma peak frequency. *GAD1* is located on chromosome 2q31, spans about 45kb and consists of 17 exons. Importantly, *GAD1* encodes glutamic acid decarboxylase 67 (GAD67), the major enzyme for synthesising cortical GABA by catalysing glutamate to GABA. GABA can also be synthesised by the GAD65 enzyme (encoded by the *glutamic acid decarboxylase 2(GAD2)* gene) but *GAD2* is primarily activated in times of high GABA demand (Martin *et al.*, 1991). The importance of *GAD1* in producing GABA has been demonstrated via gene knockout studies, as *GAD1 -/-* mice have substantially reduced GABA levels and die at birth (Asada *et al.*, 1997). In contrast, *GAD2 -/-* mice showed no significant difference in GABA levels and appeared healthy. Furthermore, genetic variation in *GAD1* is associated with *in vivo* MRS GABA+ levels (Marenco *et al.*, 2010). The effect of *GAD1* SNPs on MRS GABA+ levels may be mediated via its effect on transcriptional regulation, as *GAD1* SNPs have been associated with *GAD1* mRNA levels (Straub *et al.*, 2007). Establishing the effect of genetic variation in *GAD1* on GABA+ and gamma frequency is clinically relevant, as *GAD1* SNPs have been associated with schizophrenia (Addington *et al.*, 2005, Du *et al.*, 2008, Lundorf *et al.*, 2005, Straub *et al.*, 2007) and reduced *GAD1* mRNA expression from post-mortem brain tissue is one of the most consistent findings in schizophrenia individuals (Hashimoto *et al.*, 2008, Thompson *et al.*, 2009). In conjunction, the *GAD1* mRNA deficits are especially pronounced in parvalbumin neurons (Curley *et al.*, 2011, Hashimoto *et al.*, 2003), an interneuron cell-type that is specifically important for

gamma activity (Sohal *et al.*, 2009). Therefore, investigating the effects of genetic variations within *GAD1* is biologically valid for both GABA+ and gamma.

The second approach assesses the contribution of genetic variation in genes encoding $GABA_A$ receptor ($GABA_AR$) subunits on GABA+ and gamma frequency. $GABA_AR$ are the major inhibitory receptors in the central nervous system (CNS) and mediate the fast neurotransmission of GABA in the CNS. The receptors are ligand-gated chloride ion channels and are made up of five subunits, each of which has several isoforms (α1–6, β1–3, γ1–3, δ, ϵ, θ, and π) (Barnard *et al.*, 1998, Olsen and Sieghart, 2008). Most receptors consist of 2 α's, 2 β's and 1 γ subunit. The genes for these three main receptor subunit types (α, β and γ) cluster in three chromosomal regions, on chromosome 4, 5 and 15. Variants from these three subunit genes (*GABRG1*, *GABRA2*, *GABRA4*, *GABRB1*, *GABRB2*, *GABRA1*, *GABRG2*, *GABRB3*, *GABRA5* and *GABRG3*) have been chosen for this analysis. Differences in the subunit composition affect the functional properties and pharmacology of the receptor (Olsen and Sieghart, 2009). Therefore, SNPs in these subunits may also alter the functionality and pharmacology of the receptor, leading to changes in GABA and gamma activity. Variation in the function of the $GABA_AR$ is particularly relevant in the context of gamma oscillations as gamma activity relies on the fast activation and kinetics of the $GABA_AR$ (Buzsaki and Wang, 2012, Whittington *et al.*, 2011, Whittington *et al.*, 1997). In addition, modulation of the $GABA_AR$ via alcohol (an agonist of the $GABA_AR$) decreases visual gamma peak frequency (Campbell *et al.*, 2014). In terms of clinical relevance, alterations in the expression of a range of $GABA_AR$ subunits have been implicated in schizophrenia (Benham *et al.*, 2014). Several SNPs in the α and β subunit of the $GABA_AR$ have been associated with schizophrenia (Lo *et al.*, 2004, Petryshen *et al.*, 2005) and these SNPs were hypothesised to be functionally relevant in predisposing to schizophrenia as they affect $GABA_AR$ mRNA expression levels.

Whether variation in $GABA_AR$ subunit SNPs/genes consequently leads to alterations on *in vivo* GABA levels and gamma oscillations has yet to be investigated.

Lastly, the third approach determines whether schizophrenia polygenic risk scores predict GABA+ and gamma frequency. Schizophrenia polygenic risk scores were chosen as GABAergic dysfunction is a well-known feature of schizophrenia (Gonzalez-Burgos *et al.*, 2010) and the polygenic score may reflect alterations in the GABAergic pathways. The polygenic risk score approach is a relatively new concept but of the few reported studies, this approach is providing promising results. For example, Walton et al. (2013) reported a positive relationship between schizophrenia risk score and left DLPFC inefficiency during working memory processing (Walton *et al.*, 2013). In addition, Whally et al. (2012) found bipolar affective disorder risk score to be associated with increased activation in limbic regions during an executive processing task (Whalley *et al.*, 2012).

Therefore, the aim of this study was to use three promising genetic imaging approaches to provide novel insights into the link between genetic variants, variability in GABA+ and gamma frequency and schizophrenia.

4.3 Methods:

4.3.1 Participants

The imaging and genetic data in this study was obtained from the homogenous group of 91 healthy participants (described in Chapter 3) that took part in the '100 Brains' study. The 91 subjects consisted of 33 males and 58 females and were aged between 19-34 years (mean 23.5, SD 3.4). All subjects were healthy, Caucasian, right-handed and had completed or were completing a university bachelor's degree. All individuals were of Caucasian ethnicity

because ethnic matching is vital in genetic imaging (Hariri and Weinberger, 2003). Out of the 91 participants, following imaging quality control procedures, GABA+ data was available for 87 participants and gamma frequency data for 78 participants (Chapter 3). Genetic data was available for 87 of the 91 participants as one subject did not provide a saliva sample and three were excluded due to low genotyping completeness.

4.3.2 Gamma Frequency and GABA+ Acquisition

Details of gamma frequency and GABA+ acquisition are provided in Chapter 3. Briefly, participants viewed an optimised high-contrast square-wave grating to induce visual gamma oscillations in the occipital cortex. Gamma band oscillations were localised to the visual cortex using synthetic aperture magnetometry (SAM) (Robinson and Vrba, 1999) and a virtual sensor was placed at the location of peak gamma activity. Time-frequency analysis was performed using the Hilbert transform to create time- frequency spectra. From the resulting spectra, the induced peak gamma frequency over the sustained time window (0-1.5s) was obtained for each individual.

GABA+ was quantified in a 3cm x 3cm x 3cm voxel optimally placed in the occipital cortex. GABA spectra were acquired using a MEGA-PRESS sequence and GABA+ was quantified using GANNET (http://gabamrs.blogspot.co.uk/). The GABA peak at 3.0ppm in the difference edited spectrum was fitted with a single Gaussian model. To reduce multiple testing, analyses were conducted using GABA+ concentrations quantified using creatine as an internal concentration reference as creatine has been shown to be more repeatable than using water as the internal reference (Bogner *et al.*, 2010). However, to ensure the reliability of any significant findings for GABA+/creatine were not due to using creatine as a reference,

post-hoc analysis using water as an internal reference (GABA+/H_20 (IU)) was subsequently tested.

4.3.3 Genotyping

Genomic DNA was obtained from saliva using Oragene OG-500 saliva kits. Genotyping was performed using custom Illumina HumanCoreExome-24 BeadChip genotyping arrays which contain 570,038 genetic variants (Illumina, Inc., San Diego, CA). Standard genotype quality control (QC) procedures were implemented using PLINK v1.07 (Purcell *et al.*, 2007). Individuals were excluded for ambiguous sex, cryptic relatedness up to third degree relatives ascertained using identity by descent, genotyping completeness less than 97%, and non-European ethnicity admixture detected as outliers in iterative EIGENSTRAT analyses of an LD-pruned dataset (Price *et al.*, 2006). SNPs were excluded where the minor allele frequency was less than 1%, if the call rate was less than 98% or if the $\chi 2$-test for Hardy-Weinberg Equilibrium had a p-value less than 1 e-04. Individuals genotypes were imputed using the pre-phasing/imputation stepwise approach implemented in IMPUTE2/SHAPEIT (Delaneau *et al.*, 2012, Howie *et al.*, 2011) and 1000 Genomes (1000 Genomes haplotypes Phase I integrated variant set release, December 2013) as the reference dataset. Details of the subsequent acquisition and analysis for the three genetic approaches are detailed below.

4.3.4 Candidate SNP Approach

Following standard quality control of the genetic data, four *GAD1* SNPs that were genotyped using the Illumina chip remained for analysis: rs2241165, rs3828275, rs701492, rs16858988. In addition, the genotypes for four *GAD1* SNPs (rs1043240, rs1978340, rs3749034, rs769390) that have previously been shown to impact GABA+ (Marenco *et al.*, 2010) and/or are associated with schizophrenia (Addington *et al.*, 2005, Lundorf *et al.*, 2005, Straub *et al.*,

2007) were available through imputation with high quality scores (imputation quality more than 0.9). Genotype imputation predicts the genotype for SNPs that are not directly genotyped by using genetic data from those that are directly genotyped on the chip (Marchini and Howie, 2010). Thus, a total of eight *GAD1* SNPs were analysed. Although two pairs of SNPs (rs2241165 and rs3749034; rs769390 and rs701492) were in strong linkage disequilibrium (LD) (r^2 >0.8), all SNPS were kept for analysis. The effect of these eight SNPs on gene expression in the primary visual cortex was assessed using the brain eQTL Almanac (Braineac) (Ramasamy *et al.*, 2014). Braineac is a web-based resource that contains data from 134 healthy Caucasian post-mortem brains to determine whether a gene or SNP is operating as an expression quantitative trait loci (eQTL), meaning altering the mRNA levels of the gene. Detailed information for the eight SNPs is provided in Table 1.

Table 1. Summary of the Genotyped and Imputed *GAD1* SNPs

dbSNP ID	Base Position on chromosome 2[1]	Location within gene	Allele (major/minor)	Schizophrenia Risk Associated Allele	Effect of Risk Associated allele on mRNA expression[2]
rs10432420	171660312	5'flanking	G/A	G	G increased expression
rs1978340	171670121	5'flanking	G/A	A	A increased expression
rs3749034	171673475	5'UTR	G/A	G	G increased expression
rs2241165	171678379	Intron 2	A/G	A	A increased expression
rs3828275	171682740	Intron 3	G/A	N/A	A lowered expression
rs769390	171693455	Intron 6	A/C	C	C increased expression
rs701492	171702480	Intron 9	G/A	N/A	A increased expression
rs16858988	171702960	Intron 10	G/A	N/A	A increased expression

[1]Position According to National Center for Biotechnology Information (NCBI, September, 2014). [2]For the three SNPs which have not been associated with schizophrenia the effect of the minor allele on mRNA expression is reported.

The effect of genetic variation in *GAD1* on GABA+ and gamma frequency was tested with linear regression analyses using an additive genetic model and a recessive genetic model (post-hoc analysis) in PLINK (Table 2). The additive model assumes that for each copy of the minor allele there is a uniform, linear increased impact on the phenotype. The recessive model assumes that two copies of the minor allele are needed to alter the phenotype, so individuals homozygous for the minor allele are compared to individuals homozygous for the major allele and heterozygotes. A recessive model was performed for three SNPs post-hoc as figures displaying GABA+ levels according to genotype group suggested a recessive effect (Figure 1) and previous studies have shown *GAD1* SNPs to have recessive effects (Marenco *et al.*, 2010). As age, gender and V1 structural parameters were not found to affect gamma frequency in this dataset (Chapter 3) we did not need to co-vary for these variables. In addition age, gender and GM fraction are not associated with GABA+ in this dataset and so were not added as covariates in the linear regression analyses.

4.3.5 Aggregate SNP (gene-level) Approach

SNPs from the $GABA_AR$ subunit genes lying in clusters on chromosomes 4, 5 and 15 that had been genotyped on the chip, in the 87 individuals were extracted for analysis. Genotype data was available for 187 SNPs, which grouped onto ten $GABA_AR$ subunit genes (Table 3). SNPs from all ten genes were included as all ten $GABA_AR$ subunit genes are highly expressed in the occipital cortex. To assess the impact of these set of SNPs from the $GABA_AR$ subunit gene on GABA+ and gamma frequency, a gene-based approach was performed using a sequence kernel association test (SKAT) within the SKAT package (Wu *et al.*, 2010, Wu *et al.*, 2011) in R (R Development Core Team, 2013). SKAT is a flexible test for the joint effects of multiple SNPs in a region (gene) on a phenotype (Wu *et al.*, 2011). The test uses a multiple regression model to regress the phenotype on genetic variants in a

region and on covariates. This allows for different variants to have different directions and magnitude of effects, including no effects.

4.3.6 Polygenic Scoring Approach

Five individual polygenic schizophrenia risk scores were computed using the score function in PLINK (Purcell *et al.*, 2007). SNPs to include in the score were selected from the Psychiatric GWAS Consortium (PGC2) database for schizophrenia (https://pgc.unc.edu/), with a statistical threshold of P ≤0.5, P ≤0.3, P ≤0.1, P ≤0.01 and P ≤0.0001. The PGC2 schizophrenia database contains genome-wide genetic data for 36, 989 schizophrenia subjects and 113,075 controls (Consortium, 2014). The polygenic score was calculated as the sum of the number of susceptibility alleles weighted by the logarithm of the corresponding odds ratios (ORs) from the schizophrenia case-controls study performed by PGC2. Linear regressions were performed in SPSS by regressing the polygenic risk score against the phenotypes GABA+ and gamma frequency.

Acknowledgements for data analysis

Special thanks to Kathryn Tansey for helping with the genetic analysis.

4.4 Results

4.4.1 Impact of Variation in GAD1 SNPs

Using the additive genetic model, variation in one SNP (rs2241165) was significantly associated with GABA+/Cr levels (p=0.024) and two SNPs (rs10432420 and rs3749034) showed a trend towards significance (p=0.057 and p=0.067, respectively, Table 2). Plotting GABA levels by genotype group for these three SNPs suggested a recessive effect of the minor allele on GABA+/Cr (Figure 1) and so post-hoc analysis with the recessive model was

performed for these three SNPs. Rs10432420 was associated with GABA+/Cr under a recessive model ($p=1.58*10^{-4}$). Only the association between rs10432420 and GABA+/Cr using the recessive model remained significant after correcting for multiple comparisons ($p<0.05$). To ensure the findings were not due to using creatine as a reference, the effect of genotype on GABA+/H_20 values was also assessed. This revealed a similar direction of effect of these three *GAD1* SNPs on GABA+/H_20 but was not significant using either the additive or recessive model. Figure 1 shows the direction of effect on GABA+/Cr and GABA+/H_20 by genetic variation in these three *GAD1* SNPs. None of the SNPs had a significant effect on gamma frequency with the additive model ($p>0.05$, Table 2).

Table 2: Effect of Variation in *GAD1* SNPs on GABA+ and Gamma Frequency

	GABA+/Creatine					**GABA+/H20**				**Gamma Frequency**		
		Additive Model		Recessive Model		Additive Model		Recessive Model			Additive Model	
GAD1 SNP	N	Beta (SE)	P	Beta (SE)	P	Beta (SE)	P	Beta (SE)	P	N	Beta (SE)	P
rs10432420	80	0.214 (0.111)	0.057	0.410 (0.103)	**$1.58*10^{-4}$**	0.103 (0.113)	0.366	0.172 (0.112)	0.129	73	-0.079 (0.118)	0.504
rs1978340	76	-0.039 (0.116)	0.738							70	0.037 (0.121)	0.760
rs3749034	82	0.203 (0.110)	0.067	0.255 (0.108)	**0.021**	0.114 (0.111)	0.309	0.075 (0.112)	0.505	76	-0.085 (0.116)	0.465
rs2241165	83	0.248 (0.108)	**0.024**	0.245 (0.108)	**0.025**	0.117 (0.110)	0.291	0.073 (0.111)	0.510	76	-0.086 (0.116)	0.460
rs3828275	83	-0.096 (0.111)	0.388							76	0.052 (0.116)	0.657
rs769390	78	-0.105 (0.114)	0.359							72	0.005 (0.120)	0.966
rs701492	83	-0.035 (0.111)	0.753							76	0.079 (0.116)	0.498
rs16858988	83	-0.050 (0.111)	0.651							76	-0.022 (0.116)	0.852

Beta is the regression coefficient. Beta values are standardised to enable comparison across SNPs and across GABA+ and gamma frequency. SE is the standard error of the Beta. P values are uncorrected for multiple comparisons (bold = $p<0.05$).

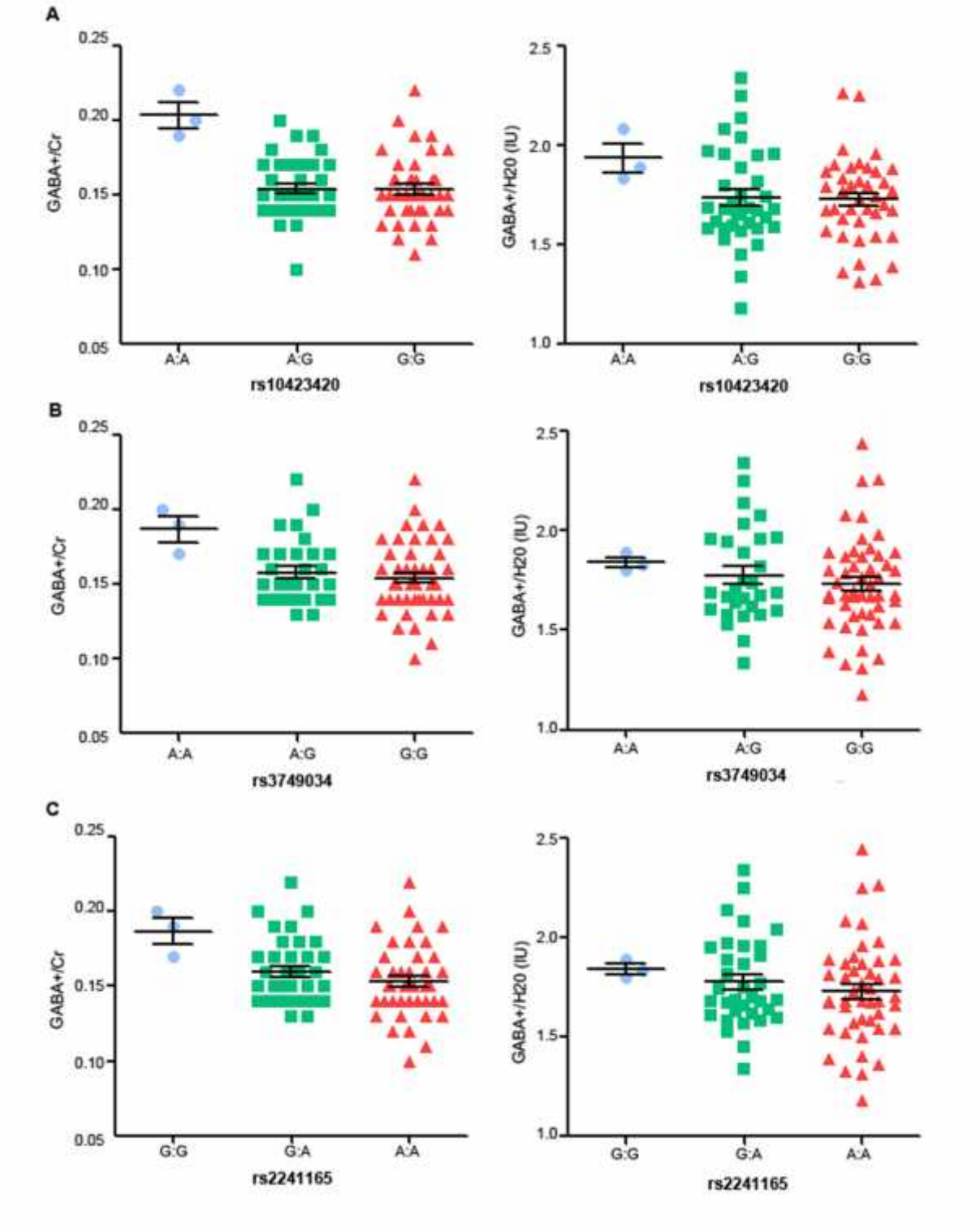

Figure 1: Effect of *GAD1* genotype on GABA+/Cr and GABA+/H_20 for (A) rs10423420 (B) rs3749034 and (C) rs2241165. Black lines represent the genotype group mean and standard error of the mean.

All three *GAD1* SNPs show the same direction of effect on GABA+/Cr, in which individuals with the schizophrenia risk associated allele, (G for rs10423420 and rs379034 and A for rs2241165) have decreased levels of GABA+/Cr. Post-hoc analysis reveals a recessive effect of the minor allele as individuals homozygous and heterozygous for the major allele (the risk associated allele) have decreased levels of GABA+/Cr in comparison to the group homozygous for the minor allele. For rs2241165, the A:A and G:A groups have decreased levels of GABA+/Cr in comparison to the G:G genotype, for rs1043240, the G:G and A:G groups have decreased GABA+/Cr in comparison to the A:A group and for rs3749034, the G:G and A:G group have decreased levels of GABA+/Cr in comparison to the A:A genotype. Although non-significant, a similar pattern can be seen for GABA+/$H_2$0, in which individuals with the risk associated allele have lower GABA+/$H_2$0 levels.

4.4.2 Impact of Variation in GABA$_A$R Subunit Genes

None of the 10 GABA$_A$R subunit genes had a significant association with GABA+/Cr or gamma frequency.

Table 3. Effect of GABA$_A$R Subunit Genes on GABA+ and Gamma Frequency

Gene	Chromosome	GABA$_A$ Receptor Subunit	Number of SNPs	GABA+/Cr n=83	Gamma Frequency n=76
				P	P
GABRG1	4	γ_1, gamma-1	5	0.578	0.468
GABRA2	4	α_2, alpha-2	9	0.890	0.110
GABRA4	4	α_4, alpha-4	5	0.465	0.407
GABRB1	4	β_1, beta-1	30	0.446	0.349
GABRB2	5	β_2, beta-2	14	0.323	0.606
GABRA1	5	α_1, alpha-1	3	0.683	0.638
GABRG2	5	γ_2, gamma-2	8	0.227	0.862
GABRB3	15	β_3, beta-3	44	0.800	0.221
GABRA5	15	α_5, alpha-5	5	0.626	0.096
GABRG3	15	γ_3, gamma-3	64	0.477	0.984

4.4.3 Impact of Schizophrenia Polygenic Risk Score

Schizophrenia polygenic risk score using any of the five training p-value thresholds was not significantly associated with GABA+/Cr or gamma frequency.

Table 4 Effect of schizophrenia polygenic risk score on GABA+/Cr and gamma frequency.

Training SNP threshold level[1]	Number of SNPs included in Schizophrenia Risk Score	GABA+/Cr		Gamma Frequency	
		R^2	P	R^2	P
$P \leq 0.0001$	914	0.004	0.579	0.021	0.209
$P \leq 0.01$	6032	0.000	0.979	0.047	0.059
$P \leq 0.1$	22263	0.007	0.467	0.036	0.099
$P \leq 0.3$	43488	0.004	0.573	0.033	0.115
$P \leq 0.5$	59226	0.003	0.626	0.028	0.146

[1] Training SNP threshold level obtained from the PGC2 schizophrenia study.

4.5 Discussion

Three different genetic imaging approaches consisting of a candidate SNP approach with *GAD1* SNPs, a candidate gene-based approach with $GABA_AR$ genes and a schizophrenia polygenic risk score approach were used to assess the influence of genetic variation on occipital GABA+ and visual gamma peak frequency. The candidate SNP approach revealed an association between three of the eight *GAD1* SNPs and occipital GABA+/Cr (Table 2). As all three SNPs are in strong or moderate LD with one another ($r^2>0.5$), they may be reflecting a common effect. Using the additive model, rs2241165 reached nominal statistical significance (p=0.024) and rs10432420 and rs3749034 showed a strong trend towards nominal significance (p=0.057 and p=0.067). Post-hoc analysis revealed that the minor A allele for two of these SNPs (rs10432420 and rs3749034) may have recessive effects as the recessive model increased the significance of the two SNPs from a strong trend to statistical significance ($p<0.05$). This is in contrast to a previous study which found a recessive effect

for the major G allele (associated with risk for schizophrenia) of rs3749034 on cortical thickness in the left parahippocampal gyrus (PHG) (Brauns *et al.*, 2013). The difference in the A minor allele having recessive effects in this study rather than the G major allele in Brauns et al. (2013) could be due to a number of differences between the two studies. Firstly, the recessive effect was found in different imaging measures (GABA+/Cr vs cortical thickness) and in different cortical areas (occipital vs PHG). Thus, major and minor alleles may have opposing effects depending on the imaging measure or the region in which they are obtained. Secondly, the differential findings could be due to the low number of individuals in the homozygous minor A allele group in this study (n=3) leading to unreliable results.

To test the robustness of these *GAD1* findings and ensure their specificity to GABA rather than using creatine as a reference, the impact of these three significant SNPs on GABA+/H_20 was also tested and although were not found to be significant, did reveal a similar pattern (Figure 1). This discrepancy in results between using creatine and water as a reference reflects the inherent 'noise' present in the GABA+ measure and highlights the small effects of single genetic variants. However, as the effect of the three *GAD1* SNPs show a similar pattern with both measures, the results are still highly viable and require further investigation.

Encouragingly, the direction of effect of the risk associated alleles was as expected and was present in all three SNPs. Individuals with the schizophrenia risk associated allele (homozygous and heterozygous) had decreased GABA+/Cr levels in comparison to those homozygous for the minor allele. This finding compliments the theory of decreased GABAergic function in schizophrenia, due to findings of decreased *GAD1* mRNA (Thompson Ray *et al.*, 2011), decreased GAD67 protein (Curley *et al.*, 2011) and decreased GABA levels (Yoon *et al.*, 2010) in clinical schizophrenia populations. However, this clear

directional effect of schizophrenia risk alleles leading to reduced *GAD1* mRNA, GAD67 protein and GABA was not present in this study as the three significant risk associated alleles reported here are associated with increased *GAD1* mRNA expression in the occipital cortex (Table 1). A pharmacological study supports this uncertain directional relationship between these components as inhibition of GABA transaminase (enzyme that metabolises GABA) increases cortical GABA levels but decreases GAD67 protein (Mason *et al.*, 2001). The reason for this dissociation between GAD67 protein and GABA could be due to *GAD1* mRNA expression being activity regulated (Benson *et al.*, 1994) and if GABA metabolism is reduced (increases GABA) this could lead to decreased *GAD1* expression and GAD67 protein. Conversely, as possible in this study if *GAD1* mRNA and GAD67 protein is increased, this could lead to decreased GABA levels. To add to this issue, this study was performed in healthy individuals and thus the discrepancy between these variables could be due to differences between healthy and schizophrenia individuals. Furthermore, measures obtained from chronic schizophrenia patients can often be confounded by other factors such as medication, difference in lifestyle and an increased prevalence of smoking, which may lead to findings that are not directly specific to schizophrenia itself (Meyer-Lindenberg, 2010a, Tomelleri *et al.*, 2009).

In contrast to our findings, the only other study to investigate genetic variation in *GAD1* on GABA+, reported two *GAD1* schizophrenia risk associated SNPs to be associated with increased MRS GABA levels in the anterior cingulate cortex of healthy individuals (Marenco *et al.*, 2010). This directional effect in the anterior cingulate cortex was unexpected and was described as being due to a compensatory change following reduced GABA production. The compensatory change was hypothesised to be due to excessive production of GABA by the GAD65 enzyme (encoded by *GAD2*) or decreased catabolism by GABA transaminase. These

are valid theories to explain the unexpected association between risk alleles and increased GABA levels and highlight the fact that GABA levels do not solely depend on the activity of *GAD1* but a number of regulatory systems. The two significant *GAD1* SNPs (rs1978340 and rs769390) reported in Marenco et al. (2010) were also tested in this study and were not found to be associated with occipital GABA levels. These contrasting findings, in terms of the direction of effect and the difference in significant SNPs may be due to the difference in cortical regions studied. SNP effects may be regional specific and compensatory mechanisms may be more prevalent in certain cortical areas. Overall, these findings suggest a complex interaction between the *GAD1* gene, mRNA, protein, GABA and schizophrenia. However, both this study and that of Marenco et al. (2010) do support the involvement of genetic variation in *GAD1* influencing the functional MRS GABA measure, which is clinically important. Further studies will need to be performed in both healthy individuals and those with schizophrenia to disentangle the complex links between these biological mechanisms.

Although the exact mechanisms by which the risk associated alleles alter occipital GABA+ levels are unknown, a strong hypothesis would be through their effect on gene expression as all three SNPs were associated with changes in gene expression (Table 2). Supporting this, the three SNPs with the strongest effect on gene expression also had the strongest effect on GABA+ levels, suggesting a link between gene expression and the functional GABA+ measure. Importantly, these three *GAD1* SNPs are not located in protein coding regions but are in the regulatory elements of the gene. Therefore, they do not affect the amino acid sequence of the protein but play an important role at the transcriptional and translational level to control gene expression (Veyrieras *et al.*, 2008). Rs10432420 is located in the 5' flanking region, a region that is not transcribed into mRNA but is important in the transcription process as it contains the promoter, other enhancers and protein binding sites. Rs3749034 lies

in the 5' untranslated region (5'UTR) of *GAD1*, an area that is transcribed into mRNA and may affect the efficiency of the transcription and translation process (Mignone *et al.*, 2002). Specifically, the risk associated G allele of rs3749034 causes the loss of two putative transcription factor binding sites (the ATP1A1 regulatory element binding factor 6 and the myoblast determining factor) which may disrupt GABAergic transmission (Addington *et al.*, 2005, Cherlyn *et al.*, 2010). Rs2241165 is located in intron 2 and although introns are removed during the transcription process to form mature mRNA, they can affect the initial transcription of the gene, polyadenylation of the pre-mRNA and the decay of mRNA (Le Hir *et al.*, 2003, Nott *et al.*, 2003). Therefore, these SNPs may affect gene expression through their effect at various genetic stages including transcription, mRNA splicing, polyadenylation, mRNA export, translational efficiency and mRNA decay. This finding of regulatory elements affecting GABA+ reveals that these SNPs are functionally important and is in keeping with the growing evidence that regulatory sequences play an important part in psychiatric disorders (Cooper, 2010, Hindorff *et al.*, 2009).

In comparison to the finding of an association between *GAD1* SNPs and GABA+, no effect of these SNPs was found on visual gamma peak frequency (Table 2). This suggests that variation in *GAD1* does not play a major role in determining peak gamma frequency. As the relationship between *GAD1* and gamma may be weaker than that between *GAD1* and GABA, a larger sample size is needed to further explore this. The lack of association also adds further evidence that *in vivo* GABA concentration estimates and gamma peak frequency are not as strongly associated as previously thought (Chapter 3). However, there is still strong experimental evidence for a prominent role of GABAergic function in the generation of gamma oscillations (Buzsaki and Wang, 2012, Cardin *et al.*, 2009, Chen *et al.*, 2014). It may be that genetic variants that influence the function of other components of the GABAergic

system such as GAT-1, VGAT, $GABA_AR$, $GABA_BR$ or those involved in excitatory neurotransmission have a stronger impact on gamma frequency.

The candidate gene approach which tested the effect of ten individual $GABA_AR$ subunit genes by aggregating multiple SNPs found no significant relationship with either GABA+/Cr or gamma frequency (Table 3). Even though no gene reached statistical significance an interesting finding is that the two genes *GABRA2* and *GABRA5*, which are closest to reaching significance with gamma frequency have been strongly implicated in schizophrenia (Benham *et al.*, 2014). In addition, several SNPs in *GABRA2* have been associated with alcohol dependence and the frequency of beta oscillations (Edenberg *et al.*, 2004). Alcohol is a positive allosteric modulator of the $GABA_AR$ and has shown to decrease visual gamma peak frequency (Campbell *et al.*, 2014). Therefore, a common pathway linking variation in *GABRA2*, alcohol and beta/gamma oscillations could be present. The significant effect of these *GABRA2* SNPs on alcohol dependence and beta oscillations was found by testing single SNPs in comparison to the multiple SNP (gene) test used in this study. This highlights a limitation of the whole gene measure test, as the gene as a whole may not exert significant effects on GABA+ or gamma frequency, but the potential effects of single SNPs are masked. Thus, investigation of genetic variants in $GABA_AR$ subunits, particularly on gamma oscillatory measures warrants further investigation with larger sample sizes and using both a candidate SNP and candidate gene approaches.

The schizophrenia polygenic risk score was also not associated with GABA+/Cr and gamma frequency. As the polygenic risk score pools the effects of multiple variants with small effects from different genes and thus different proteins and biological pathways this measure may not be specific enough to biological pathways involved in GABA and visual gamma.

Converging genetic evidence implicates common SNPs involved in the neuronal calcium pathway to predispose individuals to schizophrenia (Ripke *et al.*, 2013). Calcium is a versatile intracellular signal that regulates many different cellular processes and is a vital component of GABAergic signalling (Berridge *et al.*, 2003, Higley, 2014). Even so, the polygenic risk score may still not be specific enough to GABA and gamma and the functional imaging measures of GABA+ and gamma frequency may not be sensitive enough to detect effects of these genetic variants. Other studies that have found a functional influence of polygenic risk scores use a more global imaging measure such as working memory (Walton *et al.*, 2013). Working memory may be a more appropriate schizophrenia endophenotype as it is a core deficit of schizophrenia and may be under control by a large number of different genes, including those involved in calcium signalling.

Overall, this study had several methodological strengths and limitations. The main strength being that the study was conducted in a homogenous population in terms of age, ethnicity, handedness, well-being and education. This greatly increased the likelihood of associations between genetic variation and GABA+ or gamma frequency being specific to the genetic variation and not other confounding variables. In addition, the imaging measures GABA+ and gamma frequency are highly repeatable (Muthukumaraswamy *et al.*, 2010, Near *et al.*, 2014), which also provides confidence that significant genetic associations with GABA+ and gamma frequency are reliable and replicable. The main limitation of this study is the sample size, which although is large in terms of neuroimaging studies, is small in terms of genetic studies. This meant that when individuals were grouped based on genotype, some genotype groups had very small numbers, which questions the reliability of the findings. In particular, the recessive effect of the three *GAD1* SNPs (rs10432420, rs3749034 and rs2241165) on GABA+/Cr are open to doubt as the homozygous minor allele group in all three SNPs only

had three individuals (Figure 1). The study was also conducted in healthy controls which although limits the effects of medication, means the results may not be directly translatable to a schizophrenia population.

To conclude, this study provides strong evidence for three candidate *GAD1* SNPs impacting occipital GABA+ levels in a homogenous group of healthy Caucasian individuals. This adds to the growing evidence that genetic variation in *GAD1* is associated with downstream functional effects on structural and neurochemical imaging measures (Brauns *et al.*, 2013, Marenco *et al.*, 2010). In addition, *GAD1* SNPs have been associated with schizophrenia (Addington *et al.*, 2005, Straub *et al.*, 2007), in which altered GABAergic function has been strongly implicated (Gonzalez-Burgos *et al.*, 2011, Stan and Lewis, 2012). Thus, *GAD1* SNPs may play an important role in leading to the altered GABA levels observed in schizophrenia patients, which may consequently lead to altered behaviour. In contrast, none of the three genetic methods revealed an influence of genetic variation on gamma frequency. However, this may be due to the sample size being too small to detect genetic effects as large sample sizes are needed in genetic studies (Abbott, 2008). As visual gamma peak frequency has been reported to be under strong genetic control (van Pelt *et al.*, 2012), the genetic components determining this measure require further investigation in a larger sample size. Ultimately, by identifying the effects of genetic variants on clinically relevant biological measures this will increase our understanding of the specific biological pathways affected in disease and may lead to novel targeted treatment strategies.

Chapter 5 - Visual Gamma Oscillations and Occipital GABA in Schizoaffective Bipolar Disorder

This Chapter has been published as a peer-reviewed journal article: Brealy, J. A., et al. (2014). Increased visual gamma power in schizoaffective bipolar disorder. Psychological Medicine, 1–12.

5.1 Abstract

Background: EEG and MEG studies have identified alterations in gamma-band (30-80 Hz) cortical activity in schizophrenia and mood disorders. MRS studies have also reported group differences between psychiatric disorders and healthy controls for *in vivo* GABA levels. These findings are consistent with neural models of disturbed glutamate and GABA neuron influence over cortical pyramidal cells. Genetic evidence suggests specific deficits in $GABA_A$ receptor ($GABA_AR$) function in schizoaffective bipolar disorder (SABP), a clinical syndrome with features of both bipolar disorder and schizophrenia. This study investigated gamma oscillations and *in vivo* GABA+ levels in this under-researched disorder.

Methods: MEG was used to measure induced gamma and evoked responses to a visual grating stimulus, known to be a potent inducer of primary visual gamma oscillations. MRS was used to measure *in vivo* GABA+ levels from an occipital voxel. The GABA+ and gamma band activity measurements were acquired from 15 individuals with remitted SABP, defined using Research Diagnostic Criteria, and 22 age and sex matched healthy controls.

Results: Individuals with SABP demonstrated increased sustained visual cortical power in the gamma band ($t(35)=-2.56$, $p=0.015$) compared with controls. There were no group differences in baseline gamma power, transient or sustained gamma frequency, alpha band responses or pattern onset visual evoked responses. There was also no group difference in occipital GABA+ levels.

Conclusions: Gamma power is increased in remitted SABP, which reflects an abnormality in the cortical inhibitory-excitatory balance. Although an interaction between gamma power and

medication can not be ruled out, there were no group differences in baseline measures. Further work is needed in other clinical populations and at risk relatives. Pharmaco-magnetoencephalography studies will help to elucidate the specific GABA and glutamate pathways affected.

5.2 Introduction

Schizoaffective bipolar disorder (SABP) is a mental illness characterised by manic and depressive episodes typical of bipolar disorder and psychotic symptoms observed in schizophrenia. SABP individuals have a distinctly poor prognosis compared with the wider bipolar phenotype (Harrow *et al.*, 2000). A genome-wide association study provided strong genetic evidence for a selective influence of GABA-A receptor dysfunction in this subpopulation of bipolar individuals (Craddock *et al.*, 2010), which was recently independently replicated (Breuer *et al.*, 2011). Although these SNPs do not alter protein sequence, they may affect the expression levels of GABA-A receptor subunits, which could consequently affect the duration of inhibitory postsynaptic current onto pyramidal cells.

These genetic findings in SABP add to the increasing evidence of an abnormal glutamatergic/ GABAergic cortical balance in psychiatric disorders. Neuropathological evidence (Costa *et al.*, 2004, Lewis *et al.*, 2012) suggests that there is a cortical GABA deficit in both bipolar disorder and schizophrenia. Decreased levels of glutamic acid decarboxylase (GAD) 67 mRNA are consistently found in parvalbumin-positive interneurons, in multiple cortical regions in schizophrenia and mood disorders (Gonzalez-Burgos *et al.*, 2010, Hashimoto *et al.*, 2003, Thompson *et al.*, 2009). Complementing this, decreased MRS GABA levels have been reported in the occipital cortex (Bhagwagar *et al.*, 2007, Yoon *et al.*, 2010) and anterior cingulate (Rowland *et al.*, 2013) of schizophrenia and bipolar individuals. However, the

findings are inconsistent, as no group differences (Tayoshi *et al.*, 2010) and increases (Brady *et al.*, 2013, Kegeles *et al.*, 2012, Ongür *et al.*, 2010) have also been found across various cortical regions. Glutamate dysfunction, particularly involving the N-methyl-D-aspartate receptor (NMDAR) has also been implicated (Kirov *et al.*, 2012, Martucci *et al.*, 2006), supported by alterations in MRS glutamate levels (Rowland *et al.*, 2013).It is possible that these glutamatergic and GABAergic abnormalities are present in the SABP phenotype, which manifests features of both disorders.

Converging evidence from both computational and animal models demonstrates that high frequency (30-80 Hz) cortical gamma oscillations depend on the excitatory-inhibitory activity generated between reciprocally connected glutamatergic and GABA interneuron cell assemblies (Bartos *et al.*, 2007, Buzsaki and Wang, 2012). Thus, one might expect gamma oscillations to be similarly perturbed in psychiatric disorder. Indeed, alterations in evoked and induced gamma band measures have been found in response to a variety of tasks in schizophrenia and bipolar disorder (Ethridge *et al.*, 2012, Hall *et al.*, 2011a, Liu *et al.*, 2012, Mulert *et al.*, 2011, O'Donnell *et al.*, 2004, Spencer *et al.*, 2009, Sun *et al.*, 2013, Tan *et al.*, 2013). The majority of studies find a decrease in gamma oscillatory measures, including gamma power, frequency and phase locking. However, no differences (Uhlhaas *et al.*, 2006) and increases (Riečanský *et al.*, 2010) in gamma measures have also been reported.

Methods have been developed to induce gamma oscillations in the primary visual cortex of healthy individuals in response to visual gratings with a high degree of repeatability (Hoogenboom *et al.*, 2006, Muthukumaraswamy *et al.*, 2010). However, the link between GABA and gamma is unclear, depending on whether you look at disease, pharmaco-MEG or modelling. Positive correlations have been demonstrated between induced gamma frequency

and occipital MRS GABA measures (Muthukumaraswamy *et al.*, 2009) although this was not replicated in a larger cohort (Cousijn *et al.*, 2014). If gamma oscillations are modulated by GABA, if a GABA deficit is present in SABP (as is implicated in clinical studies of schizophrenia and bipolar disorder) then MRS GABA-gamma studies would predict that a GABA deficit would decrease gamma frequency. Pharmaco-MEG drug studies (alcohol and propofol) would suggest that enhancing GABA will boost gamma power, (Campbell *et al.*, 2014, Saxena *et al.*, 2013) so a GABA deficit may well lead to a reduction in gamma power. Conversely, computational models of an NMDAR hypofunction (which may be relevant to the aetiology of SABP) (Spencer, 2009) would predict an increase in gamma power. Therefore, in this study the oscillatory measures gamma power and frequency in the visual cortex and GABA levels in the occipital voxel were obtained from SABP individuals and healthy controls to shed light on these contradictions.

5.3 Methods

5.3.1 Participants

Fifteen SABP individuals and 24 healthy control (HC) individuals participated in the study. The study was approved by the National Research Ethics Service (England and Wales) and the School of Psychology ethics committee, Cardiff University. Informed consent was obtained from all participants. SABP participants were recruited from local genetic epidemiology studies at the MRC Centre for Neuropsychiatric Genetics & Genomics, Cardiff University, part of the Wellcome Trust Case Control Consortium (http://www.wtccc.org.uk). They had previously been diagnosed according to the research diagnostic criteria (RDC) (Spitzer *et al.*, 1978). HC were recruited from Cardiff University staff and the local community. HC had no history of axis I psychiatric disorder, determined by the MINI

(Sheehan *et al.*, 1998) and General Hospital Questionnaire (GHQ) and no history of psychiatric disorder in first-degree relatives using the RDC family history method (Andreasen *et al.*, 1977). Exclusion criteria included dyslexia, contra-indications to MRI, organic brain disease, drug or alcohol dependence (determined by the MINI) and self-reported cognitive problems or memory problems, determined by systematic interview.

SABP subjects completed the MINI, to screen for current affective or psychotic episodes, and measures of current affective and psychotic symptoms: the Scale for the Assessment of Positive Symptoms (SAPS)(Andreasen, 1984) , the Scale for the Assessment of Negative Symptoms (SANS)(Andreasen, 1983) the Young Mania Rating Scale (YMRS) (Young *et al.*, 1978) and the Calgary Depression Scale (CDS) (Addington *et al.*, 1990). In addition, a record was made of currently prescribed medications.

5.3.2 MEG Acquisition and Analysis

Participants were presented with a slightly modified version of an established visual paradigm (Muthukumaraswamy *et al.*, 2009) consisting of a vertical, stationary, maximum-contrast, 3 cycles per degree, sine-wave grating presented on a mean luminance background (Figure 1). The stimulus was presented in the lower left visual field, subtended 4° both horizontally and vertically, with the centre of the image located 2.8° along a 45° angle, extending left-inferiorly from a small red fixation point. Visual stimuli were presented on a Mitsubishi Diamond Pro 2070 monitor (1,024 × 768 pixels and 100Hz frame rate). The duration of each stimulus was 0.8–2.3s (mean duration 1.55s) followed by 1.5s of the fixation point only. Participants were instructed to maintain fixation for the entire experiment and to maintain attention, were instructed to press a response key at the termination of each stimulation period. One hundred and fifty identical visual stimuli were presented in each recording session and each recording session took approximately 8 minutes.

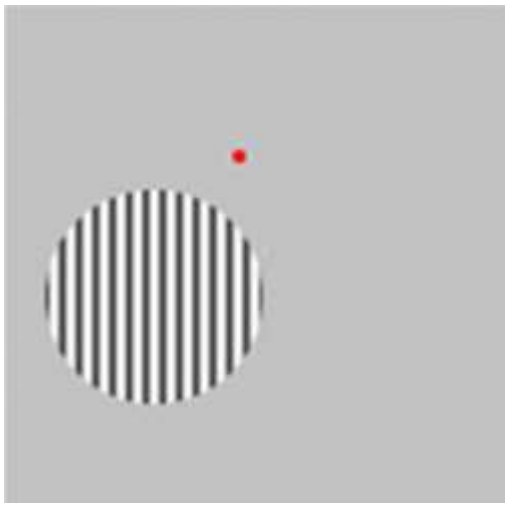

Figure 1: Visual stimulus used in this study

Whole head MEG recordings were made using a 275-channel whole head MEG system in a magnetically shielded room. Twenty nine reference channels were also recorded for noise-cancellation purposes and the primary sensors were analysed as synthetic third-order gradiometers (Vrba and Robinson, 2001). Three of the 275 channels were turned off due to excessive sensor noise. Before MEG recording, participants were fitted with three fiduciary markers in the form of electromagnetic head coils at the two pre-auricular points and nasion, and were localised relative to the MEG system immediately before and after the recording session. Previously, high resolution anatomical images had been acquired for each individual with a T1-weighted 3D FSPGR sequence (TR/TE/TI = 7.8/3.0/450ms, flip angle=20° FOV = 256*192*172mm, 1mm isotropic resolution, 8min acquisition time). After MEG recording these fiduciary markers were used to enable MEG and MRI co-registration. Two healthy controls did not participate in the MEG section of the study, so MEG analysis was conducted in 15 SABP individuals and 22 healthy controls. One SABP subject and 3 controls did not participate in the MR section of the study, so for MRI co-registration, a structural scan from a matching subject in age and gender was used.

Offline, each dataset was epoched from -0.8 to 0.8s around stimulus onset and each trial visually inspected for data quality. Trials containing gross artefacts, such as head movements and muscle clenching were excluded from further analysis. For the 15 SABP MEG datasets, on average 15.9% (SD 16.9, range 0-50.7%) of the 150 trials were removed and for the 22 healthy control datasets, on average 14.1% (SD 13.6, range 0-565) of the 150 trials were removed. Three source localisations were performed on each dataset using synthetic aperture magnetometry (SAM) (Robinson and Vrba, 1999) for gamma (30 - 70 Hz), alpha (8 – 13Hz) and evoked responses (SAMerf) (Robinson, 2004). Correspondingly, three global covariance matrices were calculated for each dataset, one for gamma, one for alpha and one for SAMerf (0 - 100 Hz). Based on these covariance matrices, using the beamformer algorithm (Robinson and Vrba, 1999) , three sets of beamformer weights were computed for the entire brain at 4mm isotropic voxel resolution.

For gamma-band SAM image reconstruction virtual sensors were constructed for each beamformer voxel and student *t* images of source power changes computed using a baseline period of -0.8 to 0s and an active period of 0 to 0.8s, while for alpha-band SAM image reconstruction a baseline period of -0.8 to -0.25s and an active period of 0.25 to 0.8s was used. The 0 to 0.25s active time window was excluded for the alpha-band SAM image reconstruction to avoid contamination of the evoked response into the alpha-band source image.

For each participant, using their source reconstruction image, the voxel with the strongest power increase in the contralateral occipital lobe was located for gamma and the voxel with the strongest source power decrease located for alpha. Time-frequency analyses of these virtual electrodes were conducted with the Hilbert transform between 1 and 100Hz, at 0.5 Hz

frequency step intervals and time-frequency spectra were computed as a percentage change from the pre-stimulus baselines (-0.8 to -0s) for each frequency band. From these spectra, the peak frequency and amplitude at that frequency for transient gamma amplitude increases (30 - 70 Hz, 0 to 0.3 s), sustained gamma amplitude increases (30 - 70 Hz, 0.3 to 0.8 s) and alpha amplitude decreases (8-13 Hz, 0.25 to 0.8s) were quantified by collapsing across the time dimension and finding the maximal (or minimal for alpha) frequency. From these spectra, the time course of gamma (30–70 Hz) was extracted and submitted to non-parametric permutation tests using 5000 permutations (Nichols and Holmes, 2002). Permuted *t* statistics were corrected for multiple comparisons using cluster-based techniques (Maris and Oostenveld, 2007). The width of the spectral peak was estimated by the full width half maximum (FWHM) of the gamma peak.

Previous studies have reported differences in baseline (pre-stimulus) gamma power between schizophrenia patients and controls (Spencer, 2012). Hence, pre-stimulus amplitudes were examined by recomputing time-frequency spectra with no baseline correction across frequency bands (0-105Hz) in the pre-stimulus period (-0.8 to 0s).

For SAMerf, the computed evoked response was passed through the 0 -100 Hz beamformer weights to generate SAMerf images (Robinson, 2004) at 10 ms intervals from 50 – 150 ms. The image window (usually 70–80 ms or 80–90 ms) with the maximal response in visual cortex was identified and the maximal voxel selected as the peak location for further analysis. For this, the evoked field was computed for this virtual sensor (-0.2 to 0 s baseline) and the peak amplitude and latency of the M80 and M150 responses quantified.

5.3.3 MRS Acquisition and Analysis

MR spectra were acquired on a GE Signa HDx 3T MRI scanner using the body coil for RF transmission and an eight-channel head coil for signal reception. MR spectra were acquired from a 3.0 x 3.0 x 3.0 cm^3 voxel in the visual cortex. The occipital voxel was orientated so that the inferior border was aligned in sagittal view with the superior border of the cerebellum and was located bilaterally to include an equal volume of both hemispheres. The posterior and superior limits of the voxel were defined by the sagittal sinus. Spectra were acquired with a MEGA-PRESS sequence (Mescher *et al.*, 1998) over an 8 minute period with the following parameters: TE = 68 ms, TR =1.8s, 256 transients of 4096 datapoints, and 16 ms editing pulses applied at 1.9 ppm (ON) and 7.5 ppm (OFF). GABA was quantified with GANNET (www.gabamrs.blogspot.co.uk/). The GABA peak at 3.0 ppm in the difference-edited spectrum was fitted with a single Gaussian model and GABA levels were quantified using both creatine and water as an internal concentration reference. For GABA+/H_20 values, the ratio of GABA+ to water was converted to institutional units (IU) by correcting for the voxel tissue fraction (grey matter and white matter) and the effective visibility of water. Grey matter, white matter and CSF fraction were determined using FAST (Zhang *et al.*, 2001). MR spectra were not acquired from one SABP individual and three controls. Thus, GABA+ data was analysed in 14 SABP individuals and 21 healthy controls.

5.3.4 GABA+ and Gamma Frequency

Correlational analysis between age-corrected GABA+/Cr concentration and sustained peak gamma frequency were carried out using the Pearson correlation coefficients (r) in SPSS 20. Age corrected values were used as the age range in this sample was large (21-61 years) and age has been shown to influence GABA levels and gamma frequency (Gaetz *et al.*, 2012, Gao *et al.*, 2013).

5.3.5 V1 Structural Properties

V1 structural properties were estimated in each individual in order to identify whether any group differences in GABA+ and gamma measures were influenced by structural group differences. FreeSurfer was used to estimate the cortical thickness and surface area of V1 for each participant from their 3D FSPGR scan (Hinds *et al.*, 2008). As the visual stimulus was presented on the left visual field, estimates of V1 surface area and thickness were calculated for the right hemisphere. As MRI data was not acquired from one SABP and three controls, V1 thickness and V1 surface area data was available for 14 SABP and 21 healthy controls.

Acknowledgements for data collection

Special thanks to Alex Shaw and Heather Richardson for assisting with data collection.

5.4 Results

5.4.1 Participant Demographic and Clinical Characteristics

Demographic and clinical characteristics for SABP and HC groups are summarized in Table 1. The SABP and HC subjects did not differ significantly by age (46.8 years (SD=9.8) versus 41.6 years (SD=10.8), $t(37)=-1.52$, $p=0.138$) and had similar female to male gender ratios. SAPS and SANS symptom scores and YMRS and CDS scores were available in 13 SABP individuals; SABP had sub-syndromal levels of depression and manic symptoms as measured with the YMRS and CDS. They also had low negative and positive symptoms as measured using the SAPS and SANS. All of the SABP patients were taking a range of medications: 14 were taking antipsychotics (Quetiapine, Aripiprazole, Olanzapine, Clozapine, Sulpiride), 7 were taking antidepressants (Citalopram, Mirtazapine, Vilazodone, Venlafaxine, Effexor), 9 were taking anticonvulsants (Depakote, Sodium Valproate, Epilim, Lamotrigine, Tegretol), 5 were taking lithium and 4 were taking benzodiazepines (Diazepam, Lorazepam, Oxazepam). SABP individuals had slightly longer key pressing response times compared to healthy

individuals (317 ms (SD 54) versus 283ms (SD 47), t=-2.056, p=0.047) but there were no group differences in the number of key presses missed (7.3 (SD 7.0) versus 4.5 (SD 4.1), t=-1.544, p=0.132).

Table 1. Demographic and Clinical Characteristics of SABP and HC groups

	SABP	HC	t value (df)	p value
Age	46 (9.8)	41 (10.8)	-1.52 (37)	0.138
Gender (F : M)	9:6	14:10		
YMRS	1.8 (2.2)			
CDS	3.8 (4.1)			
SAPS	1.4 (1.9)			
SANS	1.3 (2.0)			

Mean values are shown (with standard deviations)

5.4.2 MEG Oscillatory Measures

Figure 2A shows the grand-averaged source localisation of gamma oscillations (30-70Hz) for SABP and HC. Figure 2B shows the resulting grand-average time-frequency spectra for SABP and HC. For both groups, the time-frequency spectra showed the characteristic responses following this type of visual stimulus (Muthukumaraswamy *et al.*, 2010): there was an initial transient increase in gamma power (0-0.3s), followed by a sustained increase in gamma power (0.3-0.8s). The lower frequency band (8-13 Hz) included the early (<0.3s) visual evoked response, followed by a sustained suppression of alpha amplitude.

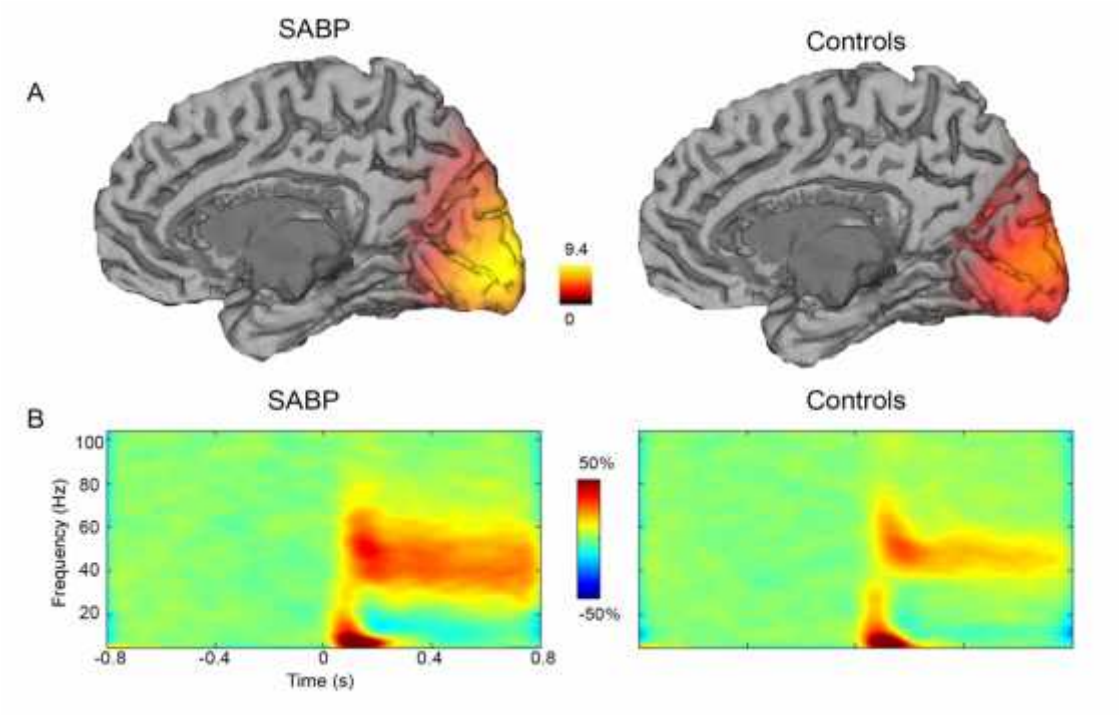

Figure 2 (A) Grand-averaged source localisation of gamma oscillations (30-70Hz) for SABP and HC individuals. Units are *t* statistics. (B) Grand-averaged time-frequency spectrograms showing source-level oscillatory power changes following visual stimulation with a circular grating patch (stimulus onset at time = 0s) for SABP and HC individuals. Spectrograms are displayed as percentage change from the pre-stimulus baseline.

For group comparisons, the grand-averaged time frequency spectra demonstrate a greater increase in sustained gamma power (30-70Hz) in the SABP group compared to the HC group. These increases in gamma power in the SABP group follow a much broader gamma band response compared to the HC (20.9 (SD 7.4) versus 15.6 (SD 7.2), t(35)=-2.170,p=0.037,95% confidence intervals of the difference = -10.253 to -0.341), calculated using FWHM of the gamma peak. In order to further investigate this group difference in the sustained gamma band response, power-frequency plots were generated for the transient (0-0.3s) and sustained gamma time windows (0.3-0.8s) (Figure 3A and B). As expected from Figure 2, in the sustained gamma time window, SABP individuals showed a significantly

higher increase of 18% in gamma power (30-70Hz) compared to a 9% increase in controls (t(35)=-2.56, p=0.015, 95% confidence intervals of the difference=-15.3 to -1.7).

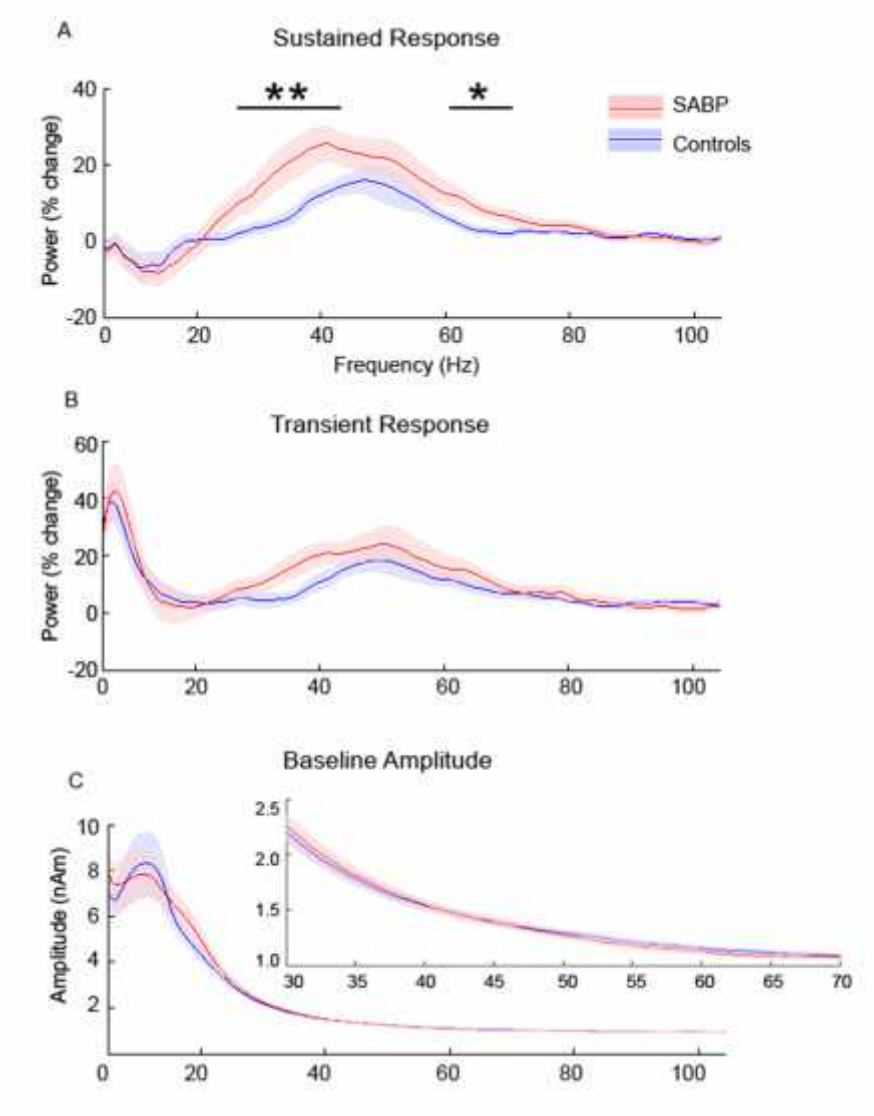

Figure 3. Grand-averaged power-frequency spectrograms, showing power changes across a broad frequency range (0-105Hz) in (B) the transient (0-0.3s) and (A) sustained response (0.3-0.8s) time window following visual stimulation. Coloured areas represent standard error of the mean. Frequency bands with significant differences in power between SABP and HC group are shown with a black bar (*p<0.05, **p<0.01, corrected for multiple comparisons across frequency bands (see text)). (C) Mean pre-stimulus baseline activity (-0.8 to 0s) in SABP and HC subjects, with an integrated and enlarged graph across 30-70Hz.

To detect the specific frequencies within the gamma frequency band at which there was increased gamma power Permuted *t* statistics were used with cluster based techniques. The power-frequency plot for sustained responses (Figure 3A) shows 2 significant clusters of increased power in the SABP group compared to HC, one at lower gamma frequencies (26.5-42.5Hz, $p<0.01$, corrected) and one at higher gamma frequencies (60.5-70Hz, $p<0.05$, corrected) (Figure 3A). At the lower gamma frequency range (26.5-42.5Hz), SABP individuals showed a 19.5% mean increase in gamma power compared to a 7.4% increase in HC. At the higher gamma frequency range (60.5Hz-70Hz), SABP individuals had a mean increase of 8.9% in gamma power compared to 3.2% in HC. There was no significant difference between groups in transient responses ($p>0.05$) (Figure 3B).

Whether the observed increase in sustained gamma power in the SABP group was due to an initial baseline (pre-stimulus) difference in the power-frequency spectrum was investigated (Figure 3C). No group differences in mean pre-stimulus (-0.8 to 0s) values were seen across the 30-70Hz frequency range ($t(35)=-0.126$, $p=0.901$, 95% confidence intervals of the difference = -0.113 to 0.100).

In order to explore if the significant difference in gamma power observed in the group comparison was consistent across the group or was influenced by only a minority of individuals, n=15 HC individuals who were age-and-sex-matched to the n=15 SABP individuals on a pair-wise basis were selected and the gamma power values were chartered for these pairs. Sustained gamma power was higher in the SABP individual than the HC individual in all but one of these pair-wise comparisons (see Figure 4A). A similar plot was made for peak sustained gamma frequency (Figure 4B). This paired age matching also ensures that small differences in age between the two groups are not affecting our results, as

although age has not been found to affect gamma power, peak gamma frequency decreases with age (Muthukumaraswamy *et al.*, 2010).

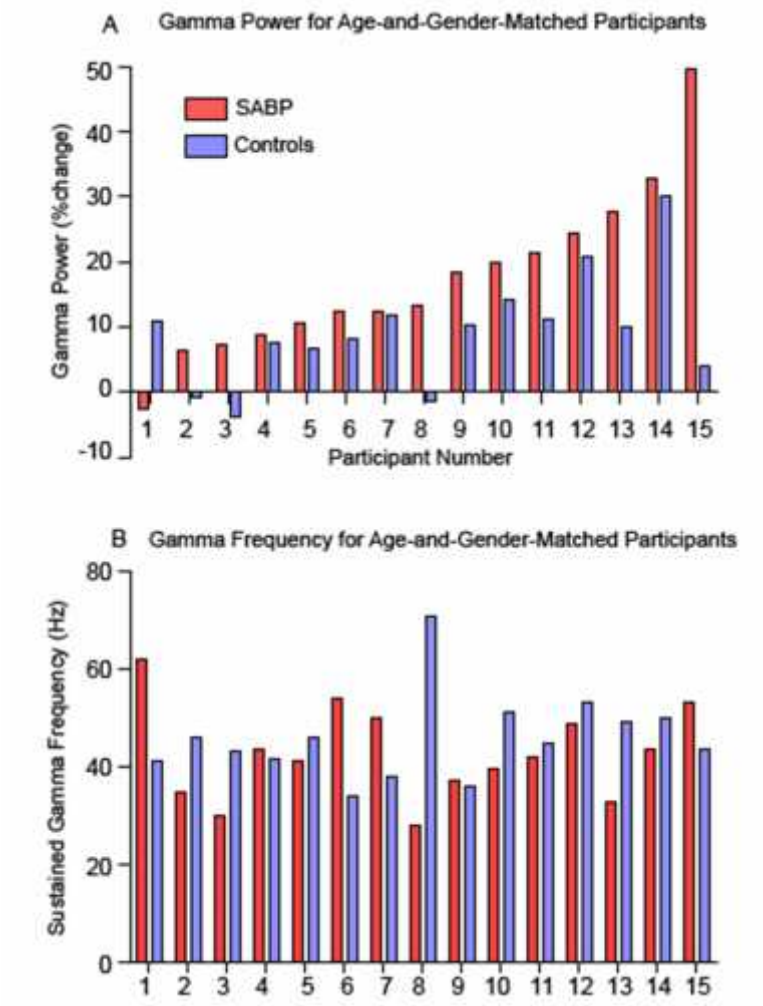

Figure 4: A histogram demonstrating individual pair-wise comparisons in (n=15) SABP and (n=15) controls for (A) mean gamma power values (30-70Hz) and (B) sustained peak gamma frequency.

The effect of medication on our finding of increased gamma power in SABP was also investigated. For the 14 patients on antipsychotics, we converted antipsychotic dosage to chlorpromazine equivalent levels (Janssen *et al.*, 2004, Woods, 2003). Chlorpromazine dosage did not correlate with gamma power (r=0.168, p=0.565). The potential effect of other medications on gamma power was investigated by group comparisons within the SABP patients, comparing those on the medication and those not on the medication. No significant

difference was found between the two groups of SABP patients for benzodiazepines (p=0.868), antidepressants (p=0.278) or lithium (p=0.789). Anticonvulsants were found to significantly reduce gamma power (p=0.01),with patients on anticonvulsants having a mean increase in gamma power of 11%, compared to a mean increase of 27% for those not medicated on anticonvulsants.

There were no group differences in transient or sustained peak gamma frequency (Figure 5A and B, p = 0.106, p = 0.280), or alpha power (Figure 5C, p = 0.900). There were also no group differences in the amplitude or latency of the M80 or M150 pattern onset evoked responses. (Figure 5D; M80 amplitude: p = 0.928, M80 latency: p = 0.072, M150 amplitude: p= 0.899, M150 latency: p = 0.143).

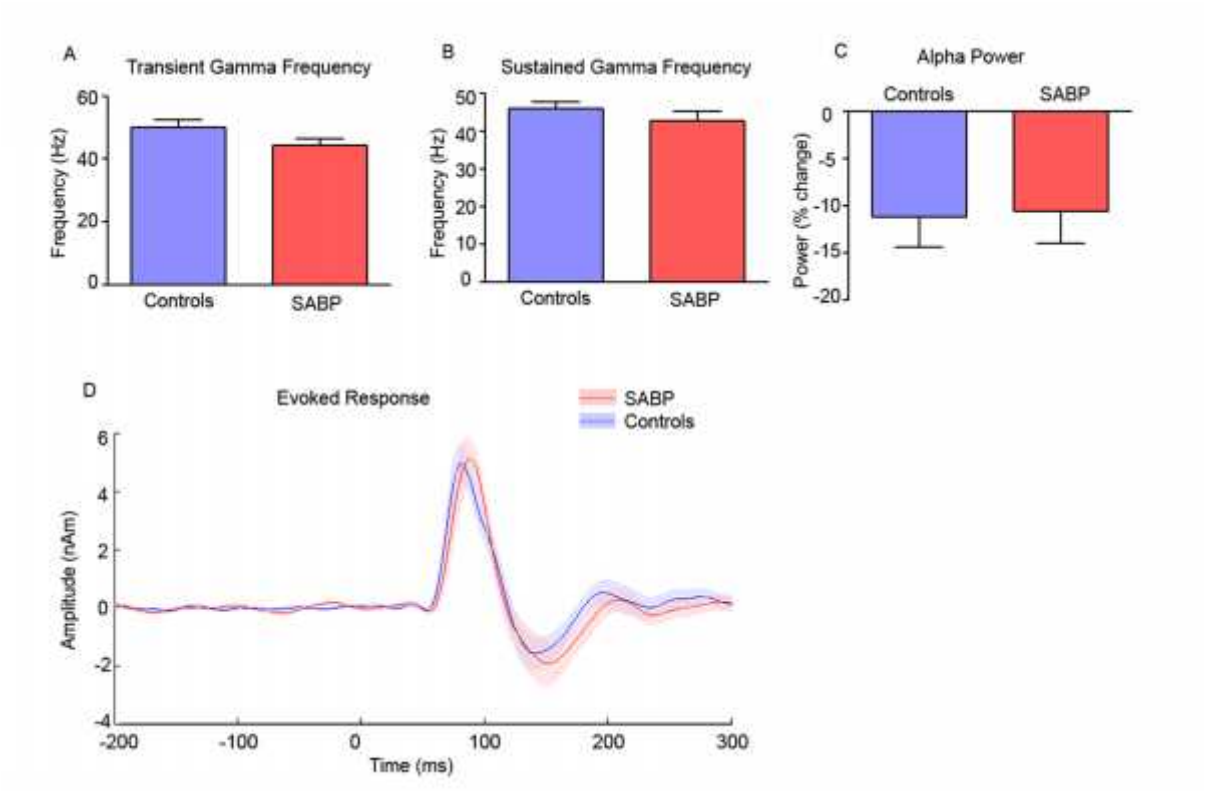

Figure 5: (A)-(C) Bar charts showing no significant group differences in (A) peak transient gamma frequency (0-0.3s), (B) peak sustained gamma frequency (0.3-0.8) and (C) alpha power (8-13Hz). Error bars represent standard errors of the mean. (D) A graph of the time

course of source level evoked responses in SABP and HC, showing no significant group differences.

5.4.3 MRS GABA+ Measures

The GABA+/Cr value for one SABP individual was identified as an outlier and excluded from further analysis. The edited MRS spectra from the occipital voxel for the remaining 13 SABP and 21 healthy individuals are shown in figure 6. All individuals show a clear GABA peak at 3ppm.

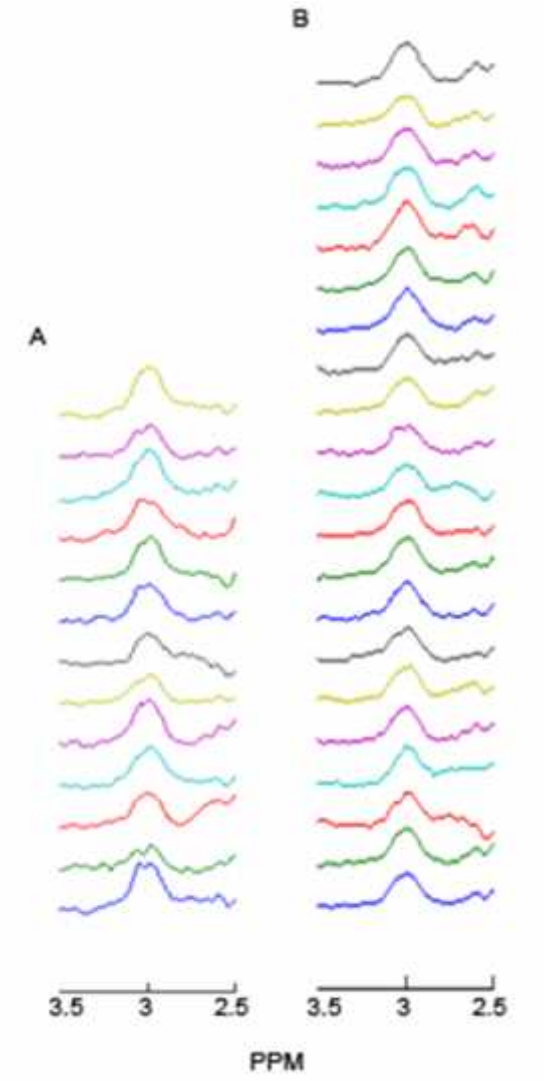

Figure 6: Edited MRS spectra for (A) 13 SABP and (B) 21 healthy controls.

For the 13 SABP and 21 control subjects, GABA+/Cr values ranged from 0.118 to 0.191 (mean 0.150 (SD 0.022) and 0.102 to 0.175 (mean 0.145 (SD 0.018)) respectively (Figure 7A). No group difference in occipital GABA+/Cr levels was found (p=0.441) and the lack of a consistent directional group difference is also shown with 13 age and gender matched pairings (Figure 7B). No group difference in GABA+ levels was also found when using GABA+/H20 values (p=0.456).

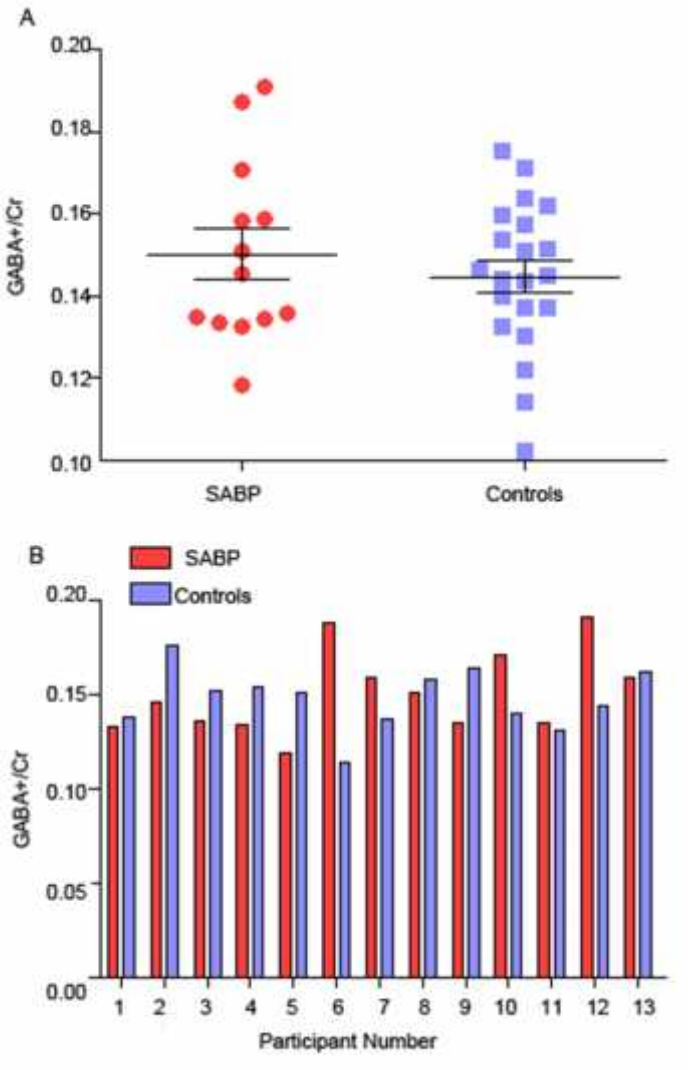

Figure 7: (A) Group comparison for GABA+/Cr values. Black lines represent the genotype group mean and standard error of the mean. (B) Histogram to compare 13 SABP individuals with an age and gender matched healthy control.

5.4.4 GABA and Gamma Frequency

There was a significant correlation between age-corrected values for GABA+/Cr and sustained peak gamma frequency in the control sample (n=19; R=0.457, p=0.049) but not in the SABP sample (R=-0.212, p=0.486) or the combined sample (R=0.106 p=0.564).

5.4.5 V1 Structural Properties

For the 14 SABP and 21 healthy controls, V1 thickness ranged from 1.58mm to 2.21mm (mean 1.91(SD 0.19)) and from 1.62mm to 2.11mm (mean 1.81 (SD 0.12)) respectively. For V1 surface area, one control was excluded as they were identified as an outlier. For the remaining 14 SABP and 20 healthy controls V1 surface area ranged from 1814cm² to 3283cm² (mean 2381 (SD 427)) and from 1905cm² to 2939cm² (mean 2325 (SD 338)) respectively. No group difference was found for either V1 thickness (p=0.102) or surface area (p=0.671).

5.5 Discussion

This study demonstrates a large increase of 18% in induced gamma power in SABP individuals compared to a 9% increase in controls, in response to a visual grating stimulus designed to maximally elicit gamma responses in the visual cortex. This was present in all but one of the pair-wise comparisons. Importantly, this increase in gamma power was not due to group differences in baseline (pre-stimulus) gamma power and could not be explained by group differences in V1 structural parameters. No group differences were found for other MEG measures, in either transient or sustained peak gamma frequency, alpha power or components of the evoked response. This dissociation between induced and evoked responses is not surprising, since previous studies have identified these measures as independent

oscillatory parameters which may be generated via different cell populations in the visual cortex (Jia *et al.*, 2013, Spaak *et al.*, 2012).

For the MRS GABA+ measure, no group differences were found using either creatine or water as a reference molecule. Given that schizophrenia and bipolar disorder are associated with decreased GABAergic function (Lewis *et al.*, 2012) and that gamma frequency and occipital GABA has previously been reported to be decreased in schizophrenia (Ferrarelli *et al.*, 2012, Yoon *et al.*, 2010), one might expect decreased gamma frequency and decreased GABA+ levels. A possible explanation for the lack of group difference in this study could be due to the relatively low sample size used. As GABA+ and gamma frequency measures show relatively high inter-individual variability, larger sample sizes may be needed to identify clear group differences. Gamma frequency has also previously been found to positively correlate with MRS GABA levels (Muthukumaraswamy *et al.*, 2009). This significant positive correlation was replicated in this study but only when using the healthy control sample and only just reached statistical significance ($p=0.049$). Therefore, this finding would need to be replicated in a large sample size as recent studies using larger sample sizes have not found a significant relationship between GABA+ and gamma frequency (Cousijn *et al.*, 2014, Robson, 2012).

In contrast to the significant finding of increased visual gamma power in SABP in this study, the majority of electrophysiological studies report reductions in gamma band responses in schizophrenia and bipolar patients during a range of cognitive and visual tasks. Many of these studies have employed evoked gamma band responses, which are phase-locked to stimuli: reduced evoked gamma power and synchrony have been observed in response to click train stimuli in chronic schizophrenia (Kwon *et al.*, 1999) and reduced gamma phase locking in

visual and auditory oddball tasks were observed in both bipolar disorder and schizophrenia (Hall *et al.*, 2011a, Spencer *et al.*, 2008a). Early visual processing deficits have also been found in schizophrenia patients, as measured by the visual backward-masking task (Wynn *et al.*, 2005). Reductions in frontal gamma power have been reported in schizophrenia individuals during more complex cognitive tasks such as working memory (Haenschel and Linden, 2011) and mental arithmetic (Kissler *et al.*, 2000). Fewer studies have focused on induced gamma oscillations. Both intact (Uhlhaas *et al.*, 2006) and impaired induced visual gamma oscillations (Grützner *et al.*, 2013) have been found in response to Mooney faces (Sun *et al.*, 2013).

Overall, several factors may explain the observed inconsistency in gamma deficits between these results and other studies. Firstly, induced gamma responses were investigated, which reflect intrinsic cortical network activity as opposed to evoked responses, which reflect driven cortical activity. Secondly, this study was in SABP individuals rather than schizophrenia patients. SABP individuals have previously been included in the schizophrenia cohort rather than as a separate cohort, which assumes a common pathophysiology. An auditory steady state response observed greater gamma amplitudes and phase locking factors in the 40Hz steady state responses to auditory stimuli in the right hemisphere of individuals with schizoaffective disorder but not schizophrenia when compared to controls (Reite *et al.*, 2010) . This suggests schizoaffective disorder may be an independent phenotype and differs in pathophysiology to schizophrenia. Thirdly, gamma responses were measured in the visual cortex rather than the auditory or prefrontal cortices. In the context of psychiatric disorders, primary abnormalities in cortical glutamate function are unlikely to be confined to the occipital cortex, but occipital measures could represent sensitive indices of more generalized pathology. Fourthly, a simple visual stimulus was used as opposed to more complex

cognitive or emotional stimuli. The advantage of using this stimulus is that responses are highly repeatable within individuals and thus represent a stable measure. Responses can also be manipulated pharmacologically in healthy individuals, providing us with a strong basis to probe GABAergic and glutamatergic function in the visual cortex of SABP individuals. Although the time window (0.5sec) over which induced sustained gamma measures are assessed is also relatively short, previous studies have investigated induced gamma power over much shorter time windows (Grützner *et al.*, 2013, Uhlhaas *et al.*, 2006). Finally, it is also possible that gamma power across psychotic disorders may be increased or decreased depending on the preponderance of positive versus negative symptoms in the illness history. The power of gamma responses to Gestalt tasks have been shown to positively correlate with positive symptoms, such as delusions and hallucinations, in the occipital region (Spencer *et al.*, 2004), and when averaged across all channels (Uhlhaas *et al.*, 2006), while gamma power has been shown to negatively correlate with the negative symptom disorganisation (Grützner *et al.*, 2013). However, as the patients in this study were remitted and had low SAPS and SANS scores, the influence of symptoms on gamma measures cannot be fully investigated.

The finding of increased gamma power in SABP supports the NMDAR hypofunction hypothesis for the aetiology of schizophrenia. Computer modelling evidence suggests gamma power may be increased by NMDAR antagonism (Spencer, 2009). In the cortical circuit model, reducing the NMDAR input by 20-100% to fast-spiking interneurons was found to increase gamma power. This increase in gamma power has been explained by reduced NMDA facilitation of fast spiking GABA interneurons which, in turn, disinhibits AMPA neurons, leading to an overall increase in cortical excitability. Preclinical work also supports this hypothesis, demonstrating increased gamma power in response to the *N*-methyl-D-aspartate (NMDA) antagonist MK-801(Arai and Kessler, 2007, Wood *et al.*, 2012) and

decreased cortical gamma power in response to the α-amino-3-hydroxy-5-methyl-4-isoxazolepropionic acid (AMPA) receptor antagonist SYM 2206 (Oke *et al.*, 2010). The anaesthetic ketamine is thought to act in a similar way, and recent *in vivo* evidence suggests that it increases glutamate release in the prefrontal cortex of healthy volunteers (Stone *et al.*, 2012). Thus, increases in gamma power may be mediated by NMDA receptor blockade, which reduces the activity of cortical GABAergic interneurons and, in consequence, increases the excitability of pyramidal cells (Homayoun and Moghaddam, 2007).

However, recent pharmacoimaging work argues against a GABA deficit mediating the effect of increased gamma responses observed in SABP. The $GABA_AR$ agonist propofol increased rather than decreased gamma power in healthy volunteers (Saxena *et al.*, 2013). Furthermore, the GABA transporter tiagabine, which increases synaptic availability of GABA, had no effect on gamma frequency or power, but suppressed the pattern onset (80ms) evoked response (Muthukumaraswamy *et al.*, 2013). It is possible, therefore, that the observed increase in gamma power reflects a primarily glutamatergic pathology. This is supported by the non-significant group differences for the GABAergic measures, gamma frequency and GABA+. The effects of NMDA antagonists (such as ketamine) and AMPA antagonists (such as perampanel) on visual gamma power need to be investigated *in vivo*.

This study had some limitations. In the context of psychiatric disorders, primary abnormalities in cortical GABAergic/glutamatergic function are unlikely to be confined to the occipital cortex. However, occipital measures could represent particularly sensitive indices of more generalized pathology. The putative advantage of using a low level visual stimulus, as opposed to more complex cognitive or emotional stimuli, is that the paradigm is tapping in to a stable and sensitive index of neurotransmitter function. While the stimuli are

simple, any abnormalities that might be discovered in mental disorder would have implications for the integration of higher level perceptual and cognitive processes seen in these disorders that are harder to detect using current MEG methods.

Medication will always be a potential confound when studying patients with schizoaffective disorder or psychosis in general. All the participants were taking medication, which could have affected gamma measures independent of any trait disturbance, and medication could have mitigated against any illness-related disturbance in this remitted group. In an auditory steady-state stimulation paradigm, patients with schizophrenia taking atypical antipsychotics showed enhanced gamma power at 40 Hz stimulation compared with patients taking conventional antipsychotics (Hong *et al.*, 2004), although there was considerable overlap. All but one of the participants was taking atypical antipsychotics. However, preclinical work suggests that atypical and conventional antipsychotics *reduce* spontaneous gamma power (Jones *et al.*, 2012), or suppress gamma power responses to acetylcholine and physostigmine (Schulz *et al.*, 2012). Hence, we might expect antipsychotics to reduce rather than explain the observed group differences. Other clinical evidence suggests that both medicated and unmedicated patients with first episode psychosis have similarly impaired gamma power during cognitive control in first-episode schizophrenia (Minzenberg *et al.*, 2010).

From the results in this study, no effect was found for chlorpromazine dosage, benzodiazepines, antidepressants or lithium on gamma power. However, patients on anticonvulsants were found to have significantly lower gamma power compared to those not on the medication. These findings coincide with a recent study, showing that the anticonvulsant sodium valproate significantly decreases visual gamma power (Perry *et al.*, 2014). This implies that anticonvulsants may in fact be normalising gamma power and that

increases in gamma power could be less detectable in patients on this type of medication. Nicotine may also be a confounding factor. Nicotine has been shown to enhance auditory evoked gamma activity (Featherstone *et al.*, 2012) but the effect of nicotine on induced oscillations in the visual cortex is unknown. Although nicotine use may be affecting our measures, as 14 of the 15 patients showed increased gamma power in comparison to their age and gender matched control it is unlikely that this can be attributed to increased nicotine intake across all SABP individuals.

In conclusion, this study demonstrates that remitted SABP is characterised by an increase in gamma power induced by a simple visual stimulus. This may be an index of a more generalised non-state-dependent dysfunction of glutamatergic and/or GABAergic activity. Further work is needed to explore these deficits in unmedicated SABP and their relatives. This will help determine if inconsistencies between the findings in this study and other clinical population studies can be explained by the visual stimulus and/or the SABP cohort. Pharmaco-MEG studies are required to examine the relative effects of glutamate and GABA receptor agonists and antagonists on induced gamma power in healthy and psychiatric populations. This may ultimately help us to understand specific mechanisms underlying the generation of gamma oscillations and improve the treatment of major mental disorders.

Chapter 6 – Individual Differences in Auditory Chirp Gamma Responses: Relationship with Auditory Structural Properties and Visual Gamma Responses

6.1 Abstract

Background: Auditory steady-state responses are increasingly being used to examine neurophysiological function in neuropsychiatric disorders. A recent study has shown that inter-individual variability is present in the peak frequency and peak power of the low and high gamma band auditory steady-state response (ASSR). However, whether the individual variation in these gamma ASSR measures is repeatable over time has not been reported. In addition, the factor(s) underlying the variation are unknown. A possible factor influencing the variation could be differences in the structural properties of the auditory cortex, as this may have downstream effects on cellular components, which are involved in the generation of the ASSR. As inter-individual variability is also present in the visual gamma response, whether this response shows a relationship with the variability in the gamma ASSR is also of interest. Thus, this study investigates (1) the repeatability of the gamma ASSR measures (2) the influence of auditory structural properties on the peak frequency and peak power of the gamma ASSR and (3) the relationship between the auditory gamma steady-state response with the induced visual gamma response.

Methods: An auditory click-chirp stimulus was developed and the individual repeatability of four ASSR measures was tested in two subjects (peak frequency in the low gamma (30-50Hz) and high gamma range (70-100Hz) and peak power in the low gamma (30-50Hz) and high gamma range (70-100Hz)). Using ASSR data from 11 healthy subjects, correlational analysis was performed to firstly assess the impact of auditory structural properties on the ASSR and secondly, to determine if visual gamma responses were correlated with gamma ASSRs.

Results: The morphology of the ASSR and the individual variability in the four ASSR measures was highly repeatable. The thickness and surface area of Heschl's gyrus (HG) was not associated with any of the four ASSR measures. Similarly, the peak frequency and peak power of the visual gamma response showed no relationship with the peak frequency and peak power of the low and high gamma auditory response.

Conclusions: These results demonstrate that peak frequency and peak power from the low (30-50Hz) and high auditory gamma responses (70-100Hz) are reproducible over time. The findings suggest that the structural parameters of the HG do not influence the ASSR and that the gamma ASSR has no relationship with the gamma visual response. However, these analyses need to be conducted in a large sample size to reliably verify these findings. Further understanding the factors underlying individual differences in the auditory domain and how these compare to other sensory domains will ultimately improve our understanding of sensory perception.

6.2 Introduction

The auditory steady-state response (ASSR) is an oscillatory response in which neurons entrain to the frequency and phase of a repeated auditory stimulus. Thus, the ASSR is a useful clinical probe for assessing the integrity of neural networks that are needed for generating auditory oscillations. ASSRs were originally obtained using sequences of clicks (click train) (Galambos *et al.*, 1981) but can also be acquired using amplitude-modulated tones (Picton *et al.*, 1987). As with many oscillatory responses, the amplitude/power of the ASSR varies across individuals (Ross *et al.*, 2000). However, an interesting feature of the ASSR is that humans show two main peak increases in amplitude which are present in the gamma frequency band; the largest being around 40Hz (Galambos *et al.*, 1981) and a second smaller peak around 80Hz (Lins *et al.*, 1995). Similarly, rats show two peak ASSRs but at

slightly different frequencies within the gamma range (Pérez-Alcázar *et al.*, 2008). The reason for this maximal response at 40Hz in humans is still unclear but has been hypothesised to be due to the preferential working frequency of the auditory system (Pastor *et al.*, 2002). Using MEG, the 40Hz response has primarily been localised to the primary auditory cortex (Herdman *et al.*, 2003) and the 80Hz response has been mainly localised subcortically (Bish *et al.*, 2004, Herdman *et al.*, 2002).

Obtaining the ASSR to multiple stimulus frequencies can be a time consuming process if different frequencies are individually tested. However, a new technique using an auditory stimulus that increases linearly in frequency from 1-120Hz (chirp) has shown that the ASSR can be measured continuously over a range of frequencies (Artieda *et al.*, 2004), greatly reducing the time needed to test the full spectrum. In addition, this stimulus has revealed that individuals exhibit variability in their peak frequency within the two main gamma components at 40Hz and 80Hz. Within the lower gamma component, individuals peaked in power from 43-50Hz and for the higher gamma component individuals peaked between 80-120Hz. This variability in peak frequency had not previously been demonstrated, as other studies use click trains or amplitude-modulated tones only at one particular frequency, the most common being 40Hz. Importantly, this variability has been shown to be functionally relevant, as lower peak frequencies in the 30-60Hz range have been associated with cognitive impairment in multiple sclerosis patients (Arrondo *et al.*, 2009).

Intriguingly, this individual variability in the peak response frequency is also found in other primary sensory cortices, including the visual cortex in response to a visual grating (Adjamian *et al.*, 2004, Hoogenboom *et al.*, 2006, Muthukumaraswamy *et al.*, 2010) and in the motor cortex following finger movements (Cheyne and Ferrari, 2013, Gaetz *et al.*, 2011,

Muthukumaraswamy, 2010). Importantly, these studies have indicated that the cortical balance between inhibitory (GABA) and excitatory (glutamate) neurotransmission in the visual and motor cortex plays a significant role in determining their respective peak gamma response frequency (Gaetz *et al.*, 2011, Muthukumaraswamy *et al.*, 2009). So far, no studies have investigated the potential factor(s) underlying individual variability in the peak gamma frequency of the ASSR. Due to the relatively consistent laminar structure and cell types found across these three primary sensory domains, the auditory peak response frequency may also share similar factors as the visual and motor domains in driving their individual gamma frequency variability (Cunningham *et al.*, 2004). Recent evidence supports GABAergic and glutamatergic function as determining factors of the auditory peak response frequency, as the 40Hz ASSR can be selectively manipulated via pharmacological modulation with a $GABA_AR$ antagonist (muscimol) and an NMDAR antagonist (ketamine) in both rats and human individuals (Plourde *et al.*, 1997, Vohs *et al.*, 2010, Vohs *et al.*, 2012). If consistent neurochemical similarities are present across sensory systems, this may lead to functional relationships across the modalities, such as individuals with a high peak gamma frequency in the visual domain may also have a high peak gamma frequency in the auditory domain.

Structural properties of the visual cortex have also been implicated in influencing its peak gamma response frequency (Gaetz *et al.*, 2012, Muthukumaraswamy *et al.*, 2010) and thus, this may also be the case in the auditory domain. Different structural divisions of the auditory cortex such as Heschl's gyrus (HG), the primary auditory cortex (A1) and the superior temporal cortex (STG) are known to vary widely in cortical thickness, volume and gyral morphology across individuals (Abdul-Kareem and Sluming, 2008, Kang *et al.*, 2012, Rademacher *et al.*, 2001). These variations may reflect differences in cell types (GABAergic

interneurons) or cell densities, which are particularly relevant factors for generating and maintaining sensory gamma oscillations (Cardin *et al.*, 2009). Thus, differences in structural properties could lead to downstream effects on functional gamma oscillatory activity. In agreement with structural properties of the auditory cortex influencing the ASSR, a recent study has shown that the *power* of the 40Hz steady-state response positively correlates with the cortical thickness of the superior temporal gyrus (Edgar *et al.*, 2013). Whether these findings are also applicable to the peak gamma frequency of the ASSR has not been explored.

Further understanding the factors underlying the individual variability in the ASSR is also important clinically, as several psychiatric populations, including schizophrenia (Kwon *et al.*, 1999, Spencer *et al.*, 2008b), bipolar disorder (O'Donnell *et al.*, 2004, Oda *et al.*, 2012) and schizoaffective disorder (Brenner *et al.*, 2003) have been found to have a reduced 40Hz ASSR. As GABAergic and glutamatergic dysfunction has been strongly implicated in the pathophysiology of psychiatric populations, the ASSR abnormalities may be reflecting neurophysiological changes in neurotransmission of inhibitory and excitatory systems. Similarly, reduced grey matter volume in the STG and Heschl's gyrus (Kasai *et al.*, 2003, Vita *et al.*, 2012), is one of the most consistent cortical changes observed in schizophrenia, and so these structural changes may also be responsible for the ASSR abnormalities. Therefore, by linking structural, neurochemical and functional information from the auditory cortex, this will help unravel the specific systems disrupted in clinical disorders and how these may lead to particular symptoms.

Hence, this study developed an auditory click-chirp stimulus to investigate the relationship between inter-subject variability in auditory peak gamma frequency and peak gamma power with auditory cortical thickness and surface area. Peak gamma frequencies and power of the

ASSR were measured from individuals by driving the auditory cortex from 10-120Hz using a click train stimulus. All individuals had previously participated in the '100 Brains' imaging project. This enabled us to determine: (1) whether the peak gamma frequency or peak gamma power in the ASSR was determined by the thickness and/or area of Heschl's gyrus (transverse temporal plane) and (2) whether peak gamma frequencies and power in the auditory domain were correlated with peak gamma frequency or power obtained in the visual domain.

6.3 Methods

6.3.1 Participants

15 healthy individuals (9 females and 6 males, all right handed) aged between 20-29 years (mean 24.1 years (SD=3.0)) and with normal hearing participated in the study. All participants had no history of neurological or neuropsychiatric disease and had previously participated in the '100 Brains' study (Chapter 3). All participants provided written informed consent.

6.3.2 Auditory Stimulus

The auditory stimulus was based upon a previously described chirp stimulus (Artieda *et al.*, 2004). However, rather than using a tone modulated in amplitude at increasing frequencies, a chirp using click trains that linearly increased in frequency was developed. This is because click trains have been shown to elicit larger ASSRs in comparison to amplitude-modulated tones (McFadden *et al.*, 2014). Auditory stimuli consisted of trains of 1-millisecond clicking sounds that either increased in frequency from 10-120Hz (chirp, Figure 1) or decreased in frequency from 120-10Hz. 120Hz was chosen as the maximum stimulation frequency as the power of the ASSR is considerably weaker beyond 120Hz (Pérez-Alcázar *et al.*, 2008). Each

chirp lasted for 1.62s followed by a 0.5s baseline period. A total of 525 chirps (500 increasing chirps and 25 decreasing chirps that were randomly ordered) were delivered binaurally through insert ear (etymotic) phones at 70dB above the participant's sound threshold level (Ross *et al.*, 2000). Subjects were instructed to listen to the chirps and in order to help maintain their attention, were asked to count how many of the chirps decreased in frequency. These 25 decreasing chirps were not used for further analysis and hence were solely presented for attention purposes. Each testing session lasted approximately 18.5 minutes. To assess the repeatability of the ASSR measures, 2 of the 15 participants repeated the testing session three times in one day at 1hr intervals. These three repeat sessions for the 2 participants were performed eight weeks after their initial participation.

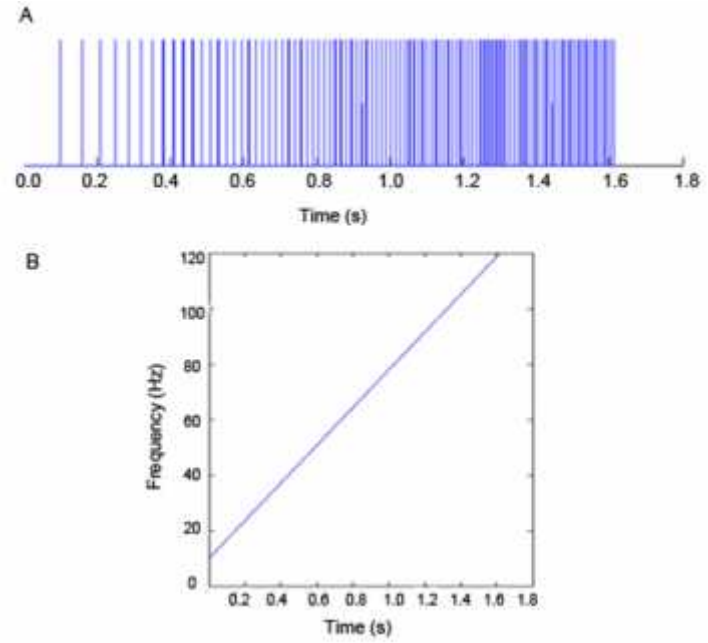

Figure 1: Auditory stimulus represented in terms of (A) click train stimulus and (B) a time-frequency figure to show the linear increase from 10-120Hz over the 1.62s stimulus period.

6.3.3 MEG Acquisition and Analysis

Whole head MEG data was acquired using a 275-channel CTF radial gradiometer system. Four of the channels were turned off due to excessive sensor noise. In addition, 29 reference

channels were recorded for noise-cancellation purposes and the primary sensors were analysed as synthetic third-order gradiometers (Vrba and Robinson, 2001). Three fiducial markers (1 nasal and 2 pre-auricular points) were placed on the participant using electromagnetic head coils and were localised relative to the MEG before and at the end of the recording session.

Offline, data sets were epoched -0.2s before stimulus onset and 1.9s after stimulus onset. Trials were visually inspected and those with large artefacts such as muscle clenching and head movement were excluded. For the 15 MEG datasets, on average 4.8% (SD 3.9, range 0-13.4%) of the 500 trials were removed. The MEG data from the axial gradiometers was converted to a planar gradient configuration (gradient tangential to the scalp) using the Fieldtrip toolbox (Oostenveld *et al.*, 2011). This conversion was performed as the power of the signal is typically largest directly above the source, which can be optimally measured using a planar gradient configuration (Bastiaansen and Knösche, 2000). Frequency analysis was performed using the Hilbert transform from 1 to 120Hz in 1Hz steps for the horizontal and vertical components of the planar gradients. Next, the two planar directions were combined to give the local maximal under the sensors.

To calculate relative changes from baseline, activity from the baseline period of -0.2 to 0s was compared to the active period of 0 to 1.9s. For each participant, the temporal sensor with the maximum response in the gamma band (30-50Hz) over the 0.35 to 0.70s time window was located for both the left and right hemisphere individually. From these maximal temporal sensors, peak frequency and peak power values in the low gamma (30-50Hz) and the high gamma (70-100Hz) band were extracted. These two gamma band ranges were chosen as all participants showed two peaks of activity within these values. This sensor-space method was

chosen over the source-space synthetic aperture magnetometry (SAM) approach, as SAM cannot accurately detect temporally correlated sources, such as bilateral auditory sources. This is due to an assumption of SAM that sources are uncorrelated in time and so for temporally correlated sources, the reconstructed source power is attenuated resulting in a reduction in the source power (Brookes *et al.*, 2007).

Visual gamma peak frequency and peak power for these 15 participants had previously been obtained from the '100 Brains' study (Chapter 3).

6.3.4 MRI Acquisition and Analysis

T_1-weighted anatomical images (FSPGR) with 1-mm isotropic resolution had previously been obtained from the '100 Brains' study (Chapter 3). From these 3D FSPGR scans, estimates for the thickness and surface area of Heschl's gyrus were obtained using an Atlas in Freesurfer template space, using Version 4.4 of the FreeSurfer package (http://surfer.nmr.mgh.harvard.edu/).

6.4 Results

6.4.1 Auditory Chirp Gamma Responses

The auditory click-chirp evoked clear sources of increased gamma activity in both the left and right temporal sensors in 11 of the 15 participants. Thus, 11 participants were included for further analysis. Figure 2A shows topographic maps with the location of increases in gamma activity (30-50Hz) for the group average (n=11) and 2 single participants. Increases in activity from baseline were stronger in the right than left hemisphere for 10 of the 11 subjects.

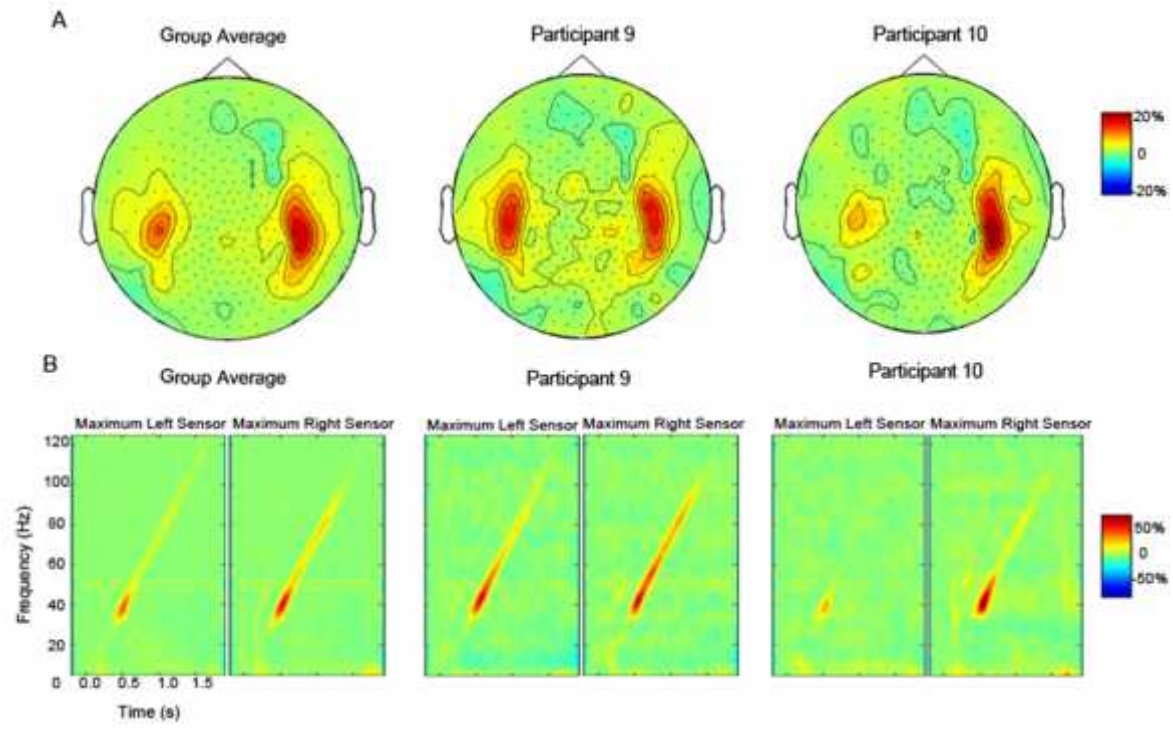

Figure 2: (A) Topographic maps showing the increased gamma activity (30-50Hz) over the left and right temporal sensors in response to the auditory click-chirp. (B) Time-frequency spectra showing the click-chirp response from the left and right maximal temporal sensor for the group average and 2 representative participants.

The time-frequency spectra from the left and right temporal sensor across individuals show a similar morphology. Characteristic components are similar to those previously reported using a 'chirp' stimulus with an amplitude-modulated tone rather than a click train (Artieda *et al.*, 2004). The ASSR starts at about 30Hz and continues linearly increasing in frequency in accordance with the frequency of stimulation until the end of the stimulus at 120Hz. The largest increase in power occurred in the 30-50Hz frequency band from 0.35 to 0.7s. A second, smaller, increase in power occurred in the 70-100Hz frequency band from 0.9 to 1.5s. In the low frequency band there is an early evoked response (M100 and P200) and an offset response at 1.7s.

As the responses showed a similar morphology in both the left and right temporal sensor but were reliably stronger in the right sensor, the peak gamma frequency and peak gamma power in the low gamma and high gamma band were extracted from the right sensor for each individual. Peak gamma frequencies in the 30-50Hz band ranged from 37 to 43Hz (mean 40.36Hz (SD= 2.11)) and ranged in power (% change from baseline) from 22 to 169 (mean 77 (SD=43), see figure 3A). Peak gamma frequencies in the 70-100Hz band had a larger range in peak frequency, from 70-84Hz (mean 78.45 (SD=4.48)) and ranged in power from 6 to 71 (mean 30 (SD =23), see figure 3B). The peak response from the low gamma frequency (30-50Hz) was not significantly correlated with the peak from the high gamma frequency (70-100Hz) (R=0.393, p=0.232), suggesting that the two responses are independent and that the high gamma response is not simply a harmonic of the low gamma response.

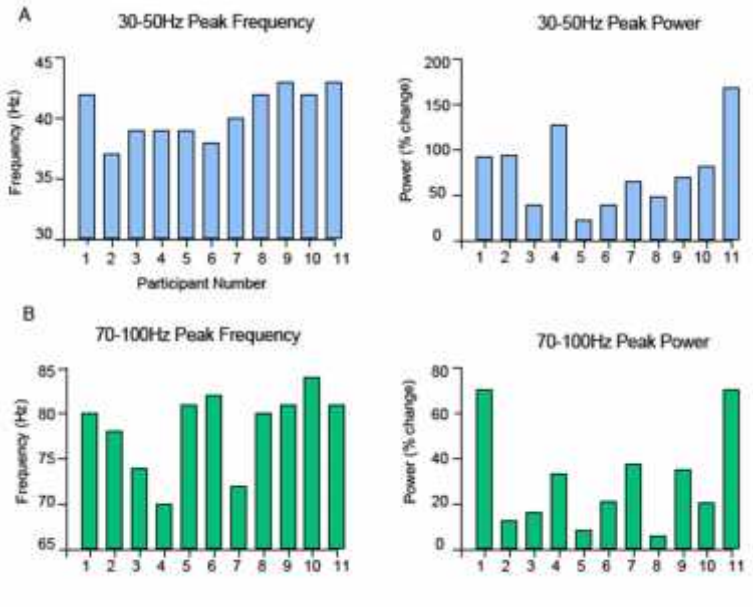

Figure 3: Peak gamma frequency and peak power in (A) the 30-50Hz gamma band and (B) the 70-100Hz gamma band for all 11 participants.

6.4.2 Repeatability of Chirp Gamma Responses

The ASSR showed a stable morphology that was repeatable across time (Figure 4).

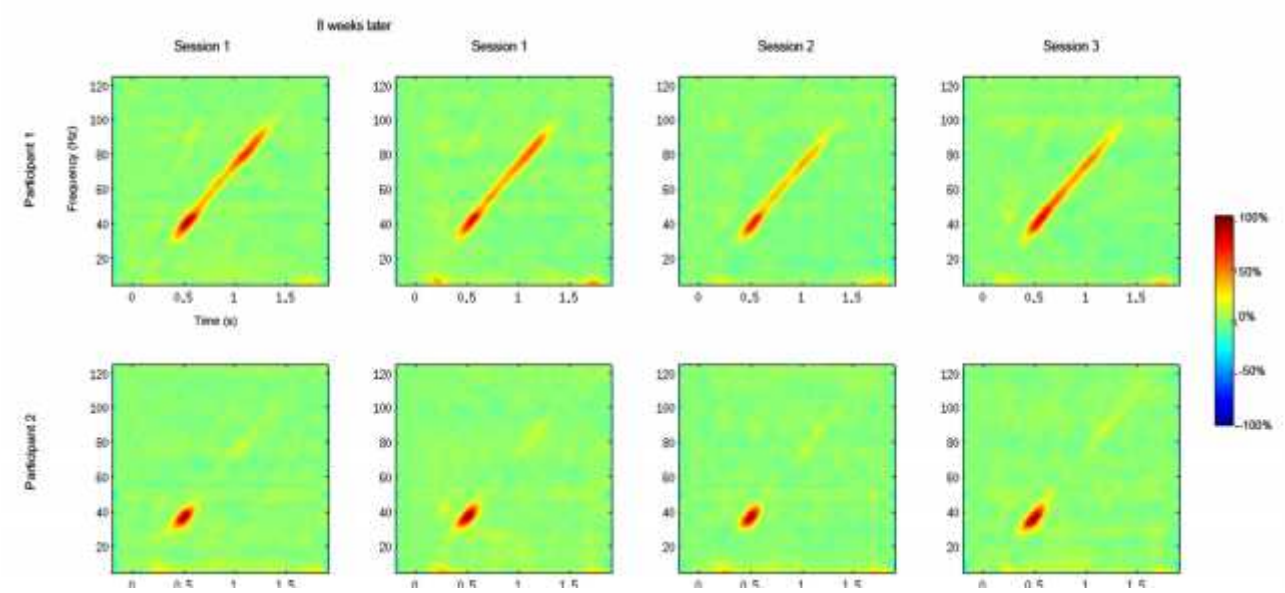

Figure 4: Time-frequency spectra from the maximal right temporal sensor of 2 participants that were scanned in the initial study (session 1) and then scanned 8 weeks later, three times in one day at 1hr intervals (session 1, 2 and 3).

The peak frequency and peak power obtained from these 2 individuals across the four sessions is displayed below and show that the 30-50Hz peak frequency measure has the strongest reliability across the sessions.

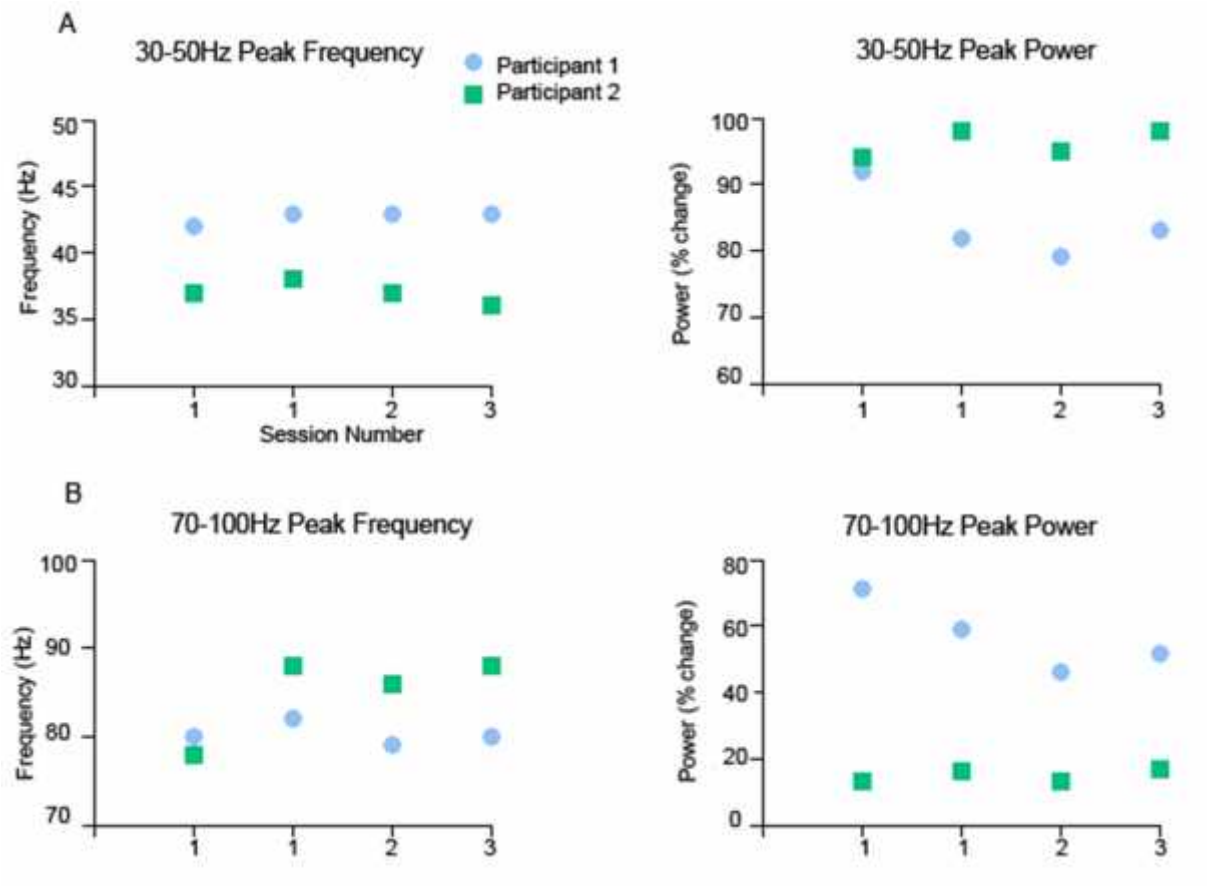

Figure 5: Plots displaying the reliability of the four gamma measures from the low gamma band (A) and the high gamma band (B) of 2 individuals, across the four different sessions.

To statistically assess the repeatability of the measures of interest (30-50Hz peak frequency, 30-50Hz peak power, 70-100Hz peak frequency and 70-100Hz peak power) the intraclass correlation coefficients (ICC) with two-way random effects and absolute agreement were calculated. The 30-50Hz peak frequency measure had a strong ICC (single measures ICC= 0.973; average measures ICC=0.993), as did the 30-50Hz peak power (single measures ICC= 0.743; average measures ICC=0.920). The 70-100Hz peak frequency measure also had a weaker ICC (single measures ICC= 0.453; average measures ICC=0.768) and the 70-100Hz peak power had a strong ICC (single measures ICC= 0.933; average measures ICC=0.982).

6.4.3 Auditory Structural Properties

From the 11 participants that produced clear ASSRs, the thickness of the right HG ranged from 2.41mm to 2.89mm (mean 2.67 (SD 0.13)) and the surface area of the right HG ranged from 298cm^2 to 394cm^2 (mean 339 (SD 34)).

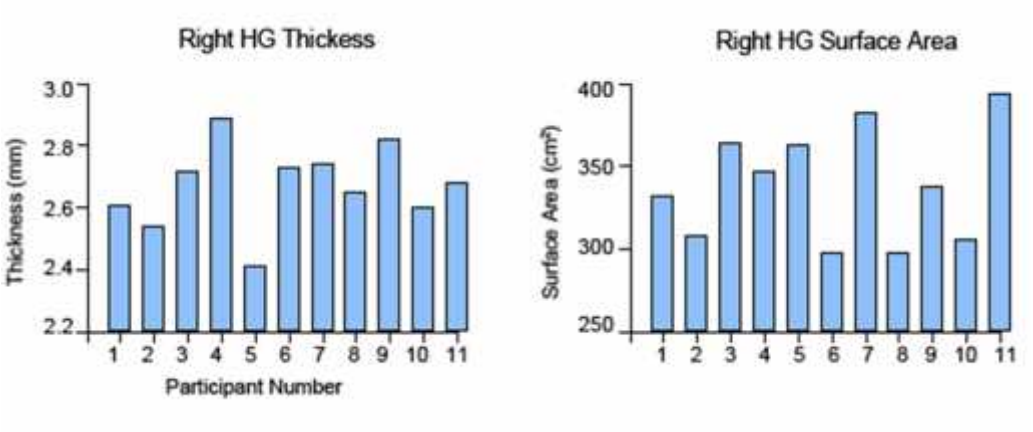

Figure 6: Histogram showing the thickness and surface of the right HG for the 11 participants.

6.4.4 Visual Gamma Responses

From the 11 participants, visual gamma peak frequency ranged from 36.5Hz to 58.5Hz (mean 50.5 (SD 5.5)) and visual gamma peak power (% change from baseline) ranged from 26.59% to 89.75% (mean 52.76 (SD 17.61)).

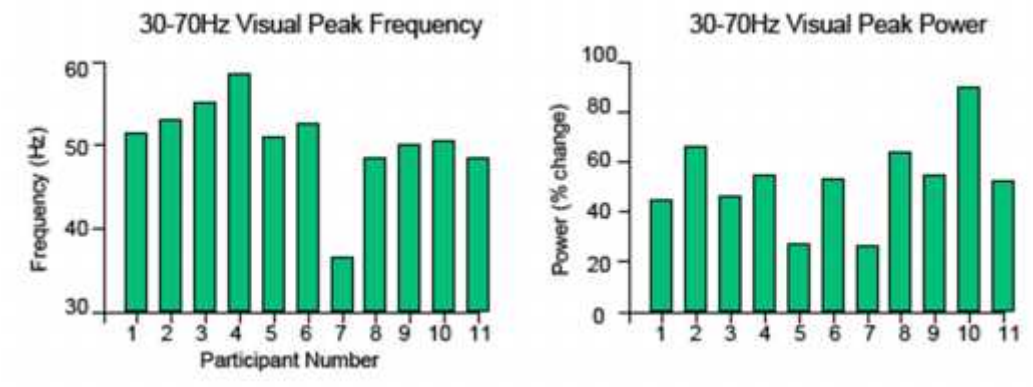

Figure 7: Histogram showing the peak visual gamma frequency and peak visual power for the 11 participants.

6.4.5 Correlational Analysis

Table 1: Correlations between ASSR gamma responses with auditory structural properties and visual gamma responses

	Age	Right HG Thickness	Right HG Surface Area	Visual Gamma Peak Frequency	Visual Gamma Peak Power
30 to 50Hz ASSR Peak Frequency	R=0.502 P=0.115	R=0.155 P=0.649	R=0.163 P=0.633	R=-0.294 P=0.380	R=0.205 P=0.546
30 to 50Hz ASSR Peak Power	R=0.391 P=0.234	R=0.305 P=0.362	R=310 P=0.354	R=0.096 P=0.778	R=0.270 P=0.423
70 to 100Hz ASSR Peak Frequency	R=0.376 P=0.254	R=-0.511 P=0.109	R=-0.426 P=0.191	R=0.008 P=0.981	R=0.411 P=0.209
70 to 100Hz ASSR Peak Power	R=0.110 P=0.748	R=0.259 P=0.441	R=0.473 P=0.142	R=-0.168 P=0.622	R=-0.178 P=0.601

Firstly, correlational analysis between age and the four ASSR measures was performed as age has previously been found to negatively correlate with the 30-50Hz peak frequency of the ASSR (Purcell *et al.*, 2004). Age was not significantly associated with any of the four auditory measures and so was not included for further analysis. None of the four ASSR measurements (30-50Hz peak frequency, 30-50Hz peak power, 70-100Hz peak frequency and 70-100Hz peak power) were significantly associated with either the structural properties of the right HG (thickness or surface area) or visual gamma responses (visual gamma peak frequency or visual gamma peak power).

6.5 Discussion

This study has developed an auditory click-chirp stimulus that reliably produces a continuous ASSR over a broad range of frequencies. This allows for both low and high gamma frequency ASSRs to be simultaneously measured. This is highly beneficial for clinical investigations as both low and high gamma oscillations have been found to be altered in schizophrenia and bipolar disorder (Grützner *et al.*, 2013, Hamm *et al.*, 2011, Oda *et al.*, 2012). Another advantage of this stimulus is that it provides further information about the

ASSR, as in addition to measuring individual differences in the *power* of the ASSR, individual differences in peak *frequency* can also be measured.

Essentially, the click-chirp revealed two main increases in gamma power, one being in the 30-50Hz range and another in the 70-100Hz range (Figure 2B and Figure 4), that were maximal in the temporal sensors of the right and left hemisphere (Figure 2). These findings coincide with previous studies that have shown the ASSR produces maximal responses in the 30-50Hz and 80-120Hz range (Alegre *et al.*, 2008, Artieda *et al.*, 2004) and have been localised to the auditory cortex (Herdman *et al.*, 2003, Pantev *et al.*, 1996, Pastor *et al.*, 2002). The high gamma response (70-100Hz) was also weaker in power than the low gamma response (30-50Hz) across all individuals. Although the ASSR produces the largest response at 40Hz (Galambos *et al.*, 1981), the significantly weaker high gamma response may be due to the source of this component being more subcortical, which MEG is less able to detect. This is supported by studies which have shown both brainstem/cerebellar and cortical (temporal lobe) sources to be active during the ASSR (Pastor *et al.*, 2002, Pastor *et al.*, 2008, Ribary *et al.*, 1991), but stronger activation is visible in cortical areas for lower frequencies (<50Hz) and above 50Hz, stronger activity is present in the brainstem (Herdman *et al.*, 2002, Mauer and Döring, 1999). As MEG is not sensitive enough to reliably measure deeper sources, the source of the 80Hz response was not investigated in this study. Further investigation into the primary source of the 80Hz response with this chirp stimulus would need to be verified using other imaging techniques with a higher spatial resolution, such as fMRI.

Interestingly, the power of the low and high gamma components was stronger in the right temporal sensor than the left temporal sensor in 10 of the 11 participants. This finding

coincides with other MEG studies that have found a right hemisphere dominance following binaural stimulation with 40Hz amplitude-modulated tones (Ross *et al.*, 2005), and click trains at 20, 30, 40 and 80Hz (Oda *et al.*, 2012). The reason for this right hemisphere dominance has been hypothesised to be due to the right hemisphere's sharper tuning to spectral processing in comparison to the left hemisphere which is more specialised for temporal processing (Liégeois-Chauvel *et al.*, 2001, Ross *et al.*, 2005). However, these findings and implications must be interpreted with caution as a recent EEG study has shown larger ASSRs in the left temporal hemisphere in response to 40Hz click trains (McFadden *et al.*, 2014).

Importantly, the chirp revealed that individuals differed in their peak power for both the low and high gamma response and also in their peak frequency within these two responses (Figure 3). The ICC values suggest these inter-individual differences present in all four measures were relatively repeatable within individuals, particularly for participant 2 (Figure 4 and 5). For participant 1, the repeatability was less consistent for the power of the 30-50Hz and 70-100Hz response across sessions. Due to the relatively long length of the recording session, this lower reliability in power may be due to fatigue and decreased attention (Alegre *et al.*, 2008). Even with the lower reliability for the power of the response, all four measures are statistically consistent and thus suitable for correlational analysis with auditory structural and visual oscillatory measures.

None of the four right temporal ASSR measures were significantly associated with the thickness or surface area of the right HG. So far, only one other study has investigated the effect of auditory structural properties on the ASSR (Edgar *et al.*, 2013). This study reported a positive correlation between the power of the 40Hz response and the thickness of the left

superior temporal gyrus (STG), using a sample size of 29 healthy controls. Several factors may explain this discrepancy in findings between that of Edgar et al. (2013) and this study. Firstly, this study investigated the impact of thickness from Heschl's gyrus rather than the STG, as Heschl's gyrus contains the primary auditory cortex, which is thought to be the main generator of the 40Hz ASSR (Herdman *et al.*, 2003). Secondly, the positive correlation was specific to the left STG as it was not found in the right STG, and this study investigated correlations in the right HG as these produced the stronger, more reliable findings. Lastly, the sample size in this study was much smaller (n=11 vs n=29), which greatly reduces the power to detect reliable relationships between variables. The power to detect a correlation of moderate effect size between pairs of relevant variables with a sample size of 11 is 25%. Therefore, further investigating this relationship in a larger sample size is required to determine whether the properties of auditory structures such as the STG and Heschl's gyrus influence individual differences in the peak power or peak frequency of the low and high gamma ASSRs.

In addition, no association was found between the peak frequency of the ASSR (30-50Hz and 70-100Hz) and the peak gamma frequency (30-70Hz) obtained from the visual cortex in response to a high-contrast grating. Similarly, the peak power of the ASSR (30-50Hz and 70-100Hz) was not associated with the peak power of the visual gamma response. These findings are not surprising, seeing as the auditory gamma activity represents a *steady-state response* and the visual gamma activity represents an *induced response*, which may have different neural sources and functional processes (Krishnan *et al.*, 2005a). In the visual system, a static grating is able to induce an oscillatory gamma response within the primary visual cortex, the frequency of which appears to be a stable trait marker within an individual and hence represents a characteristic 'resonance' of the visual system. In the auditory domain, no reliable analogue of a static visual stimulus has been found that induces auditory

gamma. However, by using an evoked design that uses varying frequency of stimulation, as with the chirp used here, the assumption is that the peak stimulus response frequency also represents a similar 'resonance' within the individual's auditory system. The lack of association between these visual and auditory oscillatory resonant frequencies suggests differences in neural circuitry between the two sensory domains, in agreement with recent evidence (Linden and Schreiner, 2003, Read *et al.*, 2002, Smith and Populin, 2001). As sensory gamma oscillations depend on the balance between GABAergic and glutamatergic neurotransmission via reciprocally connected parvalbumin expressing interneurons and excitatory pyramidal cells (Whittington *et al.*, 2011) there may be specific differences in the number, type or the strength of connectivity in these neurons.

Although no relationship was found between individual variation in gamma power and frequency with auditory structural properties, this study provides a platform for future studies to investigate the factors underlying individual differences in the ASSR. As in other sensory domains, identifying the factors underling individual variability in the ASSR is behaviourally and clinically important (Cheyne and Ferrari, 2013, Kanai and Rees, 2011). Supporting this, in healthy individuals the power of the 40Hz ASSR has been shown to positively correlate with speech recognition (Manju *et al.*, 2014) and in MS patients the frequency of the ASSR (30-50Hz) has been associated with verbal memory and attention-executive functioning tests (Arrondo *et al.*, 2009). In psychiatric populations, the power of the 80Hz ASSR negatively correlates with scores from the Hamilton Depression Rating Scale and global hallucinatory experiences (Oda *et al.*, 2012, Tsuchimoto *et al.*, 2011). In addition, the power of the 40Hz ASSR has been found to be reduced in adults with autism spectrum disorder (ASD) and parents of children with ASD, with the power of the 40Hz response being negatively correlated with the Social Responsiveness Scale (SRS) (Rojas *et al.*, 2008, Rojas *et al.*,

2011). Thus, the altered 40Hz ASSR found across different disorders may be indicating a widespread alteration in biological mechanisms, which consequently lead to various symptoms and altered behaviours.

Given that cortical gamma oscillations depend on GABAergic and glutamatergic function (Bartos *et al.*, 2007, Buzsaki and Wang, 2012), determining the effect of *in vivo* GABA and Glx (glutamate and glutamine) measures from the auditory cortex on the peak frequency and power of the ASSR would be of particular interest. The dependency of the 40Hz ASSR on GABAergic and glutamatergic function has been supported by several studies via pharmacological manipulation (Plourde *et al.*, 1997, Sivarao *et al.*, 2013, Vohs *et al.*, 2010). In conjunction, abnormal excitatory/inhibitory cortical balance is well documented in psychiatric populations and schizophrenia and bipolar individuals demonstrate altered ASSRs (O'Donnell *et al.*, 2013, Oda *et al.*, 2012, Spencer, 2012, Tsuchimoto *et al.*, 2011). Therefore, this stimulus may be of particular use to identify particular biological pathways in the auditory system that may lead to an altered ASSR, which may consequently lead to differences in auditory perception.

In addition, although the power and frequency of the gamma oscillations did not correlate across the auditory and visual cortex further understanding the similarities and differences between these two sensory modalities is clinically important. In psychiatric patients, decreased gamma power is found in both the visual and auditory cortex (Grützner *et al.*, 2013, Oda *et al.*, 2012, Rass *et al.*, 2010). As increasing GABAergic function increases the power of the gamma ASSR (Vohs *et al.*, 2010) and the power of visual gamma oscillations (Campbell *et al.*, 2014, Saxena *et al.*, 2013) this suggests these patients have a widespread

deficit in cortical GABAergic function. However, further work is needed to determine the precise GABAergic pathways affected and whether these are modality specific.

Overall, this study shows that a click-chirp stimulus provides a powerful tool in which to probe the factors underlying individual variability of the ASSR. Identifying these factors will (1) enable comparisons across other sensory modalities, (2) increase our understanding of the biological substrates that lead to altered oscillatory activity and (3) how these substrates may consequently influence perception in both health and disease.

Chapter 7 - General Discussion

This thesis used a combination of structural and functional neuroimaging measures, as well as genetic data, to increase our understanding of individual variation in genes and brain structure/function in the visual and auditory system of healthy individuals and psychiatric disorders. Specifically, four main experimental questions were investigated: firstly, (Chapter 3) whether differences in the structural and neurochemical properties of the visual cortex explain individual variation in visual gamma frequency; secondly, (Chapter 4) whether genetic variation influences individual variation in resting occipital GABA+ levels or visual gamma frequency; thirdly, (Chapter 5) to determine if occipital GABA+, V1 structure or visual gamma oscillations are altered in SABP and lastly, (Chapter 6) to determine if individual differences in auditory steady-state gamma oscillations can be explained by individual differences in the structure of the auditory cortex.

7.1 Summary of Experimental Results

Previously, positive correlations between the structural parameters of V1 (thickness and surface area) and MRS GABA+ levels with visual gamma peak frequency have been reported (Gaetz *et al.*, 2012, Muthukumaraswamy *et al.*, 2009, Muthukumaraswamy *et al.*, 2010, Robson, 2012, Schwarzkopf *et al.*, 2012). However, these studies used small sample sizes or slightly different stimulus parameters across participants. Thus, Chapter 3 investigated the relationship between these imaging variables using identical stimulus parameters in a large cohort of 100 healthy individuals that were homogenous in terms of age, ethnicity, education and handedness. Using this large homogenous cohort, neither the structural properties of the visual cortex (thickness or surface area) nor resting occipital GABA+ levels were found to be associated with visual gamma peak frequency.

Genetic variation may be another factor influencing downstream individual variation in both gamma peak frequency and cortical GABA levels (Hasler and Northoff, 2011, Marenco *et al.*, 2010, van Pelt *et al.*, 2012). Hence, Chapter 4 looked at the influence of genetic variation on individual variation in visual gamma frequency and occipital GABA+, using a candidate-SNP, a candidate-gene approach and a polygenic schizophrenia risk score approach. The *GAD1* candidate approach, revealed an association between three out of eight *GAD1* SNPs on occipital GABA+ levels. Specifically, the minor allele from all three SNPs was found to have a recessive effect, so that those individuals who were homozygous for the minor allele had increased levels of GABA+/Cr in comparison to those who were homozygous or heterozygous for the major allele. In contrast, none of the eight *GAD1* SNPs influenced visual gamma peak frequency. Genetic variation in the $GABA_AR$ subunit or polygenic schizophrenia risk scores were also not significantly associated with occipital GABA+ or visual gamma peak frequency.

Altered GABAergic and gamma oscillatory activity has been widely implicated in the pathophysiology of schizophrenia and bipolar disorder, via a wealth of genetic, pathological and physiological studies (Bhagwagar *et al.*, 2007, Gonzalez-Burgos *et al.*, 2010, Hashimoto *et al.*, 2003, Lewis *et al.*, 2012). However, some reports have identified no differences or opposing directions of effect within the same clinically defined psychiatric population (Ongür *et al.*, 2010, Riečanský *et al.*, 2010, Tan *et al.*, 2013, Tayoshi *et al.*, 2010, Yoon *et al.*, 2010). Therefore, Chapter 5 investigated visual gamma oscillations and occipital GABA+ in SABP individuals to further understand the neurochemical and neurophysiological changes present in psychiatric populations. SABP individuals were found to have increased visual gamma power compared to healthy individuals, both at the group level and individually, as 14 of the 15 SABP individuals tested had increased power relative to their matched control. No group

differences were found for other MEG visual measures (baseline gamma power, transient or sustained gamma frequency, alpha band responses and visual evoked responses) or MRS occipital GABA+ levels.

Although differences in structural and neurochemical measures have been identified as potential factors influencing individual variation in peak gamma response frequency in both the visual and motor cortex (Gaetz *et al.*, 2011, Gaetz *et al.*, 2012, Muthukumaraswamy *et al.*, 2009, Muthukumaraswamy *et al.*, 2010, Schwarzkopf *et al.*, 2012), these relationships have not been studied in the auditory domain. Determining the factors underlying the peak response frequency in the auditory domain is equally important as the visual and motor domain. Chapter 6 found neither the thickness nor surface area of the right HG to be associated with the peak gamma frequency or power of the low (30-50Hz) or high (70-100Hz) gamma ASSR in the right auditory cortex. Also, the peak response frequency in the auditory cortex was not associated with the peak response frequency in the visual cortex, suggesting these oscillatory responses are regionally specific.

7.2 Interpretation of Results and Future Directions

7.2.1 Occipital GABA, V1 Structural Properties and Visual Gamma Frequency

The lack of association between occipital GABA+ and visual gamma peak frequency opposes preclinical evidence supporting the strong dependence of gamma oscillatory activity on GABAergic circuitry (Buzsaki and Wang, 2012, Cardin *et al.*, 2009) and the initial finding of a positive correlation between the two neuroimaging measures (Muthukumaraswamy *et al.*, 2009). However, the null finding does agree with more recent research using larger sample sizes that no relationship exists between MRS measured GABA+ and MEG measured gamma frequency (Cousijn *et al.*, 2014, Shaw *et al.*, 2013). The lack of consistency between this

study and more recent studies with the initial report shows how important it is for the scientific community to use large sample sizes and replication, in order to increase the likelihood that findings reflect a true association (Button *et al.*, 2013).

Despite the lack of association between GABA+ and gamma frequency found in this study, substantial computational and experimental studies indicate that GABAergic transmission, via mutually connected interneurons and pyramidal cells is vital in the generation of gamma oscillations (Brunel and Wang, 2003, Traub *et al.*, 1997, Traub *et al.*, 1996). In addition, positive correlations between MRS GABA and gamma frequency have been reported in other brain areas, including the primary motor cortex (Gaetz *et al.*, 2011) and the left DLPFC (Chen *et al.*, 2014). Thus, these two imaging studies suggest that MRS GABA and gamma frequency are associated and that a common GABAergic mechanism in regulating gamma frequency is present across cortical regions. However, these two imaging studies have two main limitations that question the reliability of a true association between gamma frequency and GABA: small sample sizes (n=9 and n=16, respectively) and relatively large age ranges (22.7-42.7 and 21-49 years, respectively). Small sample sizes are a well-known problem in neuroimaging studies and can increase the likelihood of false positive findings. Also, gamma frequency and GABA levels change with age (Gaetz *et al.*, 2011, Gaetz *et al.*, 2012, Gao *et al.*, 2013, Muthukumaraswamy *et al.*, 2010) and previous correlations between these two measures have been proposed to be due to their mutual relationship with age (Gaetz *et al.*, 2012, Robson, 2012). Thus, before a reliable and strong association between *in vivo* GABA and gamma frequency across cortical regions can be confirmed using neuroimaging techniques, these findings need to be verified in studies with larger participant numbers and with reduced confounding variables such as age.

A crucial reason for the lack of a consistent association between GABA+ and gamma frequency across imaging studies may be due to the MRS GABA+ measure not consistently reflecting the inhibitory activity that is most relevant for gamma frequency. In the neocortex, the inhibitory activity from interneurons expressing the calcium binding protein parvalbumin (PV), plays a particularly important role in the generation of gamma oscillations (Cardin *et al.*, 2009, Sohal *et al.*, 2009) because of their fast-spiking characteristics (Bartos *et al.*, 2007). These PV-expressing interneurons are the largest subclass of inhibitory interneurons, accounting for 40% of GABAergic neurons (Xu *et al.*, 2010), but whether their activity/function is accurately represented by MRS GABA+ measures is unclear. MRS GABA+ could also not be specific enough to functional GABA, as the GABA+ measure is obtained from a large volume which may not all represent functional GABA, and up to 40% of the GABA+ MRS signal is from macromolecules (Harris *et al.*, 2014). In addition, computational and pharmacological studies have revealed that gamma *frequency* relies on a complex local network, controlled by the excitatory/ inhibitory balance (Brunel and Wang, 2003) and the kinetics of inhibitory postsynaptic potentials (IPSPs) (Bartos *et al.*, 2007). For example, Whittington et al. (1995 and 2000) has shown that increasing the decay time of $GABA_AR$ mediated IPSPs either by computer simulation or application of $GABA_AR$ modulating drugs leads to a decrease in oscillation frequency (Whittington *et al.*, 1995, Whittington *et al.*, 2000). Thus, even if GABA+ measures are accurately reflecting the activity of PV-expressing interneurons, due to the combination of factors controlling gamma frequency, accurate and consistent associations between GABA+ and gamma frequency may be difficult to obtain.

The use of small sample sizes and confounding factors such as age used in previous studies may also be accountable for unreliable relationships being previously reported between V1

structural measures and visual gamma frequency (Gaetz *et al.*, 2012, Muthukumaraswamy *et al.*, 2010, Schwarzkopf *et al.*, 2012). Given that the study in this thesis used a large and homogenous sample but still found no association between either V1 thickness or surface area with gamma frequency, this would suggest that no association exists between these measures. However, a lack of dependency of gamma frequency on the structural measures of V1 would be surprising. Given that MR-measures of structural differences are thought to reflect differences in the number and type of interneurons/pyramidal cells (Rakic, 1988) and possibly their dendritic connectivity density, these cortical circuitry changes would strongly affect the excitatory and inhibitory neurotransmission, and thus gamma frequency. This is supported by computational studies showing that varying the strength of excitatory input to interconnected interneurons and pyramidal cells alters gamma frequency (Jia *et al.*, 2013, Spencer, 2009). Therefore, as discussed with the GABA+ measure, the structural measures of V1 may in fact be strongly influencing individual variation in gamma frequency, but the structural measures lack the relevant specificity and their precise dependency on underlying neuronal structure is unknown (Eriksson *et al.*, 2009). Finally, the V1 structural measures obtained in this thesis are a global representation of V1 structure (including all 6 cortical layers), whereas only cortical layers 2, 3 and 4 are most relevant to gamma-band oscillations (Xing *et al.*, 2012). Thus, structural measures encompassing only layers 2, 3 and 4 may be more useful.

Even with the complexity of factors involved in gamma oscillatory activity, understanding the underlying mechanisms driving individual variation in frequency remains important as this will reveal more about the functional role of these oscillations. A potential factor driving inter-individual in visual peak response frequency that warrants investigation is the effective connectivity of V1. Recently, inter-individual differences in the cortical effective

connectivity of V1 (estimated using fMRI and dynamic causal modelling (DCM)) was shown to positively correlate with individual variability in the tilt illusion (Song *et al.*, 2013) and orientation perception has been shown to be predicted by GABA and peak gamma frequency (Edden *et al.*, 2009, Yoon *et al.*, 2010). Thus, effective connectivity of V1 may be driving individual variation in gamma frequency, which consequently leads to alterations in visual perception, such as orientation perception. Overall, these studies show how important it is for future studies to combine different imaging modalities with preclinical and behavioural data as significant insights into the behavioural consequences of biological variation are revealed.

7.2.2 Effect of Genetic Variation on Occipital GABA and Visual Gamma Frequency

Encouragingly, Chapter 4 revealed a significant association between three *GAD1* SNPs and *in vivo* occipital GABA+ levels. These findings build upon previous genetic imaging evidence that individual variation in *GAD1* influences individual variation of *in vivo* cortical GABA levels (Marenco *et al.*, 2010). In addition, the association implies that cortical MRS GABA measures are influenced at a genetic level and reflect a downstream biologically relevant GABAergic measure. The findings from this thesis are important from a clinical perspective, as the *GAD1* alleles (minor alleles) that were linked with decreased GABA levels have been associated with increased risk for schizophrenia, bipolar disorder and panic disorder (Addington *et al.*, 2005, Du *et al.*, 2008, Lundorf *et al.*, 2005, Straub *et al.*, 2007, Weber *et al.*, 2012). Decreased MRS GABA levels have been reported in a range of cortical regions, including the occipital cortex,(Goddard *et al.*, 2001, Yoon *et al.*, 2010) anterior cingulate (Rowland *et al.*, 2013) and prefrontal cortex (Long *et al.*, 2013, Marsman *et al.*, 2014) across major psychiatric disorders. Therefore, the findings from this thesis provide an important link between GABA pathophysiology and common genetic variation, by

suggesting that lowered GABA levels observed in disorders such as schizophrenia are the biological consequence of *GAD1* schizophrenia risk-associated alleles.

As many reports have also discovered lowered *GAD1* mRNA expression (Hashimoto *et al.*, 2008, Thompson *et al.*, 2009, Thompson Ray *et al.*, 2011, Volk *et al.*, 2012) and lowered GAD67 protein levels (Curley *et al.*, 2011, Guidotti *et al.*, 2000) across various brain regions (particularly in the DLPFC but also in the visual cortex), this leads to a strong assumption that *GAD1* risk alleles lead to decreased GABA levels via lowered mRNA expression and less translation of the corresponding GAD67 protein. However, this clear directional relationship between gene expression level, protein level and neurotransmitter level was not present in this study, as the three *GAD1* risk associated alleles that were associated with lowered occipital GABA+ levels, were associated with increased *GAD1* mRNA expression in the occipital cortex (Ramasamy *et al.*, 2014). Other studies have also reported an inconsistent directional relationship across gene expression, protein and neurotransmitter levels. Dracheva et al. (2004) found elevated levels of *GAD1* mRNA in the DLPFC and occipital cortex of elderly schizophrenia patients but the corresponding GAD67 protein levels were unchanged (Dracheva *et al.*, 2004). This shows a clear need for a further understanding of the molecular mechanisms of action of *GAD1* variants on mRNA and subsequent protein levels.

Understanding whether these molecular mechanisms of action of *GAD1* variants are similar across different *GAD1* variants, across different cortical regions and in different types of schizophrenia populations (chronic vs recently diagnosis) will also allow other key questions to be answered. For example, a major difference between this study and that of Marenco et al. (2010) is the directional effect of *GAD1* risk associated alleles on resting GABA+ levels; this thesis found schizophrenia risk-associated alleles were related to *decreased occipital* GABA

levels, whereas Marenco et al, (2010) found the risk associated alleles were related to *increased ACC* GABA levels. As the latter findings were found in the ACC rather than the occipital cortex, these opposing directional effects could be due to regional specificity of genetic variants. This is supported by post-mortem and imaging studies, showing that *GAD1* mRNA expression and *in vivo* GABA levels are differentially modulated across brain regions and so are likely to have different functional effects (Boy *et al.*, 2010, Fong *et al.*, 2005, Puts *et al.*, 2011, Ramasamy *et al.*, 2014). A further example is that although the majority of studies report a general deficit in GABAergic measures for schizophrenia individuals, elevated levels of GABA have been reported in the anterior cingulate, parieto-occipital cortices and PFC (Kegeles *et al.*, 2012, Ongür *et al.*, 2010). Understanding the mechanisms of genetic variation could help explain these type of discrepancies across studies, such as whether they are due to individuals having different *GAD1* variants that lead to opposing effects or other factors such as medication.

The findings from Chapter 4 provide crucial support for the usefulness of candidate SNP studies and strong evidence for *GAD1* variants influencing cortical GABA levels. However, the major limitation of small sample groups (when individuals are grouped based on genotype) must be acknowledged. As the majority of single genetic variants have small effect sizes on downstream functional measures the small genotype groups in this study may have led to an overestimation of *GAD1* effects on GABA. The relatively small sample size may also be a contributing factor as to why the *GAD1* variants were not found to influence peak gamma frequency. *GAD1* variation would be expected to influence the GABAergic function of PV interneurons and thus gamma frequency but as gamma frequency is likely to reflect a more downstream and less direct measure of GABAergic activity compared to MRS GABA, larger sample sizes may be needed to detect this effect. Therefore, future studies must address

that despite the time and expense required, genetic imaging studies require large sample sizes (in hundreds or thousands) in order for obtaining reliable results and to enable the detection of small effect sizes.

Another key issue that future genetic imaging studies must acknowledge is that both biological and clinically defined psychiatric phenotypes are most likely to be influenced by multiple genetic factors, which they themselves are affected by environmental elements (Consortium, 2014, Purcell *et al.*, 2009). For example, in this study the levels of occipital GABA+ are likely to be influenced by a complex network of components that regulate GABAergic circuitry/activity such as $GABA_A$ receptors, GABA transporters, or developmental growth factors (BDNF and neuregulin 1 (NRG1)-ErbB4 signalling) (Fazzari *et al.*, 2010, Marenco *et al.*, 2011, Subburaju and Benes, 2012). Therefore, the corresponding genes regulating these components also merit investigation into their effect on cortical GABA and gamma frequency. Although the effect of other components and multiple SNPs on GABA+ and gamma frequency were taken into account in this thesis by using $GABA_AR$ subunit genes and schizophrenia polygenic risk scores, neither of these approaches revealed significant associations of genetic variation with GABA+ or gamma frequency. These null findings could reflect a true lack of effect but would need to be verified in a large independent sample. Given the dependence of GABA and gamma on $GABA_AR$ function, the surprising lack of association raises the important issue of specificity when incorporating the effect of multiple SNPs/genes on imaging measures. Only certain SNPs/genes may be significantly involved in biological/clinical phenotypes and including multiple variants may be incorporating 'noise' into the analysis, masking the true effect of particular SNPs. Therefore, a major challenge for future imaging studies is to balance specificity and sensitivity, to ensure that enough genetic variation is included but that it is still specific

enough in regards to the imaging measure. Despite these caveats, it is clear that through this study and others, combining genetic and imaging data is truly advantageous in helping us bridge the gap between genes, neurobiology and behaviour (Linden, 2012, Meyer-Lindenberg, 2010b, Muñoz *et al.*, 2009).

7.2.3 GABA and Gamma in SABP

Chapter 5 revealed that SABP individuals had a significant increase in visual gamma power in comparison to their age and gender matched healthy control. These findings were not as expected, as the majority of other studies have reported that schizophrenia/SABP subjects have decreased gamma power in a range of cortical regions (Cho *et al.*, 2006, Kwon *et al.*, 1999, Minzenberg *et al.*, 2010, Wynn *et al.*, 2005), including the occipital cortex (Grützner *et al.*, 2013). As discussed in Chapter 5, several reasons may account for this discrepancy with other literature: (1) this study looked at induced responses rather than early evoked responses; (2) the visual stimulus is less cognitively demanding compared to stimuli (working memory) used in other studies and (3) the clinical population only included SABP individuals rather than schizophrenia subjects or a combination of schizophrenia and SABP subjects.

Importantly, increased visual gamma power in SABP subjects indicates that an underlying pathophysiology is present in this clinical population. As no group differences were present for MRS GABA and gamma frequency measures, this suggests the prime pathophysiology does not involve GABAergic transmission, which agrees with previous studies showing no relationship between MRS occipital GABA and visual gamma power (Cousijn *et al.*, 2014, Muthukumaraswamy *et al.*, 2009). Instead, substantial evidence points towards a key alteration in glutamatergic function, in which *NMDA receptor hypofunction* reduces the firing rate of PV interneurons, resulting in the disinhibition of pyramidal neurons and a subsequent

increase in pyramidal neuronal activity (Homayoun and Moghaddam, 2007). This proposed mechanism of action is supported by *in vitro* and *in vivo* rat studies that have shown NMDAR blockade via application of MK-801 or ketamine (NMDAR antagonists) leads to a decrease in the firing rate of interneurons but an increase in the firing rate of pyramidal neurons and increased gamma power (Anver *et al.*, 2011, Hakami *et al.*, 2009, Hiyoshi *et al.*, 2014, Homayoun and Moghaddam, 2007). In addition, genetic ablation of the NMDAR in PV interneurons of mice leads to increased gamma power (Carlén *et al.*, 2012). This hypothesis of increased gamma power due to NMDAR hypofunction is also translatable to humans, as sub-anaesthetic doses of ketamine increase gamma responses to auditory stimuli (Hong *et al.*, 2010) and increases glutamatergic transmission in the anterior cingulate cortex of healthy individuals (Stone *et al.*, 2012).

A possible dysfunction of the NMDAR in SABP subjects is highly plausible, as this adheres to the NMDAR hypofunction hypothesis of schizophrenia (Gilmour *et al.*, 2012, Moghaddam and Javitt, 2012). This hypothesis originated from the observation that administration of NMDAR antagonists to schizophrenia individuals exacerbates their psychotic and cognitive symptoms (Lahti *et al.*, 1995, LUBY *et al.*, 1959), while in healthy individuals NMDAR antagonists induce the psychotic, negative and cognitive symptoms associated with schizophrenia (DAVIES and BEECH, 1960, Krystal *et al.*, 1994, Rowland *et al.*, 2005). Further evidence has now added to the involvement of the NMDAR in the etiology and pathogenesis of schizophrenia, via genetic (Kirov *et al.*, 2012, Martucci *et al.*, 2006), post-mortem (Law and Deakin, 2001) and imaging studies (Pilowsky *et al.*, 2006, Rowland *et al.*, 2013). Therefore, the findings from this thesis and other literatures point towards a main dysfunction in the NMDAR in SABP, which leads to increased gamma power.

The finding of no group difference in MRS GABA levels or gamma frequency was not as expected, due to the substantial evidence showing that a general deficit in GABAergic function is found in schizophrenia, bipolar disorder and SABP individuals (Curley *et al.*, 2011, Ferrarelli *et al.*, 2012, Hashimoto *et al.*, 2003, Lewis *et al.*, 2012, Yoon *et al.*, 2010). Based on the assumption that a reduction in GABAergic activity is secondary to the NMDAR hypofunction, alterations in GABA or gamma frequency may be less prominent and so larger sample sizes may be needed to detect these differences. Interestingly, a crucial mechanistic link between NMDAR dysfunction and diminished GABAergic function has been identified, which may explain how both altered glutamatergic and GABAergic function are found in psychiatric disorders. Behrens et al. (2007) have shown that in primary neuronal cultures, prolonged exposure to ketamine causes the activation of NADPH oxidase (an enzyme that generates the toxic reactive oxygen species superoxide) and subsequent toxic levels of free radicals lead to a down regulation of GAD67 enzyme in PV expressing interneurons (Behrens *et al.*, 2007). Therefore, it may be that psychiatric populations including SABP have alterations in both inhibitory and excitatory transmission, partly due to this intracellular mechanism that link the two together.

Understanding how these alterations in visual gamma parameters (power or frequency) may translate into functional differences is important, as this may explain why clinical populations experience certain dysfunctions in visual processing/perception (discrimination of orientation, motion and object size (Butler *et al.*, 2008, Chen, 2011, Tadin *et al.*, 2006, Yoon *et al.*, 2010)). As patients in this thesis were remitted and had low symptom scores, any possible relationship between increased gamma power and visual symptoms or broader symptom measures (SAPS or SANS) could not be investigated. Other studies have found associations of visual gamma power with the positive (hallucinations and delusions) (Spencer

et al., 2004, Uhlhaas *et al.*, 2006) and negative symptoms (disorganisation) (Grützner *et al.*, 2013) of schizophrenia, which supports a general role of gamma band oscillations in visual processing. However, exactly what role gamma band oscillations play in visual processing/perception is still under considerable debate (Fries, 2009, Mazaheri and Van Diepen, 2014, Ray and Maunsell, 2010). In terms of narrowband gamma oscillations obtained in this thesis, it is clear that the parameters (power and frequency) depend on the size, (Perry *et al.*, 2013), contrast, (Hall *et al.*, 2005) orientation (Koelewijn *et al.*, 2011), and motion (Swettenham *et al.*, 2009) of the grating stimuli, and so imply these oscillations have a role in encoding stimulus properties. However, whether these oscillations are essential for all types of visual processing is not clear as a recent study has shown that narrow gamma band oscillations are not elicited by all types of visual stimuli (Hermes *et al.*, 2014). Therefore, a challenge for future studies is to determine the exact role of gamma band oscillations in visual perception and what particular visual deficits arise when abnormalities are present.

In order to advance our understanding of the role of gamma band oscillations in clinical populations, it is essential that centres work together in obtaining data by using the same experimental procedures, so that data across centres can be combined. This will greatly reduce inconsistencies across studies which may arise from using small sample sizes or different experimental techniques which lead to different types of participant responses. More studies also need to focus on comparing different patients populations (i.e. schizophrenia, SABP and bipolar disorder) and compare medicated vs unmedicated populations. This may ultimately reveal whether similarities or differences are present in the pathophysiology of these clinically defined populations and will help the development of more targeted treatment strategies.

7.2.4 A1 Structural Properties and Auditory Gamma Oscillations

Chapter 7 showed the development of an auditory click-chirp stimulus that has the advantage of measuring the auditory steady-state response (ASSR) across a broad frequency range, while still efficiently detecting the two largest responses at 40Hz and 80Hz. This provides a richer representation of the ASSR in comparison to other studies that typically only measure the ASSR to 40Hz or 80Hz stimulation independently (Oda *et al.*, 2012, Pastor *et al.*, 2002, Ross *et al.*, 2005, Spencer *et al.*, 2009). Interestingly, the ASSR showed inter-individual variability in the peak frequency and peak power of the response in the gamma band, as is found in the visual domain in response to a static visual grating (Hoogenboom *et al.*, 2006, Muthukumaraswamy *et al.*, 2010). The similarity of these gamma response parameters (peak frequency and power) between the visual and auditory system would suggest that similar variables may be driving these oscillatory responses and that they may be analogous in representing the 'resonance' of their respective sensory domain. If similar factors are driving the variability in peak frequency and power in both sensory domains, then investigating the influence of GABA/glutamate levels and structural parameters on the ASSR is of great interest, as these measures have been implicated in visual peak frequency and visual peak power (Gaetz *et al.*, 2012, Muthukumaraswamy *et al.*, 2009, Schwarzkopf *et al.*, 2012, Spencer, 2009).

In this thesis, no correlational relationship was found between the structural parameters of the right HG (thickness or surface area) with the peak frequency or peak power of the ASSR (within either 30-50Hz or 70-100Hz range) from the right hemisphere. Only one other study has reported an association between an auditory structural measure and the ASSR, in which the power of the 40Hz response was positively correlated with the thickness of the left STG (Edgar *et al.*, 2013). A similar association may not have been found in this thesis because: (1)

associations were tested in the HG rather than the STG, and although both are auditory structures they have different morphologies (Abdul-Kareem and Sluming, 2008, Taylor *et al.*, 2005); (2) positive associations detected by Edgar et al. (2013) were in the left STG but not in the right STG, and this thesis only tested associations in the right HG due to their stronger reliability; (3) a small sample was used in this thesis. Thus, it is possible that variability in auditory structural properties may play a role in determining the variability in peak frequency and/or power of the gamma ASSR but this will need to be explored by other studies.

Future studies should also investigate the influence of GABAergic/glutamatergic circuitry in the auditory cortex on individual variability in the peak frequency and power of the ASSR, as inhibitory/excitatory transmission plays a key role in the generation of synchronous ASSRs in the gamma frequency range (Lewis *et al.*, 2005). Vohs et al. (2010 and 2012) has shown that enhancing GABAergic activity via application of the $GABA_AR$ agonist muscimol increases the power of the 40 Hz ASSR in sham rats but decreases the power in the neonatal ventral hippocampal lesion (NVHL) rat model of schizophrenia (Vohs *et al.*, 2010, Vohs *et al.*, 2012). This suggests a $GABA_AR$ dysfunction is present in the NVHL schizophrenia model, which could be responsible for the decreased power of the 40Hz ASSR in the NVHL rats compared to sham rats. These findings can also be applied to human schizophrenia populations, by implying that the widely reported reduction in the 40Hz ASSR of schizophrenia (Brenner *et al.*, 2003, Krishnan *et al.*, 2005b, Kwon *et al.*, 1999) and their relatives (Hong *et al.*, 2004) is due to alterations in inhibitory function. This agrees with the few studies that have investigated cellular inhibitory function in auditory areas of schizophrenia individuals, in which decreased *GAD1* mRNA and a reduced density of GAT1-immunoreactive axon cartridges are found (Impagnatiello *et al.*, 1998, Konopaske *et al.*, 2006).

Glutamatergic function has also been shown to influence the power of the gamma ASSR, as ketamine increases the power of the 40Hz ASSR in humans (Plourde *et al.*, 1997). As abnormal increases in the power of the auditory 40Hz response are also observed in schizoaffective bipolar individuals (Reite *et al.*, 2010), this may be driven by an NMDAR hypofunction in the auditory cortex, which has also been hypothesised in the visual cortex (Chapter 5). Therefore, evidence exists for both GABAergic and glutamatergic function playing a role in the power of the 40Hz ASSR. However, it is not clear whether these neurochemical factors also influence the variability in the power of the high gamma ASSR (70-100Hz) or the peak frequency of the low (30-50Hz) or high gamma (70-100Hz) ASSR, which can be studied using the click-chirp stimulus. As has been done in the visual system, the impact of GABA and glutamate levels on the peak frequency and power of the gamma ASSR can be assessed using MRS and by pharmaco-MEG. This will ultimately provide information into the specific cellular pathways that generate the different ASSR components which can then be applied to understanding the factors underlying ASSR abnormalities in clinical populations.

In addition, it would be interesting to study whether individual differences in ASSR gamma parameters lead to differences in behavioural measures of auditory perception. So far, other studies have found the power of the 40Hz ASSR to positively correlate with speech recognition ability (Manju *et al.*, 2014) and with the auditory hallucinations symptom rating of the SAPS (Spencer *et al.*, 2009). Thus, a high 40Hz ASSR up to a certain threshold may be advantageous for auditory perception, but responses above this threshold may predispose individuals to experiencing auditory hallucinations. In particular, it would be interesting to see if auditory peak gamma frequency and power play a role in encoding auditory stimulus

parameters (discriminating the pitch of a sound), similar to the hypothesised encoding role (contrast, motion and size) of gamma oscillations described in the visual domain.

Lastly, it is clear that similarities exist between gamma oscillations in the auditory and visual domain, such as in their microcircuitry and neurochemical systems. Despite this, no correlational relationship was found between gamma peak frequency or power responses in the auditory domain with those in the visual domain. These findings suggest that these oscillatory responses are regionally specific and functionally tuned. This agrees with evidence showing that MRS GABA levels are region-specific in the motor and visual cortex (Boy *et al.*, 2010).

Overall, it is clear that the exact biological determinants of gamma ASSRs needs further investigation in human individuals and can be studied using the click-chirp described in this thesis. As most studies have focused on identifying ASSR abnormalities in schizophrenia, more research on the ASSR in other clinical populations such as bipolar disorder needs to be conducted. This will not only allow similarities and differences in oscillatory activity to be identified across psychiatric disorders but will provide further insights into the biological pathways within these disorders, with the aim of improving current treatment.

7.3 Conclusion

To conclude, this thesis has shown the clear advantage of combining different brain imaging modalities (MEG and MRS) and genetic information to provide a more detailed insight into the biological mechanisms underpinning visual and auditory processing in healthy and disease states. For example, Chapter 4 has reinforced that genetic variation in *GAD1* is associated with variation in occipital MRS GABA levels and that lower occipital GABA

function in schizophrenia individuals may be partly due to the effect of specific *GAD1* variants. The association between *GAD1* and MRS GABA levels also reinforces the usefulness of MRS as a biological marker, as variability in MRS occipital GABA levels was sensitive to variation at the genetic level by *GAD1*.

Chapter 3 and 4 both show the importance of using large homogenous sample sizes, whether this is for producing reliable and strong associations between imaging measures or for statistical power in order to detect the small effect sizes of genes on imaging measures. Similarly, although Chapter 5 did not reveal the expected directional group difference in gamma measures between SABP and healthy individuals, these findings highlight how researchers need to work together in order to identify whether these differences between studies reflect true differences across patient populations, (SABP vs schizophrenia) differences between cortical regions studied or are solely due to the use of different stimuli.

Lastly, as in Chapter 5 and 6, it is important that researchers transfer their knowledge from their particular research area and apply it to less well researched areas such as from the visual to the auditory system or in SABP individuals rather than solely schizophrenia individuals. This will ultimately provide a more fruitful picture of the function and dysfunction of systems across different brain areas and in different clinical populations.

References

Abbott, A. (2008). Psychiatric genetics: The brains of the family. *Nature* **454**, 154-7.

Abdul-Kareem, I. A. & Sluming, V. (2008). Heschl gyrus and its included primary auditory cortex: structural MRI studies in healthy and diseased subjects. *J Magn Reson Imaging* **28**, 287-99.

Addington, A. M., Gornick, M., Duckworth, J., Sporn, A., Gogtay, N., Bobb, A., Greenstein, D., Lenane, M., Gochman, P., Baker, N., Balkissoon, R., Vakkalanka, R. K., Weinberger, D. R., Rapoport, J. L. & Straub, R. E. (2005). GAD1 (2q31.1), which encodes glutamic acid decarboxylase (GAD67), is associated with childhood-onset schizophrenia and cortical gray matter volume loss. *Mol Psychiatry* **10**, 581-8.

Addington, D., Addington, J. & Schissel, B. (1990). A depression rating scale for schizophrenics. In *Schizophr Res*, pp. 247-51: Netherlands.

Adjamian, P., Holliday, I. E., Barnes, G. R., Hillebrand, A., Hadjipapas, A. & Singh, K. D. (2004). Induced visual illusions and gamma oscillations in human primary visual cortex. *Eur J Neurosci* **20**, 587-92.

Alegre, M., Barbosa, C., Valencia, M., Pérez-Alcázar, M., Iriarte, J. & Artieda, J. (2008). Effect of reduced attention on auditory amplitude-modulation following responses: a study with chirp-evoked potentials. *J Clin Neurophysiol* **25**, 42-7.

Amos, W., Driscoll, E. & Hoffman, J. I. (2011). Candidate genes versus genome-wide associations: which are better for detecting genetic susceptibility to infectious disease? *Proc Biol Sci* **278**, 1183-8.

Andreasen, N. C. (1983). *The Scale for the Assessment of Negative Symptoms (SANS)*. University of Iowa: Iowa City.

Andreasen, N. C. (1984). *The Scale for the Assessment of Positive Symptoms (SAPS)*. University of Iowa: Iowa City.

Andreasen, N. C., Endicott, J., Spitzer, R. L. & Winokur, G. (1977). The family history method using diagnostic criteria. Reliability and validity. *Arch Gen Psychiatry* **34**, 1229-35.

Anver, H., Ward, P. D., Magony, A. & Vreugdenhil, M. (2011). NMDA receptor hypofunction phase couples independent γ-oscillations in the rat visual cortex. *Neuropsychopharmacology* **36**, 519-28.

Arai, A. C. & Kessler, M. (2007). Pharmacology of ampakine modulators: From AMPA receptors to synapses and behavior. *Current Drug Targets* **8**, 583-602.

Arrondo, G., Alegre, M., Sepulcre, J., Iriarte, J., Artieda, J. & Villoslada, P. (2009). Abnormalities in brain synchronization are correlated with cognitive impairment in multiple sclerosis. *Mult Scler* **15**, 509-16.

Artieda, J., Valencia, M., Alegre, M., Olaziregi, O., Urrestarazu, E. & Iriarte, J. (2004). Potentials evoked by chirp-modulated tones: a new technique to evaluate oscillatory activity in the auditory pathway. *Clin Neurophysiol* **115**, 699-709.

Asada, H., Kawamura, Y., Maruyama, K., Kume, H., Ding, R. G., Kanbara, N., Kuzume, H., Sanbo, M., Yagi, T. & Obata, K. (1997). Cleft palate and decreased brain gamma-aminobutyric acid in mice lacking the 67-kDa isoform of glutamic acid decarboxylase. *Proc Natl Acad Sci U S A* **94**, 6496-9.

Banissy, M. J., Kanai, R., Walsh, V. & Rees, G. (2012). Inter-individual differences in empathy are reflected in human brain structure. *Neuroimage* **62**, 2034-9.

Barnard, E. A., Skolnick, P., Olsen, R. W., Mohler, H., Sieghart, W., Biggio, G., Braestrup, C., Bateson, A. N. & Langer, S. Z. (1998). International Union of Pharmacology. XV. Subtypes of gamma-aminobutyric acidA receptors: classification on the basis of subunit structure and receptor function. *Pharmacol Rev* **50**, 291-313.

Barnes, G. R., Furlong, P. L., Singh, K. D. & Hillebrand, A. (2006). A verifiable solution to the MEG inverse problem. *Neuroimage* **31**, 623-6.

Bartos, M., Vida, I. & Jonas, P. (2007). Synaptic mechanisms of synchronized gamma oscillations in inhibitory interneuron networks. *Nature Reviews Neuroscience* **8**, 45-56.

Bastiaansen, M. C. & Knösche, T. R. (2000). Tangential derivative mapping of axial MEG applied to event-related desynchronization research. *Clin Neurophysiol* **111**, 1300-5.

Başar, E. (2013). A review of gamma oscillations in healthy subjects and in cognitive impairment. *Int J Psychophysiol* **90**, 99-117.
Başar, E. & Güntekin, B. (2008). A review of brain oscillations in cognitive disorders and the role of neurotransmitters. *Brain Res* **1235**, 172-93.
Bear, M., Connors, B. & Paradiso, M. (2007). *Neuroscience: Exploring the Brain*. Lippincott Williams and Wilkins.
Behrens, M. M., Ali, S. S., Dao, D. N., Lucero, J., Shekhtman, G., Quick, K. L. & Dugan, L. L. (2007). Ketamine-induced loss of phenotype of fast-spiking interneurons is mediated by NADPH-oxidase. *Science* **318**, 1645-7.
Benham, R. S., Engin, E. & Rudolph, U. (2014). Diversity of neuronal inhibition: a path to novel treatments for neuropsychiatric disorders. *JAMA Psychiatry* **71**, 91-3.
Benson, D. L., Huntsman, M. M. & Jones, E. G. (1994). Activity-dependent changes in GAD and preprotachykinin mRNAs in visual cortex of adult monkeys. *Cereb Cortex* **4**, 40-51.
Berridge, M. J., Bootman, M. D. & Roderick, H. L. (2003). Calcium signalling: dynamics, homeostasis and remodelling. *Nat Rev Mol Cell Biol* **4**, 517-29.
Bertholdo, D., Watcharakorn, A. & Castillo, M. (2013). Brain proton magnetic resonance spectroscopy: introduction and overview. *Neuroimaging Clin N Am* **23**, 359-80.
Bhagwagar, Z., Wylezinska, M., Jezzard, P., Evans, J., Ashworth, F., Sule, A., Matthews, P. M. & Cowen, P. J. (2007). Reduction in occipital cortex gamma-aminobutyric acid concentrations in medication-free recovered unipolar depressed and bipolar subjects. *Biol Psychiatry* **61**, 806-12.
Bigal, M. E., Hetherington, H., Pan, J., Tsang, A., Grosberg, B., Avdievich, N., Friedman, B. & Lipton, R. B. (2008). Occipital levels of GABA are related to severe headaches in migraine. *Neurology* **70**, 2078-80.
Bish, J. P., Martin, T., Houck, J., Ilmoniemi, R. J. & Tesche, C. (2004). Phase shift detection in thalamocortical oscillations using magnetoencephalography in humans. *Neurosci Lett* **362**, 48-52.
Bogner, W., Gruber, S., Doelken, M., Stadlbauer, A., Ganslandt, O., Boettcher, U., Trattnig, S., Doerfler, A., Stefan, H. & Hammen, T. (2010). In vivo quantification of intracerebral GABA by single-voxel (1)H-MRS-How reproducible are the results? *Eur J Radiol* **73**, 526-31.
Boy, F., Evans, C. J., Edden, R. A., Singh, K. D., Husain, M. & Sumner, P. (2010). Individual differences in subconscious motor control predicted by GABA concentration in SMA. *Curr Biol* **20**, 1779-85.
Brady, R. O., McCarthy, J. M., Prescot, A. P., Jensen, J. E., Cooper, A. J., Cohen, B. M., Renshaw, P. F. & Ongür, D. (2013). Brain gamma-aminobutyric acid (GABA) abnormalities in bipolar disorder. *Bipolar Disord* **15**, 434-9.
Brauns, S., Gollub, R. L., Walton, E., Hass, J., Smolka, M. N., White, T., Wassink, T. H., Calhoun, V. D. & Ehrlich, S. (2013). Genetic variation in GAD1 is associated with cortical thickness in the parahippocampal gyrus. *J Psychiatr Res* **47**, 872-9.
Brenner, C. A., Sporns, O., Lysaker, P. H. & O'Donnell, B. F. (2003). EEG synchronization to modulated auditory tones in schizophrenia, schizoaffective disorder, and schizotypal personality disorder. *Am J Psychiatry* **160**, 2238-40.
Breuer, R., Hamshere, M. L., Strohmaier, J., Mattheisen, M., Degenhardt, F., Meier, S., Paul, T., O'Donovan, M. C., Mühleisen, T. W., Schulze, T. G., Nöthen, M. M., Cichon, S., Craddock, N. & Rietschel, M. (2011). Independent evidence for the selective influence of GABA(A) receptors on one component of the bipolar disorder phenotype. *Mol Psychiatry* **16**, 587-9.
Brookes, M. J., Hale, J. R., Zumer, J. M., Stevenson, C. M., Francis, S. T., Barnes, G. R., Owen, J. P., Morris, P. G. & Nagarajan, S. S. (2011). Measuring functional connectivity using MEG: methodology and comparison with fcMRI. *Neuroimage* **56**, 1082-104.
Brookes, M. J., Stevenson, C. M., Barnes, G. R., Hillebrand, A., Simpson, M. I., Francis, S. T. & Morris, P. G. (2007). Beamformer reconstruction of correlated sources using a modified source model. *Neuroimage* **34**, 1454-65.

Brunel, N. & Wang, X. J. (2003). What determines the frequency of fast network oscillations with irregular neural discharges? I. Synaptic dynamics and excitation-inhibition balance. *J Neurophysiol* **90**, 415-30.
Butler, P. D., Silverstein, S. M. & Dakin, S. C. (2008). Visual perception and its impairment in schizophrenia. *Biol Psychiatry* **64**, 40-7.
Button, K. S., Ioannidis, J. P., Mokrysz, C., Nosek, B. A., Flint, J., Robinson, E. S. & Munafò, M. R. (2013). Power failure: why small sample size undermines the reliability of neuroscience. *Nat Rev Neurosci* **14**, 365-76.
Buzsaki, G. & Wang, X. J. (2012). Mechanisms of Gamma Oscillations. *Annual Review of Neuroscience, Vol 35* **35**, 203-225.
Callaway, E. M. (1998). Local circuits in primary visual cortex of the macaque monkey. *Annu Rev Neurosci* **21**, 47-74.
Campbell, A. E., Sumner, P., Singh, K. D. & Muthukumaraswamy, S. D. (2014). Acute Effects of Alcohol on Stimulus-Induced Gamma Oscillations in Human Primary Visual and Motor Cortices. *Neuropsychopharmacology*.
Cardin, J. A., Carlen, M., Meletis, K., Knoblich, U., Zhang, F., Deisseroth, K., Tsai, L. H. & Moore, C. I. (2009). Driving fast-spiking cells induces gamma rhythm and controls sensory responses. *Nature* **459**, 663-U63.
Cardno, A. G. & Owen, M. J. (2014). Genetic relationships between schizophrenia, bipolar disorder, and schizoaffective disorder. *Schizophr Bull* **40**, 504-15.
Carlén, M., Meletis, K., Siegle, J. H., Cardin, J. A., Futai, K., Vierling-Claassen, D., Rühlmann, C., Jones, S. R., Deisseroth, K., Sheng, M., Moore, C. I. & Tsai, L. H. (2012). A critical role for NMDA receptors in parvalbumin interneurons for gamma rhythm induction and behavior. *Mol Psychiatry* **17**, 537-48.
Castro, J. B. & Kandler, K. (2010). Changing tune in auditory cortex. *Nat Neurosci* **13**, 271-3.
Chen, C. M., Stanford, A. D., Mao, X., Abi-Dargham, A., Shungu, D. C., Lisanby, S. H., Schroeder, C. E. & Kegeles, L. S. (2014). GABA level, gamma oscillation, and working memory performance in schizophrenia. *Neuroimage Clin* **4**, 531-9.
Chen, Y. (2011). Abnormal visual motion processing in schizophrenia: a review of research progress. *Schizophr Bull* **37**, 709-15.
Chen, Y., Levy, D. L., Sheremata, S. & Holzman, P. S. (2006). Bipolar and schizophrenic patients differ in patterns of visual motion discrimination. *Schizophr Res* **88**, 208-16.
Cherlyn, S. Y. T., Woon, P. S., Liu, J. J., Ong, W. Y., Tsai, G. C. & Sim, K. (2010). Genetic association studies of glutamate, GABA and related genes in schizophrenia and bipolar disorder: A decade of advance. *Neuroscience and Biobehavioral Reviews* **34**, 958-977.
Cheyne, D. & Ferrari, P. (2013). MEG studies of motor cortex gamma oscillations: evidence for a gamma "fingerprint" in the brain? *Front Hum Neurosci* **7**, 575.
Cho, R. Y., Konecky, R. O. & Carter, C. S. (2006). Impairments in frontal cortical gamma synchrony and cognitive control in schizophrenia. *Proceedings of the National Academy of Sciences of the United States of America* **103**, 19878-19883.
Cohen, D. (1968). Magnetoencephalography: evidence of magnetic fields produced by alpha-rhythm currents. *Science* **161**, 784-6.
Consortium, S. P. G.-W. A. S. G. (2011). Genome-wide association study identifies five new schizophrenia loci. *Nat Genet* **43**, 969-76.
Consortium, S. W. G. o. t. P. G. (2014). Biological insights from 108 schizophrenia-associated genetic loci. *Nature* **511**, 421-7.
Cooper, D. N. (2010). Functional intronic polymorphisms: Buried treasure awaiting discovery within our genes. *Hum Genomics* **4**, 284-8.
Costa, E., Davis, J. M., Dong, E., Grayson, D. R., Guidotti, A., Tremolizzo, L. & Veldic, M. (2004). A GABAergic cortical deficit dominates schizophrenia pathophysiology. *Crit Rev Neurobiol* **16**, 1-23.

Cousijn, H., Haegens, S., Wallis, G., Near, J., Stokes, M. G., Harrison, P. J. & Nobre, A. C. (2014). Resting GABA and glutamate concentrations do not predict visual gamma frequency or amplitude. *Proc Natl Acad Sci U S A* **111**, 9301-6.

Craddock, N., Jones, L., Jones, I. R., Kirov, G., Green, E. K., Grozeva, D., Moskvina, V., Nikolov, I., Hamshere, M. L., Vukcevic, D., Caesar, S., Gordon-Smith, K., Fraser, C., Russell, E., Norton, N., Breen, G., St Clair, D., Collier, D. A., Young, A. H., Ferrier, I. N., Farmer, A., McGuffin, P., Holmans, P. A., Donnelly, P., Owen, M. J., O'Donovan, M. C. & Wellcome Trust Case Control, C. (2010). Strong genetic evidence for a selective influence of GABA(A) receptors on a component of the bipolar disorder phenotype (vol 15, pg 146, 2010). *Molecular Psychiatry* **15**, 1121-1121.

Cunningham, M. O., Whittington, M. A., Bibbig, A., Roopun, A., LeBeau, F. E., Vogt, A., Monyer, H., Buhl, E. H. & Traub, R. D. (2004). A role for fast rhythmic bursting neurons in cortical gamma oscillations in vitro. *Proc Natl Acad Sci U S A* **101**, 7152-7.

Curley, A. A., Arion, D., Volk, D. W., Asafu-Adjei, J. K., Sampson, A. R., Fish, K. N. & Lewis, D. A. (2011). Cortical deficits of glutamic acid decarboxylase 67 expression in schizophrenia: clinical, protein, and cell type-specific features. *Am J Psychiatry* **168**, 921-9.

DAVIES, B. M. & BEECH, H. R. (1960). The effect of 1-arylcylohexylamine (sernyl) on twelve normal volunteers. *J Ment Sci* **106**, 912-24.

Delaneau, O., Marchini, J. & Zagury, J. F. (2012). A linear complexity phasing method for thousands of genomes. *Nat Methods* **9**, 179-81.

Dougherty, R. F., Koch, V. M., Brewer, A. A., Fischer, B., Modersitzki, J. & Wandell, B. A. (2003). Visual field representations and locations of visual areas V1/2/3 in human visual cortex. *J Vis* **3**, 586-98.

Dracheva, S., Elhakem, S. L., McGurk, S. R., Davis, K. L. & Haroutunian, V. (2004). GAD67 and GAD65 mRNA and protein expression in cerebrocortical regions of elderly patients with schizophrenia. *J Neurosci Res* **76**, 581-92.

Du, J., Duan, S., Wang, H., Chen, W., Zhao, X., Zhang, A., Wang, L., Xuan, J., Yu, L., Wu, S., Tang, W., Li, X., Li, H., Feng, G., Xing, Q. & He, L. (2008). Comprehensive analysis of polymorphisms throughout GAD1 gene: a family-based association study in schizophrenia. *J Neural Transm* **115**, 513-9.

Dudbridge, F. (2013). Power and predictive accuracy of polygenic risk scores. *PLoS Genet* **9**, e1003348.

Edden, R. A., Muthukumaraswamy, S. D., Freeman, T. C. & Singh, K. D. (2009). Orientation discrimination performance is predicted by GABA concentration and gamma oscillation frequency in human primary visual cortex. *J Neurosci* **29**, 15721-6.

Edenberg, H. J., Dick, D. M., Xuei, X., Tian, H., Almasy, L., Bauer, L. O., Crowe, R. R., Goate, A., Hesselbrock, V., Jones, K., Kwon, J., Li, T. K., Nurnberger, J. I., O'Connor, S. J., Reich, T., Rice, J., Schuckit, M. A., Porjesz, B., Foroud, T. & Begleiter, H. (2004). Variations in GABRA2, encoding the alpha 2 subunit of the GABA(A) receptor, are associated with alcohol dependence and with brain oscillations. *Am J Hum Genet* **74**, 705-14.

Edgar, J. C., Chen, Y. H., Lanza, M., Howell, B., Chow, V. Y., Heiken, K., Liu, S., Wootton, C., Hunter, M. A., Huang, M., Miller, G. A. & Cañive, J. M. (2013). Cortical thickness as a contributor to abnormal oscillations in schizophrenia? *Neuroimage Clin* **4**, 122-9.

Engel, A. K., Fries, P. & Singer, W. (2001). Dynamic predictions: oscillations and synchrony in top-down processing. *Nat Rev Neurosci* **2**, 704-16.

Eriksson, S. H., Free, S. L., Thom, M., Symms, M. R., Martinian, L., Duncan, J. S. & Sisodiya, S. M. (2009). Quantitative grey matter histological measures do not correlate with grey matter probability values from in vivo MRI in the temporal lobe. *J Neurosci Methods* **181**, 111-8.

Erk, S., Meyer-Lindenberg, A., Linden, D. E., Lancaster, T., Mohnke, S., Grimm, O., Degenhardt, F., Holmans, P., Pocklington, A., Schmierer, P., Haddad, L., Mühleisen, T. W., Mattheisen, M., Witt, S. H., Romanczuk-Seiferth, N., Tost, H., Schott, B. H., Cichon, S., Nöthen, M. M., Rietschel, M., Heinz,

A. & Walter, H. (2014). Replication of brain function effects of a genome-wide supported psychiatric risk variant in the CACNA1C gene and new multi-locus effects. *Neuroimage* **94**, 147-54.
Erk, S., Meyer-Lindenberg, A., Schnell, K., Opitz von Boberfeld, C., Esslinger, C., Kirsch, P., Grimm, O., Arnold, C., Haddad, L., Witt, S. H., Cichon, S., Nöthen, M. M., Rietschel, M. & Walter, H. (2010). Brain function in carriers of a genome-wide supported bipolar disorder variant. *Arch Gen Psychiatry* **67**, 803-11.
Ethridge, L. E., Hamm, J. P., Shapiro, J. R., Summerfelt, A. T., Keedy, S. K., Stevens, M. C., Pearlson, G., Tamminga, C. A., Boutros, N. N., Sweeney, J. A., Keshavan, M. S., Thaker, G. & Clementz, B. A. (2012). Neural Activations During Auditory Oddball Processing Discriminating Schizophrenia and Psychotic Bipolar Disorder. *Biological Psychiatry* **72**, 766-774.
Evans, C. J., McGonigle, D. J. & Edden, R. A. (2010). Diurnal stability of gamma-aminobutyric acid concentration in visual and sensorimotor cortex. *J Magn Reson Imaging* **31**, 204-9.
Fawcett, I. P., Barnes, G. R., Hillebrand, A. & Singh, K. D. (2004). The temporal frequency tuning of human visual cortex investigated using synthetic aperture magnetometry. *Neuroimage* **21**, 1542-53.
Fazzari, P., Paternain, A. V., Valiente, M., Pla, R., Luján, R., Lloyd, K., Lerma, J., Marín, O. & Rico, B. (2010). Control of cortical GABA circuitry development by Nrg1 and ErbB4 signalling. *Nature* **464**, 1376-80.
Featherstone, R. E., Phillips, J. M., Thieu, T., Ehrlichman, R. S., Halene, T. B., Leiser, S. C., Christian, E., Johnson, E., Lerman, C. & Siegel, S. J. (2012). Nicotine receptor subtype-specific effects on auditory evoked oscillations and potentials. *PLoS One* **7**, e39775.
Ferrarelli, F., Sarasso, S., Guller, Y., Riedner, B. A., Peterson, M. J., Bellesi, M., Massimini, M., Postle, B. R. & Tononi, G. (2012). Reduced natural oscillatory frequency of frontal thalamocortical circuits in schizophrenia. *Arch Gen Psychiatry* **69**, 766-74.
Flint, J. & Munafò, M. R. (2007). The endophenotype concept in psychiatric genetics. *Psychol Med* **37**, 163-80.
Fong, A. Y., Stornetta, R. L., Foley, C. M. & Potts, J. T. (2005). Immunohistochemical localization of GAD67-expressing neurons and processes in the rat brainstem: subregional distribution in the nucleus tractus solitarius. *J Comp Neurol* **493**, 274-90.
Frangou, S. & Williams, S. C. (1996). Magnetic resonance spectroscopy in psychiatry: basic principles and applications. *Br Med Bull* **52**, 474-85.
Fries, P. (2009). Neuronal gamma-band synchronization as a fundamental process in cortical computation. *Annu Rev Neurosci* **32**, 209-24.
Gaetz, W., Cheyne, D., Rutka, J. T., Drake, J., Benifla, M., Strantzas, S., Widjaja, E., Holowka, S., Tovar-Spinoza, Z., Otsubo, H. & Pang, E. W. (2009). Presurgical localization of primary motor cortex in pediatric patients with brain lesions by the use of spatially filtered magnetoencephalography. *Neurosurgery* **64**, ons177-85; discussion ons186.
Gaetz, W., Edgar, J. C., Wang, D. J. & Roberts, T. P. (2011). Relating MEG measured motor cortical oscillations to resting γ-aminobutyric acid (GABA) concentration. *Neuroimage* **55**, 616-21.
Gaetz, W., Roberts, T. P., Singh, K. D. & Muthukumaraswamy, S. D. (2012). Functional and structural correlates of the aging brain: relating visual cortex (V1) gamma band responses to age-related structural change. *Hum Brain Mapp* **33**, 2035-46.
Galambos, R., Makeig, S. & Talmachoff, P. J. (1981). A 40-Hz auditory potential recorded from the human scalp. *Proc Natl Acad Sci U S A* **78**, 2643-7.
Gallagher, T. A., Nemeth, A. J. & Hacein-Bey, L. (2008). An introduction to the Fourier transform: relationship to MRI. *AJR Am J Roentgenol* **190**, 1396-405.
Gao, F., Edden, R. A., Li, M., Puts, N. A., Wang, G., Liu, C., Zhao, B., Wang, H., Bai, X., Zhao, C., Wang, X. & Barker, P. B. (2013). Edited magnetic resonance spectroscopy detects an age-related decline in brain GABA levels. *Neuroimage* **78**, 75-82.
Gilmour, G., Dix, S., Fellini, L., Gastambide, F., Plath, N., Steckler, T., Talpos, J. & Tricklebank, M. (2012). NMDA receptors, cognition and schizophrenia--testing the validity of the NMDA receptor hypofunction hypothesis. *Neuropharmacology* **62**, 1401-12.

Gitlin, M. J., Swendsen, J., Heller, T. L. & Hammen, C. (1995). Relapse and impairment in bipolar disorder. *Am J Psychiatry* **152**, 1635-40.
Goddard, A. W., Mason, G. F., Almai, A., Rothman, D. L., Behar, K. L., Petroff, O. A., Charney, D. S. & Krystal, J. H. (2001). Reductions in occipital cortex GABA levels in panic disorder detected with 1h-magnetic resonance spectroscopy. *Arch Gen Psychiatry* **58**, 556-61.
Gonchar, Y., Wang, Q. & Burkhalter, A. (2007). Multiple distinct subtypes of GABAergic neurons in mouse visual cortex identified by triple immunostaining. *Front Neuroanat* **1**, 3.
Gonzalez-Burgos, G., Fish, K. N. & Lewis, D. A. (2011). GABA neuron alterations, cortical circuit dysfunction and cognitive deficits in schizophrenia. *Neural Plast* **2011**, 723184.
Gonzalez-Burgos, G., Hashimoto, T. & Lewis, D. A. (2010). Alterations of Cortical GABA Neurons and Network Oscillations in Schizophrenia. *Current Psychiatry Reports* **12**, 335-344.
Gonzalez-Burgos, G. & Lewis, D. A. (2012). NMDA receptor hypofunction, parvalbumin-positive neurons, and cortical gamma oscillations in schizophrenia. *Schizophr Bull* **38**, 950-7.
Gottesman, I. I. & Gould, T. D. (2003). The endophenotype concept in psychiatry: etymology and strategic intentions. *Am J Psychiatry* **160**, 636-45.
Grill-Spector, K. & Malach, R. (2004). The human visual cortex. *Annu Rev Neurosci* **27**, 649-77.
Group, P. G. C. B. D. W. (2011). Large-scale genome-wide association analysis of bipolar disorder identifies a new susceptibility locus near ODZ4. *Nat Genet* **43**, 977-83.
Grützner, C., Wibral, M., Sun, L., Rivolta, D., Singer, W., Maurer, K. & Uhlhaas, P. J. (2013). Deficits in high- (>60 Hz) gamma-band oscillations during visual processing in schizophrenia. *Front Hum Neurosci* **7**, 88.
Guidotti, A., Auta, J., Davis, J. M., Di-Giorgi-Gerevini, V., Dwivedi, Y., Grayson, D. R., Impagnatiello, F., Pandey, G., Pesold, C., Sharma, R., Uzunov, D., Costa, E. & DiGiorgi Gerevini, V. (2000). Decrease in reelin and glutamic acid decarboxylase67 (GAD67) expression in schizophrenia and bipolar disorder: a postmortem brain study. *Arch Gen Psychiatry* **57**, 1061-9.
Haenschel, C. & Linden, D. (2011). Exploring intermediate phenotypes with EEG: Working memory dysfunction in schizophrenia. *Behavioural Brain Research* **216**, 481-495.
Hakami, T., Jones, N. C., Tolmacheva, E. A., Gaudias, J., Chaumont, J., Salzberg, M., O'Brien, T. J. & Pinault, D. (2009). NMDA receptor hypofunction leads to generalized and persistent aberrant gamma oscillations independent of hyperlocomotion and the state of consciousness. *PLoS One* **4**, e6755.
Hall, M. H., Spencer, K. M., Schulze, K., McDonald, C., Kalidindi, S., Kravariti, E., Kane, F., Murray, R. M., Bramon, E., Sham, P. & Rijsdijk, F. (2011a). The genetic and environmental influences of event-related gamma oscillations on bipolar disorder. *Bipolar Disorders* **13**, 260-271.
Hall, M. H., Taylor, G., Sham, P., Schulze, K., Rijsdijk, F., Picchioni, M., Toulopoulou, T., Ettinger, U., Bramon, E., Murray, R. M. & Salisbury, D. F. (2011b). The early auditory gamma-band response is heritable and a putative endophenotype of schizophrenia. *Schizophr Bull* **37**, 778-87.
Hall, S. D., Holliday, I. E., Hillebrand, A., Singh, K. D., Furlong, P. L., Hadjipapas, A. & Barnes, G. R. (2005). The missing link: analogous human and primate cortical gamma oscillations. *Neuroimage* **26**, 13-7.
Hamm, J. P., Gilmore, C. S., Picchetti, N. A., Sponheim, S. R. & Clementz, B. A. (2011). Abnormalities of neuronal oscillations and temporal integration to low- and high-frequency auditory stimulation in schizophrenia. *Biol Psychiatry* **69**, 989-96.
Hannula, D. E., Simons, D. J. & Cohen, N. J. (2005). Imaging implicit perception: promise and pitfalls. *Nat Rev Neurosci* **6**, 247-55.
Hariri, A. R. & Weinberger, D. R. (2003). Imaging genomics. *Br Med Bull* **65**, 259-70.
Harris, A. D., Puts, N. A., Barker, P. B. & Edden, R. A. (2014). Spectral-editing measurements of GABA in the human brain with and without macromolecule suppression. *Magn Reson Med*.
Harrow, M., Grossman, L. S., Herbener, E. S. & Davies, E. W. (2000). Ten-year outcome: patients with schizoaffective disorders, schizophrenia, affective disorders and mood-incongruent psychotic symptoms. *British Journal of Psychiatry* **177**, 421-426.

Hashimoto, T., Bazmi, H. H., Mirnics, K., Wu, Q., Sampson, A. R. & Lewis, D. A. (2008). Conserved regional patterns of GABA-related transcript expression in the neocortex of subjects with schizophrenia. *Am J Psychiatry* **165**, 479-89.

Hashimoto, T., Volk, D. W., Eggan, S. M., Mirnics, K., Pierri, J. N., Sun, Z. X., Sampson, A. R. & Lewis, D. A. (2003). Gene expression deficits in a subclass of GABA neurons in the prefrontal cortex of subjects with schizophrenia. *Journal of Neuroscience* **23**, 6315-6326.

Hasler, G. & Northoff, G. (2011). Discovering imaging endophenotypes for major depression. *Mol Psychiatry* **16**, 604-19.

Hendry, S. H., Schwark, H. D., Jones, E. G. & Yan, J. (1987). Numbers and proportions of GABA-immunoreactive neurons in different areas of monkey cerebral cortex. *J Neurosci* **7**, 1503-19.

Henriksen, O. (1995). In vivo quantitation of metabolite concentrations in the brain by means of proton MRS. *NMR Biomed* **8**, 139-48.

Henry, P. G., Dautry, C., Hantraye, P. & Bloch, G. (2001). Brain GABA editing without macromolecule contamination. *Magn Reson Med* **45**, 517-20.

Herdman, A. T., Lins, O., Van Roon, P., Stapells, D. R., Scherg, M. & Picton, T. W. (2002). Intracerebral sources of human auditory steady-state responses. *Brain Topogr* **15**, 69-86.

Herdman, A. T., Wollbrink, A., Chau, W., Ishii, R., Ross, B. & Pantev, C. (2003). Determination of activation areas in the human auditory cortex by means of synthetic aperture magnetometry. *Neuroimage* **20**, 995-1005.

Hermes, D., Miller, K. J., Wandell, B. A. & Winawer, J. (2014). Stimulus Dependence of Gamma Oscillations in Human Visual Cortex. *Cereb Cortex*.

Herrmann, C. S. (2001). Human EEG responses to 1-100 Hz flicker: resonance phenomena in visual cortex and their potential correlation to cognitive phenomena. *Exp Brain Res* **137**, 346-53.

Higley, M. J. (2014). Localized GABAergic inhibition of dendritic Ca(2+) signalling. *Nat Rev Neurosci* **15**, 567-72.

Hillebrand, A. & Barnes, G. R. (2005). Beamformer analysis of MEG data. *Int Rev Neurobiol* **68**, 149-71.

Hindorff, L. A., Sethupathy, P., Junkins, H. A., Ramos, E. M., Mehta, J. P., Collins, F. S. & Manolio, T. A. (2009). Potential etiologic and functional implications of genome-wide association loci for human diseases and traits. *Proc Natl Acad Sci U S A* **106**, 9362-7.

Hinds, O. P., Rajendran, N., Polimeni, J. R., Augustinack, J. C., Wiggins, G., Wald, L. L., Diana Rosas, H., Potthast, A., Schwartz, E. L. & Fischl, B. (2008). Accurate prediction of V1 location from cortical folds in a surface coordinate system. *Neuroimage* **39**, 1585-99.

Hirayasu, Y., McCarley, R. W., Salisbury, D. F., Tanaka, S., Kwon, J. S., Frumin, M., Snyderman, D., Yurgelun-Todd, D., Kikinis, R., Jolesz, F. A. & Shenton, M. E. (2000). Planum temporale and Heschl gyrus volume reduction in schizophrenia: a magnetic resonance imaging study of first-episode patients. *Arch Gen Psychiatry* **57**, 692-9.

Hiyoshi, T., Kambe, D., Karasawa, J. & Chaki, S. (2014). Involvement of glutamatergic and GABAergic transmission in MK-801-increased gamma band oscillation power in rat cortical electroencephalograms. *Neuroscience* **280**, 262-74.

Hogstrom, L. J., Westlye, L. T., Walhovd, K. B. & Fjell, A. M. (2013). The structure of the cerebral cortex across adult life: age-related patterns of surface area, thickness, and gyrification. *Cereb Cortex* **23**, 2521-30.

Homayoun, H. & Moghaddam, B. (2007). NMDA receptor hypofunction produces opposite effects on prefrontal cortex interneurons and pyramidal neurons. *J Neurosci* **27**, 11496-500.

Hong, L. E., Summerfelt, A., Buchanan, R. W., O'Donnell, P., Thaker, G. K., Weiler, M. A. & Lahti, A. C. (2010). Gamma and delta neural oscillations and association with clinical symptoms under subanesthetic ketamine. *Neuropsychopharmacology* **35**, 632-40.

Hong, L. E., Summerfelt, A., McMahon, R., Adami, H., Francis, G., Elliott, A., Buchanan, R. W. & Thaker, G. K. (2004). Evoked gamma band synchronization and the liability for schizophrenia. *Schizophrenia Research* **70**, 293-302.

Hoogenboom, N., Schoffelen, J. M., Oostenveld, R., Parkes, L. M. & Fries, P. (2006). Localizing human visual gamma-band activity in frequency, time and space. *Neuroimage* **29**, 764-773.
Howie, B., Marchini, J. & Stephens, M. (2011). Genotype imputation with thousands of genomes. *G3 (Bethesda)* **1**, 457-70.
Hubel, D. H. & Wiesel, T. N. (1962). Receptive fields, binocular interaction and functional architecture in the cat's visual cortex. *J Physiol* **160**, 106-54.
Iliadou, V. V., Apalla, K., Kaprinis, S., Nimatoudis, I., Kaprinis, G. & Iacovides, A. (2013). Is central auditory processing disorder present in psychosis? *Am J Audiol* **22**, 201-8.
Impagnatiello, F., Guidotti, A. R., Pesold, C., Dwivedi, Y., Caruncho, H., Pisu, M. G., Uzunov, D. P., Smalheiser, N. R., Davis, J. M., Pandey, G. N., Pappas, G. D., Tueting, P., Sharma, R. P. & Costa, E. (1998). A decrease of reelin expression as a putative vulnerability factor in schizophrenia. *Proc Natl Acad Sci U S A* **95**, 15718-23.
Janssen, B., Weinmann, S., Berger, M. & Gaebel, W. (2004). Validation of polypharmacy process measures in inpatient schizophrenia care. *Schizophr Bull* **30**, 1023-33.
Javitt, D. C. (2009). When doors of perception close: bottom-up models of disrupted cognition in schizophrenia. *Annu Rev Clin Psychol* **5**, 249-75.
Javitt, D. C., Shelley, A. & Ritter, W. (2000). Associated deficits in mismatch negativity generation and tone matching in schizophrenia. *Clin Neurophysiol* **111**, 1733-7.
Jefferys, J. G., Traub, R. D. & Whittington, M. A. (1996). Neuronal networks for induced '40 Hz' rhythms. *Trends Neurosci* **19**, 202-8.
Jia, X. X., Xing, D. J. & Kohn, A. (2013). No Consistent Relationship between Gamma Power and Peak Frequency in Macaque Primary Visual Cortex. *Journal of Neuroscience* **33**, 17-U421.
Jones, N. C., Reddy, M., Anderson, P., Salzberg, M. R., O'Brien, T. J. & Pinault, D. (2012). Acute administration of typical and atypical antipsychotics reduces EEG gamma power, but only the preclinical compound LY379268 reduces the ketamine-induced rise in gamma power. *International Journal of Neuropsychopharmacology* **15**, 657-668.
Kanai, R. & Rees, G. (2011). The structural basis of inter-individual differences in human behaviour and cognition. *Nat Rev Neurosci* **12**, 231-42.
Kandel, E., Schwartz, J. & Jessel, T. (2000). *Principles of Neuroscience*. McGraw-Hill: New York.
Kang, X., Herron, T. J., Cate, A. D., Yund, E. W. & Woods, D. L. (2012). Hemispherically-unified surface maps of human cerebral cortex: reliability and hemispheric asymmetries. *PLoS One* **7**, e45582.
Kasai, K., Shenton, M. E., Salisbury, D. F., Hirayasu, Y., Lee, C. U., Ciszewski, A. A., Yurgelun-Todd, D., Kikinis, R., Jolesz, F. A. & McCarley, R. W. (2003). Progressive decrease of left superior temporal gyrus gray matter volume in patients with first-episode schizophrenia. *Am J Psychiatry* **160**, 156-64.
.
Kaufman, R. E., Ostacher, M. J., Marks, E. H., Simon, N. M., Sachs, G. S., Jensen, J. E., Renshaw, P. F. & Pollack, M. H. (2009). Brain GABA levels in patients with bipolar disorder. *Prog Neuropsychopharmacol Biol Psychiatry* **33**, 427-34.
Kegeles, L. S., Mao, X., Stanford, A. D., Girgis, R., Ojeil, N., Xu, X., Gil, R., Slifstein, M., Abi-Dargham, A., Lisanby, S. H. & Shungu, D. C. (2012). Elevated prefrontal cortex γ-aminobutyric acid and glutamate-glutamine levels in schizophrenia measured in vivo with proton magnetic resonance spectroscopy. *Arch Gen Psychiatry* **69**, 449-59.
King, A. J. & Nelken, I. (2009). Unraveling the principles of auditory cortical processing: can we learn from the visual system? *Nat Neurosci* **12**, 698-701.
Kirov, G., Pocklington, A. J., Holmans, P., Ivanov, D., Ikeda, M., Ruderfer, D., Moran, J., Chambert, K., Toncheva, D., Georgieva, L., Grozeva, D., Fjodorova, M., Wollerton, R., Rees, E., Nikolov, I., van de Lagemaat, L. N., Bayés, A., Fernandez, E., Olason, P. I., Böttcher, Y., Komiyama, N. H., Collins, M. O., Choudhary, J., Stefansson, K., Stefansson, H., Grant, S. G., Purcell, S., Sklar, P., O'Donovan, M. C. & Owen, M. J. (2012). De novo CNV analysis implicates specific abnormalities of postsynaptic signalling complexes in the pathogenesis of schizophrenia. *Mol Psychiatry* **17**, 142-53.

Kissler, J., Muller, M. M., Fehr, T., Rockstroh, B. & Elbert, T. (2000). MEG gamma band activity in schizophrenia patients smd healthy subjects in a mental arithmetic task and at rest. *Clinical Neurophysiology* **111**, 2079-2087.
Koelewijn, L., Dumont, J. R., Muthukumaraswamy, S. D., Rich, A. N. & Singh, K. D. (2011). Induced and evoked neural correlates of orientation selectivity in human visual cortex. *Neuroimage* **54**, 2983-93.
Konopaske, G. T., Sweet, R. A., Wu, Q., Sampson, A. & Lewis, D. A. (2006). Regional specificity of chandelier neuron axon terminal alterations in schizophrenia. *Neuroscience* **138**, 189-96.
Krause, F., Lindemann, O., Toni, I. & Bekkering, H. (2014). Different brains process numbers differently: structural bases of individual differences in spatial and nonspatial number representations. *J Cogn Neurosci* **26**, 768-76.
Krishnan, G. P., Skosnik, P. D., Vohs, J. L., Busey, T. A. & O'Donnell, B. F. (2005a). Relationship between steady-state and induced gamma activity to motion. *Neuroreport* **16**, 625-30.
Krishnan, G. P., Vohs, J. L., Hetrick, W. P., Carroll, C. A., Shekhar, A., Bockbrader, M. A. & O'Donnell, B. F. (2005b). Steady state visual evoked potential abnormalities in schizophrenia. *Clin Neurophysiol* **116**, 614-24.
Krystal, J. H., Karper, L. P., Seibyl, J. P., Freeman, G. K., Delaney, R., Bremner, J. D., Heninger, G. R., Bowers, M. B. & Charney, D. S. (1994). Subanesthetic effects of the noncompetitive NMDA antagonist, ketamine, in humans. Psychotomimetic, perceptual, cognitive, and neuroendocrine responses. *Arch Gen Psychiatry* **51**, 199-214.
Kwon, J. S., O'Donnell, B. F., Wallenstein, G. V., Greene, R. W., Hirayasu, Y., Nestor, P. G., Hasselmo, M. E., Potts, G. F., Shenton, M. E. & McCarley, R. W. (1999). Gamma frequency-range abnormalities to auditory stimulation in schizophrenia. *Arch Gen Psychiatry* **56**, 1001-5.
Lahti, A. C., Holcomb, H. H., Medoff, D. R. & Tamminga, C. A. (1995). Ketamine activates psychosis and alters limbic blood flow in schizophrenia. *Neuroreport* **6**, 869-72.
Lahti, A. C., Weiler, M. A., Tamara Michaelidis, B. A., Parwani, A. & Tamminga, C. A. (2001). Effects of ketamine in normal and schizophrenic volunteers. *Neuropsychopharmacology* **25**, 455-67.
Lauterbur, P. C. (1989). Image formation by induced local interactions. Examples employing nuclear magnetic resonance. 1973. *Clin Orthop Relat Res*, 3-6.
Law, A. J. & Deakin, J. F. (2001). Asymmetrical reductions of hippocampal NMDAR1 glutamate receptor mRNA in the psychoses. *Neuroreport* **12**, 2971-4.
Lawrence, R. W., Evans, D. M. & Cardon, L. R. (2005). Prospects and pitfalls in whole genome association studies. *Philos Trans R Soc Lond B Biol Sci* **360**, 1589-95.
Le Hir, H., Nott, A. & Moore, M. J. (2003). How introns influence and enhance eukaryotic gene expression. *Trends Biochem Sci* **28**, 215-20.
Le Van Quyen, M., Foucher, J., Lachaux, J., Rodriguez, E., Lutz, A., Martinerie, J. & Varela, F. J. (2001). Comparison of Hilbert transform and wavelet methods for the analysis of neuronal synchrony. *J Neurosci Methods* **111**, 83-98.
Lewis, D. A., Curley, A. A., Glausier, J. R. & Volk, D. W. (2012). Cortical parvalbumin interneurons and cognitive dysfunction in schizophrenia. *Trends in Neurosciences* **35**, 57-67.
Lewis, D. A., Hashimoto, T. & Volk, D. W. (2005). Cortical inhibitory neurons and schizophrenia. *Nat Rev Neurosci* **6**, 312-24.
Linden, D. E. (2012). The challenges and promise of neuroimaging in psychiatry. *Neuron* **73**, 8-22.
Linden, J. F. & Schreiner, C. E. (2003). Columnar transformations in auditory cortex? A comparison to visual and somatosensory cortices. *Cereb Cortex* **13**, 83-9.
Lins, O. G., Picton, P. E., Picton, T. W., Champagne, S. C. & Durieux-Smith, A. (1995). Auditory steady-state responses to tones amplitude-modulated at 80-110 Hz. *J Acoust Soc Am* **97**, 3051-63.
Liu, C. S., Bryan, R. N., Miki, A., Woo, J. H., Liu, G. T. & Elliott, M. A. (2006). Magnocellular and parvocellular visual pathways have different blood oxygen level-dependent signal time courses in human primary visual cortex. *AJNR Am J Neuroradiol* **27**, 1628-34.

Liu, T. Y., Chen, Y. S., Su, T. P., Hsieh, J. C. & Chen, L. F. (2014). Abnormal early gamma responses to emotional faces differentiate unipolar from bipolar disorder patients. *Biomed Res Int* **2014**, 906104.
Liu, T. Y., Hsieh, J. C., Chen, Y. S., Tu, P. C., Su, T. P. & Chen, L. F. (2012). Different patterns of abnormal gamma oscillatory activity in unipolar and bipolar disorder patients during an implicit emotion task. *Neuropsychologia* **50**, 1514-1520.
Liégeois-Chauvel, C., Giraud, K., Badier, J. M., Marquis, P. & Chauvel, P. (2001). Intracerebral evoked potentials in pitch perception reveal a functional asymmetry of the human auditory cortex. *Ann N Y Acad Sci* **930**, 117-32.
Lo, W. S., Lau, C. F., Xuan, Z., Chan, C. F., Feng, G. Y., He, L., Cao, Z. C., Liu, H., Luan, Q. M. & Xue, H. (2004). Association of SNPs and haplotypes in GABAA receptor beta2 gene with schizophrenia. *Mol Psychiatry* **9**, 603-8.
Long, Z., Medlock, C., Dzemidzic, M., Shin, Y. W., Goddard, A. W. & Dydak, U. (2013). Decreased GABA levels in anterior cingulate cortex/medial prefrontal cortex in panic disorder. *Prog Neuropsychopharmacol Biol Psychiatry* **44**, 131-5.
LUBY, E. D., COHEN, B. D., ROSENBAUM, G., GOTTLIEB, J. S. & KELLEY, R. (1959). Study of a new schizophrenomimetic drug; sernyl. *AMA Arch Neurol Psychiatry* **81**, 363-9.
Lund, J. S. (1988). Anatomical organization of macaque monkey striate visual cortex. *Annu Rev Neurosci* **11**, 253-88.
Lundorf, M. D., Buttenschøn, H. N., Foldager, L., Blackwood, D. H., Muir, W. J., Murray, V., Pelosi, A. J., Kruse, T. A., Ewald, H. & Mors, O. (2005). Mutational screening and association study of glutamate decarboxylase 1 as a candidate susceptibility gene for bipolar affective disorder and schizophrenia. *Am J Med Genet B Neuropsychiatr Genet* **135B**, 94-101.
Manju, V., Gopika, K. K. & Arivudai Nambi, P. M. (2014). Association of auditory steady state responses with perception of temporal modulations and speech in noise. *ISRN Otolaryngol* **2014**, 374035.
Mansfield, P. & Maudsley, A. A. (1977). Medical imaging by NMR. *Br J Radiol* **50**, 188-94.
Marchini, J. & Howie, B. (2010). Genotype imputation for genome-wide association studies. *Nat Rev Genet* **11**, 499-511.
Marenco, S., Geramita, M., van der Veen, J. W., Barnett, A. S., Kolachana, B., Shen, J., Weinberger, D. R. & Law, A. J. (2011). Genetic association of ErbB4 and human cortical GABA levels in vivo. *J Neurosci* **31**, 11628-32.
Marenco, S., Savostyanova, A. A., van der Veen, J. W., Geramita, M., Stern, A., Barnett, A. S., Kolachana, B., Radulescu, E., Zhang, F., Callicott, J. H., Straub, R. E., Shen, J. & Weinberger, D. R. (2010). Genetic modulation of GABA levels in the anterior cingulate cortex by GAD1 and COMT. *Neuropsychopharmacology* **35**, 1708-17.
Maris, E. & Oostenveld, R. (2007). Nonparametric statistical testing of EEG- and MEG-data. *Journal of Neuroscience Methods* **164**, 177-190.
Marsman, A., Mandl, R. C., Klomp, D. W., Bohlken, M. M., Boer, V. O., Andreychenko, A., Cahn, W., Kahn, R. S., Luijten, P. R. & Hulshoff Pol, H. E. (2014). GABA and glutamate in schizophrenia: a 7 T ^{1}H-MRS study. *Neuroimage Clin* **6**, 398-407.
Martin, D. L., Martin, S. B., Wu, S. J. & Espina, N. (1991). Regulatory properties of brain glutamate decarboxylase (GAD): the apoenzyme of GAD is present principally as the smaller of two molecular forms of GAD in brain. *J Neurosci* **11**, 2725-31.
Martinez, L. M., Wang, Q., Reid, R. C., Pillai, C., Alonso, J. M., Sommer, F. T. & Hirsch, J. A. (2005). Receptive field structure varies with layer in the primary visual cortex. *Nat Neurosci* **8**, 372-9.
Martucci, L., Wong, A. H., De Luca, V., Likhodi, O., Wong, G. W., King, N. & Kennedy, J. L. (2006). N-methyl-D-aspartate receptor NR2B subunit gene GRIN2B in schizophrenia and bipolar disorder: Polymorphisms and mRNA levels. *Schizophr Res* **84**, 214-21.
Mason, G. F., Martin, D. L., Martin, S. B., Manor, D., Sibson, N. R., Patel, A., Rothman, D. L. & Behar, K. L. (2001). Decrease in GABA synthesis rate in rat cortex following GABA-transaminase inhibition correlates with the decrease in GAD(67) protein. *Brain Res* **914**, 81-91.

Mauer, G. & Döring, W. H. (1999). Generators of amplitude modulation following response (AMFR). *Paper presented at 16th meeting of the Evoked Response Audiometry Study Group, Tromso, Norway.*
Mazaheri, A. & Van Diepen, R. (2014). Gamma Oscillations in a Bind?†. *Cereb Cortex*.
McFadden, K. L., Steinmetz, S. E., Carroll, A. M., Simon, S. T., Wallace, A. & Rojas, D. C. (2014). Test-retest reliability of the 40 Hz EEG auditory steady-state response. *PLoS One* **9**, e85748.
Merikangas, K. R., Akiskal, H. S., Angst, J., Greenberg, P. E., Hirschfeld, R. M., Petukhova, M. & Kessler, R. C. (2007). Lifetime and 12-month prevalence of bipolar spectrum disorder in the National Comorbidity Survey replication. *Arch Gen Psychiatry* **64**, 543-52.
Mescher, M., Merkle, H., Kirsch, J., Garwood, M. & Gruetter, R. (1998). Simultaneous in vivo spectral editing and water suppression. *NMR Biomed* **11**, 266-72.
Meyer-Lindenberg, A. (2010a). From maps to mechanisms through neuroimaging of schizophrenia. *Nature* **468**, 194-202.
Meyer-Lindenberg, A. (2010b). Imaging genetics of schizophrenia. *Dialogues Clin Neurosci* **12**, 449-56.
Mignone, F., Gissi, C., Liuni, S. & Pesole, G. (2002). Untranslated regions of mRNAs. *Genome Biol* **3**, REVIEWS0004.
Minzenberg, M. J., Firl, A. J., Yoon, J. H., Gomes, G. C., Reinking, C. & Carter, C. S. (2010). Gamma oscillatory power is impaired during cognitive control independent of medication status in first-episode schizophrenia. *Neuropsychopharmacology* **35**, 2590-9.
Miyamoto, S., Miyake, N., Jarskog, L. F., Fleischhacker, W. W. & Lieberman, J. A. (2012). Pharmacological treatment of schizophrenia: a critical review of the pharmacology and clinical effects of current and future therapeutic agents. *Mol Psychiatry* **17**, 1206-27.
Moghaddam, B. & Javitt, D. (2012). From revolution to evolution: the glutamate hypothesis of schizophrenia and its implication for treatment. *Neuropsychopharmacology* **37**, 4-15.
Mulert, C., Kirsch, V., Pascual-Marqui, R., McCarley, R. W. & Spencer, K. M. (2011). Long-range synchrony of gamma oscillations and auditory hallucination symptoms in schizophrenia. *International Journal of Psychophysiology* **79**, 55-63.
Mullins, P. G., McGonigle, D. J., O'Gorman, R. L., Puts, N. A., Vidyasagar, R., Evans, C. J., Edden, R. A. & GABA, C. S. o. M. o. (2014). Current practice in the use of MEGA-PRESS spectroscopy for the detection of GABA. *Neuroimage* **86**, 43-52.
Muthukumaraswamy, S. D. (2010). Functional properties of human primary motor cortex gamma oscillations. *J Neurophysiol* **104**, 2873-85.
Muthukumaraswamy, S. D., Edden, R. A. E., Jones, D. K., Swettenham, J. B. & Singh, K. D. (2009). Resting GABA concentration predicts peak gamma frequency and fMRI amplitude in response to visual stimulation in humans. *Proceedings of the National Academy of Sciences of the United States of America* **106**, 8356-8361.
Muthukumaraswamy, S. D., Myers, J. F., Wilson, S. J., Nutt, D. J., Hamandi, K., Lingford-Hughes, A. & Singh, K. D. (2013). Elevating Endogenous GABA Levels with GAT-1 Blockade Modulates Evoked but Not Induced Responses in Human Visual Cortex. *Neuropsychopharmacology*.
.
Muthukumaraswamy, S. D., Singh, K. D., Swettenham, J. B. & Jones, D. K. (2010). Visual gamma oscillations and evoked responses: Variability, repeatability and structural MRI correlates. *Neuroimage* **49**, 3349-3357.
Muñoz, K. E., Hyde, L. W. & Hariri, A. R. (2009). Imaging genetics. *J Am Acad Child Adolesc Psychiatry* **48**, 356-61.
Nakazawa, K., Zsiros, V., Jiang, Z., Nakao, K., Kolata, S., Zhang, S. & Belforte, J. E. (2012). GABAergic interneuron origin of schizophrenia pathophysiology. *Neuropharmacology* **62**, 1574-83.
Near, J., Ho, Y. C., Sandberg, K., Kumaragamage, C. & Blicher, J. U. (2014). Long-term reproducibility of GABA magnetic resonance spectroscopy. *Neuroimage* **99**, 191-6.
Near, J., Simpson, R., Cowen, P. & Jezzard, P. (2011). Efficient γ-aminobutyric acid editing at 3T without macromolecule contamination: MEGA-SPECIAL. *NMR Biomed* **24**, 1277-85.

Nichols, T. E. & Holmes, A. P. (2002). Nonparametric permutation tests for functional neuroimaging: A primer with examples. *Human Brain Mapping* **15**, 1-25.
Nott, A., Meislin, S. H. & Moore, M. J. (2003). A quantitative analysis of intron effects on mammalian gene expression. *RNA* **9**, 607-17.
O'Bryan, R. A., Brenner, C. A., Hetrick, W. P. & O'Donnell, B. F. (2014). Disturbances of visual motion perception in bipolar disorder. *Bipolar Disord* **16**, 354-65.
O'Donnell, B. F., Hetrick, W. P., Vohs, J. L., Krishnan, G. P., Carroll, C. A. & Shekhar, A. (2004). Neural synchronization deficits to auditory stimulation in bipolar disorder. *Neuroreport* **15**, 1369-1372.
O'Donnell, B. F., Vohs, J. L., Krishnan, G. P., Rass, O., Hetrick, W. P. & Morzorati, S. L. (2013). The auditory steady-state response (ASSR): a translational biomarker for schizophrenia. *Suppl Clin Neurophysiol* **62**, 101-12.
O'Gorman, R. L., Michels, L., Edden, R. A., Murdoch, J. B. & Martin, E. (2011). In vivo detection of GABA and glutamate with MEGA-PRESS: reproducibility and gender effects. *J Magn Reson Imaging* **33**, 1262-7.
Oda, Y., Onitsuka, T., Tsuchimoto, R., Hirano, S., Oribe, N., Ueno, T., Hirano, Y., Nakamura, I., Miura, T. & Kanba, S. (2012). Gamma band neural synchronization deficits for auditory steady state responses in bipolar disorder patients. *PLoS One* **7**, e39955.
Okada, Y. C. (1989). *Recent Developments on the Physiological Basis of Magnetoencephalography (MEG)*. Plenum Press: New York
Oke, O. O., Magony, A., Anver, H., Ward, P. D., Jiruska, P., Jefferys, J. G. R. & Vreugdenhil, M. (2010). High-frequency gamma oscillations coexist with low-frequency gamma oscillations in the rat visual cortex in vitro. *European Journal of Neuroscience* **31**, 1435-1445.
Oldfield, R. C. (1971). The assessment and analysis of handedness: the Edinburgh inventory. *Neuropsychologia* **9**, 97-113.
Olsen, R. W. & Sieghart, W. (2008). International Union of Pharmacology. LXX. Subtypes of gamma-aminobutyric acid(A) receptors: classification on the basis of subunit composition, pharmacology, and function. Update. *Pharmacol Rev* **60**, 243-60.
Olsen, R. W. & Sieghart, W. (2009). GABA A receptors: subtypes provide diversity of function and pharmacology. *Neuropharmacology* **56**, 141-8.
Ongür, D., Prescot, A. P., McCarthy, J., Cohen, B. M. & Renshaw, P. F. (2010). Elevated gamma-aminobutyric acid levels in chronic schizophrenia. *Biol Psychiatry* **68**, 667-70.
Oostenveld, R., Fries, P., Maris, E. & Schoffelen, J. M. (2011). FieldTrip: Open source software for advanced analysis of MEG, EEG, and invasive electrophysiological data. *Comput Intell Neurosci* **2011**, 156869.
Pantev, C. (1995). Evoked and induced gamma-band activity of the human cortex. *Brain Topogr* **7**, 321-30.
Pantev, C., Roberts, L. E., Elbert, T., Ross, B. & Wienbruch, C. (1996). Tonotopic organization of the sources of human auditory steady-state responses. *Hear Res* **101**, 62-74.
Pastor, M. A., Artieda, J., Arbizu, J., Marti-Climent, J. M., Peñuelas, I. & Masdeu, J. C. (2002). Activation of human cerebral and cerebellar cortex by auditory stimulation at 40 Hz. *J Neurosci* **22**, 10501-6.
Pastor, M. A., Vidaurre, C., Fernández-Seara, M. A., Villanueva, A. & Friston, K. J. (2008). Frequency-specific coupling in the cortico-cerebellar auditory system. *J Neurophysiol* **100**, 1699-705.
Perry, G., Adjamian, P., Thai, N. J., Holliday, I. E., Hillebrand, A. & Barnes, G. R. (2011). Retinotopic mapping of the primary visual cortex - a challenge for MEG imaging of the human cortex. *Eur J Neurosci* **34**, 652-61.
Perry, G., Brindley, L. M., Muthukumaraswamy, S. D., Singh, K. D. & Hamandi, K. (2014). Evidence for increased visual gamma responses in photosensitive epilepsy. *Epilepsy Research* **In Press**.

Perry, G., Hamandi, K., Brindley, L. M., Muthukumaraswamy, S. D. & Singh, K. D. (2013). The properties of induced gamma oscillations in human visual cortex show individual variability in their dependence on stimulus size. *Neuroimage* **68**, 83-92.

Petryshen, T. L., Middleton, F. A., Tahl, A. R., Rockwell, G. N., Purcell, S., Aldinger, K. A., Kirby, A., Morley, C. P., McGann, L., Gentile, K. L., Waggoner, S. G., Medeiros, H. M., Carvalho, C., Macedo, A., Albus, M., Maier, W., Trixler, M., Eichhammer, P., Schwab, S. G., Wildenauer, D. B., Azevedo, M. H., Pato, M. T., Pato, C. N., Daly, M. J. & Sklar, P. (2005). Genetic investigation of chromosome 5q GABAA receptor subunit genes in schizophrenia. *Mol Psychiatry* **10**, 1074-88, 1057.

Pfurtscheller, G. & Lopes da Silva, F. H. (1999). Event-related EEG/MEG synchronization and desynchronization: basic principles. *Clin Neurophysiol* **110**, 1842-57.

Picton, T. W., Skinner, C. R., Champagne, S. C., Kellett, A. J. & Maiste, A. C. (1987). Potentials evoked by the sinusoidal modulation of the amplitude or frequency of a tone. *J Acoust Soc Am* **82**, 165-78.

Pilowsky, L. S., Bressan, R. A., Stone, J. M., Erlandsson, K., Mulligan, R. S., Krystal, J. H. & Ell, P. J. (2006). First in vivo evidence of an NMDA receptor deficit in medication-free schizophrenic patients. *Mol Psychiatry* **11**, 118-9.

Plourde, G., Baribeau, J. & Bonhomme, V. (1997). Ketamine increases the amplitude of the 40-Hz auditory steady-state response in humans. *Br J Anaesth* **78**, 524-9.

Poels, E. M., Kegeles, L. S., Kantrowitz, J. T., Slifstein, M., Javitt, D. C., Lieberman, J. A., Abi-Dargham, A. & Girgis, R. R. (2014). Imaging glutamate in schizophrenia: review of findings and implications for drug discovery. *Mol Psychiatry* **19**, 20-9.

Pontious, A., Kowalczyk, T., Englund, C. & Hevner, R. F. (2008). Role of intermediate progenitor cells in cerebral cortex development. *Dev Neurosci* **30**, 24-32.

Potkin, S. G., Turner, J. A., Guffanti, G., Lakatos, A., Fallon, J. H., Nguyen, D. D., Mathalon, D., Ford, J., Lauriello, J., Macciardi, F. & FBIRN (2009a). A genome-wide association study of schizophrenia using brain activation as a quantitative phenotype. *Schizophr Bull* **35**, 96-108.

Potkin, S. G., Turner, J. A., Guffanti, G., Lakatos, A., Torri, F., Keator, D. B. & Macciardi, F. (2009b). Genome-wide strategies for discovering genetic influences on cognition and cognitive disorders: methodological considerations. *Cogn Neuropsychiatry* **14**, 391-418.

Prathikanti, S. & Weinberger, D. R. (2005). Psychiatric genetics--the new era: genetic research and some clinical implications. *Br Med Bull* **73-74**, 107-22.

Price, A. L., Patterson, N. J., Plenge, R. M., Weinblatt, M. E., Shadick, N. A. & Reich, D. (2006). Principal components analysis corrects for stratification in genome-wide association studies. *Nat Genet* **38**, 904-9.

Purcell, D. W., John, S. M., Schneider, B. A. & Picton, T. W. (2004). Human temporal auditory acuity as assessed by envelope following responses. *J Acoust Soc Am* **116**, 3581-93.

Purcell, S., Neale, B., Todd-Brown, K., Thomas, L., Ferreira, M. A., Bender, D., Maller, J., Sklar, P., de Bakker, P. I., Daly, M. J. & Sham, P. C. (2007). PLINK: a tool set for whole-genome association and population-based linkage analyses. *Am J Hum Genet* **81**, 559-75.

Purcell, S. M., Wray, N. R., Stone, J. L., Visscher, P. M., O'Donovan, M. C., Sullivan, P. F., Sklar, P. & Consortium, I. S. (2009). Common polygenic variation contributes to risk of schizophrenia and bipolar disorder. *Nature* **460**, 748-52.

Puts, N. A. & Edden, R. A. (2012). In vivo magnetic resonance spectroscopy of GABA: a methodological review. *Prog Nucl Magn Reson Spectrosc* **60**, 29-41.

Puts, N. A., Edden, R. A., Evans, C. J., McGlone, F. & McGonigle, D. J. (2011). Regionally specific human GABA concentration correlates with tactile discrimination thresholds. *J Neurosci* **31**, 16556-60.

Pérez-Alcázar, M., Nicolás, M. J., Valencia, M., Alegre, M., Iriarte, J. & Artieda, J. (2008). Chirp-evoked potentials in the awake and anesthetized rat. A procedure to assess changes in cortical oscillatory activity. *Exp Neurol* **210**, 144-53.

R Development Core Team (2013). R: A language and environment for statistical computing. R Foundation for Statistical Computing: Vienna, Austria.
Rademacher, J., Morosan, P., Schormann, T., Schleicher, A., Werner, C., Freund, H. J. & Zilles, K. (2001). Probabilistic mapping and volume measurement of human primary auditory cortex. *Neuroimage* **13**, 669-83.
Rakic, P. (1988). Specification of cerebral cortical areas. *Science* **241**, 170-6.
Ramasamy, A., Trabzuni, D., Guelfi, S., Varghese, V., Smith, C., Walker, R., De, T., Coin, L., de Silva, R., Cookson, M. R., Singleton, A. B., Hardy, J., Ryten, M., Weale, M. E., Consortium, U. B. E. & Consortium, N. A. B. E. (2014). Genetic variability in the regulation of gene expression in ten regions of the human brain. *Nat Neurosci* **17**, 1418-28.
Rass, O., Krishnan, G., Brenner, C. A., Hetrick, W. P., Merrill, C. C., Shekhar, A. & O'Donnell, B. F. (2010). Auditory steady state response in bipolar disorder: relation to clinical state, cognitive performance, medication status, and substance disorders. *Bipolar Disorders* **12**, 793-803.
Ray, S. & Maunsell, J. H. (2010). Differences in gamma frequencies across visual cortex restrict their possible use in computation. *Neuron* **67**, 885-96.
Read, H. L., Winer, J. A. & Schreiner, C. E. (2002). Functional architecture of auditory cortex. *Curr Opin Neurobiol* **12**, 433-40.
Regier, D. A., Narrow, W. E., Rae, D. S., Manderscheid, R. W., Locke, B. Z. & Goodwin, F. K. (1993). The de facto US mental and addictive disorders service system. Epidemiologic catchment area prospective 1-year prevalence rates of disorders and services. *Arch Gen Psychiatry* **50**, 85-94.
Reite, M., Teale, P., Collins, D. & Rojas, D. C. (2010). Schizoaffective disorder - A possible MEG auditory evoked field biomarker. *Psychiatry Research-Neuroimaging* **182**, 284-286.
Ribary, U., Ioannides, A. A., Singh, K. D., Hasson, R., Bolton, J. P., Lado, F., Mogilner, A. & Llinás, R. (1991). Magnetic field tomography of coherent thalamocortical 40-Hz oscillations in humans. *Proc Natl Acad Sci U S A* **88**, 11037-41.
Riečanský, I., Kašpárek, T., Rehulová, J., Katina, S. & Přikryl, R. (2010). Aberrant EEG responses to gamma-frequency visual stimulation in schizophrenia. *Schizophr Res* **124**, 101-9.
Ripke, S., O'Dushlaine, C., Chambert, K., Moran, J. L., Kähler, A. K., Akterin, S., Bergen, S. E., Collins, A. L., Crowley, J. J., Fromer, M., Kim, Y., Lee, S. H., Magnusson, P. K., Sanchez, N., Stahl, E. A., Williams, S., Wray, N. R., Xia, K., Bettella, F., Borglum, A. D., Bulik-Sullivan, B. K., Cormican, P., Craddock, N., de Leeuw, C., Durmishi, N., Gill, M., Golimbet, V., Hamshere, M. L., Holmans, P., Hougaard, D. M., Kendler, K. S., Lin, K., Morris, D. W., Mors, O., Mortensen, P. B., Neale, B. M., O'Neill, F. A., Owen, M. J., Milovancevic, M. P., Posthuma, D., Powell, J., Richards, A. L., Riley, B. P., Ruderfer, D., Rujescu, D., Sigurdsson, E., Silagadze, T., Smit, A. B., Stefansson, H., Steinberg, S., Suvisaari, J., Tosato, S., Verhage, M., Walters, J. T., Levinson, D. F., Gejman, P. V., Laurent, C., Mowry, B. J., O'Donovan, M. C., Pulver, A. E., Schwab, S. G., Wildenauer, D. B., Dudbridge, F., Shi, J., Albus, M., Alexander, M., Campion, D., Cohen, D., Dikeos, D., Duan, J., Eichhammer, P., Godard, S., Hansen, M., Lerer, F. B., Liang, K. Y., Maier, W., Mallet, J., Nertney, D. A., Nestadt, G., Norton, N., Papadimitriou, G. N., Ribble, R., Sanders, A. R., Silverman, J. M., Walsh, D., Williams, N. M., Wormley, B., Arranz, M. J., Bakker, S., Bender, S., Bramon, E., Collier, D., Crespo-Facorro, B., Hall, J., Iyegbe, C., Jablensky, A., Kahn, R. S., Kalaydjieva, L., Lawrie, S., Lewis, C. M., Linszen, D. H., Mata, I., McIntosh, A., Murray, R. M., Ophoff, R. A., Van Os, J., Walshe, M., Weisbrod, M., Wiersma, D., Donnelly, P., Barroso, I., Blackwell, J. M., Brown, M. A., Casas, J. P., Corvin, A. P., Deloukas, P., Duncanson, A., Jankowski, J., Markus, H. S., Mathew, C. G., Palmer, C. N., Plomin, R., Rautanen, A., Sawcer, S. J., Trembath, R. C., Viswanathan, A. C., Wood, N. W., Spencer, C. C., Band, G., Bellenguez, C., Freeman, C., Hellenthal, G., Giannoulatou, E., Pirinen, M., Pearson, R. D., Strange, A., Su, Z., Vukcevic, D., Langford, C., Hunt, S. E., Edkins, S., Gwilliam, R., Blackburn, H., Bumpstead, S. J., Dronov, S., Gillman, M., Gray, E., Hammond, N., Jayakumar, A., McCann, O. T., Liddle, J., Potter, S. C., Ravindrarajah, R., Ricketts, M., Tashakkori-Ghanbaria, A., Waller, M. J., Weston, P., Widaa, S., Whittaker, P., McCarthy, M. I., Stefansson, K., Scolnick, E., Purcell, S., McCarroll, S. A., Sklar, P., Hultman, C. M., Sullivan, P. F., Consortium, M. G. S. o. S., Consortium, P.

E. I. & 2, W. T. C. C. C. (2013). Genome-wide association analysis identifies 13 new risk loci for schizophrenia. *Nat Genet* **45**, 1150-9.
Robinson, S. E. (2004). Localization of event-related activity by SAM(erf). In *Neurol Clin Neurophysiol*, p. 109: United States.
Robinson, S. E. & Vrba, J. (1999). Functional neuroimaging by syntheticaperture magnetometry ({SAM}). In *Recent Advances in Biomagnetism* (ed. T. Yoshimoto, M. Kotani, S. Kuriki, H. Karibe and N. Nakasato), pp. 302-305. Tohoku Univ. Press: Sendai, Japan.
Robson, S. (2012). Individual Differences in Excitation and Inhibition in Visual Cortex. In *Psychology*, p. 179. Cardiff University.
Rojas, D. C., Maharajh, K., Teale, P. & Rogers, S. J. (2008). Reduced neural synchronization of gamma-band MEG oscillations in first-degree relatives of children with autism. *BMC Psychiatry* **8**, 66.
Rojas, D. C., Teale, P. D., Maharajh, K., Kronberg, E., Youngpeter, K., Wilson, L. B., Wallace, A. & Hepburn, S. (2011). Transient and steady-state auditory gamma-band responses in first-degree relatives of people with autism spectrum disorder. *Mol Autism* **2**, 11.
Ross, B., Borgmann, C., Draganova, R., Roberts, L. E. & Pantev, C. (2000). A high-precision magnetoencephalographic study of human auditory steady-state responses to amplitude-modulated tones. *J Acoust Soc Am* **108**, 679-91.
Ross, B., Herdman, A. T. & Pantev, C. (2005). Right hemispheric laterality of human 40 Hz auditory steady-state responses. *Cereb Cortex* **15**, 2029-39.
Rowland, L. M., Astur, R. S., Jung, R. E., Bustillo, J. R., Lauriello, J. & Yeo, R. A. (2005). Selective cognitive impairments associated with NMDA receptor blockade in humans. *Neuropsychopharmacology* **30**, 633-9.
Rowland, L. M., Kontson, K., West, J., Edden, R. A., Zhu, H., Wijtenburg, S. A., Holcomb, H. H. & Barker, P. B. (2013). In vivo measurements of glutamate, GABA, and NAAG in schizophrenia. *Schizophr Bull* **39**, 1096-104.
Salat, D. H., Buckner, R. L., Snyder, A. Z., Greve, D. N., Desikan, R. S., Busa, E., Morris, J. C., Dale, A. M. & Fischl, B. (2004). Thinning of the cerebral cortex in aging. *Cereb Cortex* **14**, 721-30.
Saxena, N., Muthukumaraswamy, S. D., Diukova, A., Singh, K., Hall, J. & Wise, R. (2013). Enhanced Stimulus-Induced Gamma Activity in Humans during Propofol-Induced Sedation. In *PLoS One*, p. e57685: United States.
Schnitzler, A. & Gross, J. (2005). Normal and pathological oscillatory communication in the brain. *Nat Rev Neurosci* **6**, 285-96.
Schulz, S. B., Heidmann, K. E., Mike, A., Klaft, Z. J., Heinemann, U. & Gerevich, Z. (2012). First and second generation antipsychotics influence hippocampal gamma oscillations by interactions with 5-HT3 and D-3 receptors. *British Journal of Pharmacology* **167**, 1480-1491.
Schwarzkopf, D. S., Robertson, D. J., Song, C., Barnes, G. R. & Rees, G. (2012). The frequency of visually induced gamma-band oscillations depends on the size of early human visual cortex. *J Neurosci* **32**, 1507-12.
Schwarzkopf, D. S., Song, C. & Rees, G. (2011). The surface area of human V1 predicts the subjective experience of object size. *Nat Neurosci* **14**, 28-30.
Shaw, A., Brealy, J., Richardson, H., Muthukumaraswamy, S. D., Edden, R. A., John Evans, C., Puts, N. A., Singh, K. D. & Keedwell, P. A. (2013). Marked reductions in visual evoked responses but not gamma-aminobutyric acid concentrations or gamma-band measures in remitted depression. *Biol Psychiatry* **73**, 691-8.
Sheehan, D. V., Lecrubier, Y., Sheehan, K. H., Amorim, P., Janavs, J., Weiller, E., Hergueta, T., Baker, R. & Dunbar, G. C. (1998). The Mini-International Neuropsychiatric Interview (M.I.N.I.): the development and validation of a structured diagnostic psychiatric interview for DSM-IV and ICD-10. *J Clin Psychiatry* **59 Suppl 20**, 22-33;quiz 34-57.
Sivarao, D. V., Frenkel, M., Chen, P., Healy, F. L., Lodge, N. J. & Zaczek, R. (2013). MK-801 disrupts and nicotine augments 40 Hz auditory steady state responses in the auditory cortex of the urethane-anesthetized rat. *Neuropharmacology* **73**, 1-9.

Smith, P. H. & Populin, L. C. (2001). Fundamental differences between the thalamocortical recipient layers of the cat auditory and visual cortices. *J Comp Neurol* **436**, 508-19.
Sohal, V. S., Zhang, F., Yizhar, O. & Deisseroth, K. (2009). Parvalbumin neurons and gamma rhythms enhance cortical circuit performance. *Nature* **459**, 698-702.
Song, C., Schwarzkopf, D. S., Lutti, A., Li, B., Kanai, R. & Rees, G. (2013). Effective connectivity within human primary visual cortex predicts interindividual diversity in illusory perception. *J Neurosci* **33**, 18781-91.
Soto, D., Rotshtein, P. & Kanai, R. (2014). Parietal structure and function explain human variation in working memory biases of visual attention. *Neuroimage* **89**, 289-96.
Spaak, E., Bonnefond, M., Maier, A., Leopold, D. A. & Jensen, O. (2012). Layer-Specific Entrainment of Gamma-Band Neural Activity by the Alpha Rhythm in Monkey Visual Cortex. *Current Biology* **22**, 2313-2318.
Spencer, K. M. (2009). The functional consequences of cortical circuit abnormalities on gamma oscillations in schizophrenia: insights from computational modeling. *Frontiers in Human Neuroscience* **3**.
Spencer, K. M. (2012). Baseline gamma power during auditory steady-state stimulation in schizophrenia. *Frontiers in Human Neuroscience* **5**.
Spencer, K. M., Nestor, P. G., Niznikiewicz, M. A., Salisbury, D. F., Shenton, M. E. & McCarley, R. W. (2003). Abnormal neural synchrony in schizophrenia. *J Neurosci* **23**, 7407-11.
Spencer, K. M., Nestor, P. G., Perlmutter, R., Niznikiewicz, M. A., Klump, M. C., Frumin, M., Shenton, M. E. & McCarley, R. W. (2004). Neural synchrony indexes disordered perception and cognition in schizophrenia. *Proceedings of the National Academy of Sciences of the United States of America* **101**, 17288-17293.
Spencer, K. M., Niznikiewicz, M. A., Nestor, P. G., Shenton, M. E. & McCarley, R. W. (2009). Left auditory cortex gamma synchronization and auditory hallucination symptoms in schizophrenia. *Bmc Neuroscience* **10**.
Spencer, K. M., Niznikiewicz, M. A., Shenton, M. E. & McCarley, R. W. (2008a). Sensory-evoked gamma oscillations in chronic schizophrenia. *Biological Psychiatry* **63**, 744-747.
Spencer, K. M., Salisbury, D. F., Shenton, M. E. & McCarley, R. W. (2008b). gamma-band auditory steady-state responses are impaired in first episode psychosis. *Biological Psychiatry* **64**, 369-375.
Spitzer, R. L., Endicott, J. & Robins, E. (1978). Research diagnostic criteria: rationale and reliability. *Arch Gen Psychiatry* **35**, 773-82.
Stagg, C. J., Bachtiar, V. & Johansen-Berg, H. (2011a). The role of GABA in human motor learning. *Curr Biol* **21**, 480-4.
Stagg, C. J., Bachtiar, V. & Johansen-Berg, H. (2011b). What are we measuring with GABA magnetic resonance spectroscopy? *Commun Integr Biol* **4**, 573-5.
Stan, A. D. & Lewis, D. A. (2012). Altered cortical GABA neurotransmission in schizophrenia: insights into novel therapeutic strategies. *Curr Pharm Biotechnol* **13**, 1557-62.
Stanley, J. A. (2002). In vivo magnetic resonance spectroscopy and its application to neuropsychiatric disorders. *Can J Psychiatry* **47**, 315-26.
Stone, J. M., Dietrich, C., Edden, R., Mehta, M. A., De Simoni, S., Reed, L. J., Krystal, J. H., Nutt, D. & Barker, G. J. (2012). Ketamine effects on brain GABA and glutamate levels with 1H-MRS: relationship to ketamine-induced psychopathology. *Mol Psychiatry* **17**, 664-5.
Storey, P. (2006). Introduction to magnetic resonance imaging and spectroscopy. *Methods Mol Med* **124**, 3-57.
Straub, R. E., Lipska, B. K., Egan, M. F., Goldberg, T. E., Callicott, J. H., Mayhew, M. B., Vakkalanka, R. K., Kolachana, B. S., Kleinman, J. E. & Weinberger, D. R. (2007). Allelic variation in GAD1 (GAD67) is associated with schizophrenia and influences cortical function and gene expression. *Mol Psychiatry* **12**, 854-69.
Subburaju, S. & Benes, F. M. (2012). Induction of the GABA cell phenotype: an in vitro model for studying neurodevelopmental disorders. *PLoS One* **7**, e33352.

Sullivan, P. F., Daly, M. J. & O'Donovan, M. (2012). Genetic architectures of psychiatric disorders: the emerging picture and its implications. *Nat Rev Genet* **13**, 537-51.
Sumner, P., Edden, R. A., Bompas, A., Evans, C. J. & Singh, K. D. (2010). More GABA, less distraction: a neurochemical predictor of motor decision speed. *Nat Neurosci* **13**, 825-7.
Sun, L., Castellanos, N., Grützner, C., Koethe, D., Rivolta, D., Wibral, M., Kranaster, L., Singer, W., Leweke, M. F. & Uhlhaas, P. J. (2013). Evidence for dysregulated high-frequency oscillations during sensory processing in medication-naïve, first episode schizophrenia. *Schizophr Res* **150**, 519-25.
Swettenham, J. B., Muthukumaraswamy, S. D. & Singh, K. D. (2009). Spectral properties of induced and evoked gamma oscillations in human early visual cortex to moving and stationary stimuli. *J Neurophysiol* **102**, 1241-53.
Symms, M., Jäger, H. R., Schmierer, K. & Yousry, T. A. (2004). A review of structural magnetic resonance neuroimaging. *J Neurol Neurosurg Psychiatry* **75**, 1235-44.
Tadin, D., Kim, J., Doop, M. L., Gibson, C., Lappin, J. S., Blake, R. & Park, S. (2006). Weakened center-surround interactions in visual motion processing in schizophrenia. *J Neurosci* **26**, 11403-12.
Tan, H. R., Lana, L. & Uhlhaas, P. J. (2013). High-frequency neural oscillations and visual processing deficits in schizophrenia. *Front Psychol* **4**, 621.
Taylor, J. L., Blanton, R. E., Levitt, J. G., Caplan, R., Nobel, D. & Toga, A. W. (2005). Superior temporal gyrus differences in childhood-onset schizophrenia. *Schizophr Res* **73**, 235-41.
Tayoshi, S., Nakataki, M., Sumitani, S., Taniguchi, K., Shibuya-Tayoshi, S., Numata, S., Iga, J., Ueno, S., Harada, M. & Ohmori, T. (2010). GABA concentration in schizophrenia patients and the effects of antipsychotic medication: a proton magnetic resonance spectroscopy study. *Schizophr Res* **117**, 83-91.
Thompson, M., Weickert, C. S., Wyatt, E. & Webster, M. J. (2009). Decreased glutamic acid decarboxylase(67) mRNA expression in multiple brain areas of patients with schizophrenia and mood disorders. *Journal of Psychiatric Research* **43**, 970-977.
Thompson Ray, M., Weickert, C. S., Wyatt, E. & Webster, M. J. (2011). Decreased BDNF, trkB-TK+ and GAD67 mRNA expression in the hippocampus of individuals with schizophrenia and mood disorders. *J Psychiatry Neurosci* **36**, 195-203.
Todd, J., Michie, P. T. & Jablensky, A. V. (2003). Association between reduced duration mismatch negativity (MMN) and raised temporal discrimination thresholds in schizophrenia. *Clin Neurophysiol* **114**, 2061-70.
Tomelleri, L., Jogia, J., Perlini, C., Bellani, M., Ferro, A., Rambaldelli, G., Tansella, M., Frangou, S., Brambilla, P. & initiative, N. N. o. t. E. n. (2009). Brain structural changes associated with chronicity and antipsychotic treatment in schizophrenia. *Eur Neuropsychopharmacol* **19**, 835-40.
Traub, R. D., Jefferys, J. G. & Whittington, M. A. (1997). Simulation of gamma rhythms in networks of interneurons and pyramidal cells. *J Comput Neurosci* **4**, 141-50.
Traub, R. D., Whittington, M. A., Colling, S. B., Buzsáki, G. & Jefferys, J. G. (1996). Analysis of gamma rhythms in the rat hippocampus in vitro and in vivo. *J Physiol* **493 (Pt 2)**, 471-84.
Tsuchimoto, R., Kanba, S., Hirano, S., Oribe, N., Ueno, T., Hirano, Y., Nakamura, I., Oda, Y., Miura, T. & Onitsuka, T. (2011). Reduced high and low frequency gamma synchronization in patients with chronic schizophrenia. *Schizophr Res* **133**, 99-105.
Uhlhaas, P. J., Linden, D. E. J., Singer, W., Haenschel, C., Lindner, M., Maurer, K. & Rodriguez, E. (2006). Dysfunctional long-range coordination of neural activity during Gestalt perception in schizophrenia. *Journal of Neuroscience* **26**, 8168-8175.
Uhlhaas, P. J. & Singer, W. (2010). Abnormal neural oscillations and synchrony in schizophrenia. *Nature Reviews Neuroscience* **11**, 100-113.
van Beijsterveldt, C. E., Molenaar, P. C., de Geus, E. J. & Boomsma, D. I. (1996). Heritability of human brain functioning as assessed by electroencephalography. *Am J Hum Genet* **58**, 562-73.
van Beijsterveldt, C. E. & van Baal, G. C. (2002). Twin and family studies of the human electroencephalogram: a review and a meta-analysis. *Biol Psychol* **61**, 111-38.

van der Graaf, M. (2010). In vivo magnetic resonance spectroscopy: basic methodology and clinical applications. *Eur Biophys J* **39**, 527-40.
van Pelt, S., Boomsma, D. I. & Fries, P. (2012). Magnetoencephalography in twins reveals a strong genetic determination of the peak frequency of visually induced γ-band synchronization. *J Neurosci* **32**, 3388-92.
van Pelt, S. & Fries, P. (2013). Visual stimulus eccentricity affects human gamma peak frequency. *Neuroimage* **78**, 439-47.
Veyrieras, J. B., Kudaravalli, S., Kim, S. Y., Dermitzakis, E. T., Gilad, Y., Stephens, M. & Pritchard, J. K. (2008). High-resolution mapping of expression-QTLs yields insight into human gene regulation. *PLoS Genet* **4**, e1000214.
Vita, A., De Peri, L., Deste, G. & Sacchetti, E. (2012). Progressive loss of cortical gray matter in schizophrenia: a meta-analysis and meta-regression of longitudinal MRI studies. *Transl Psychiatry* **2**, e190.
Vohs, J. L., Chambers, R. A., Krishnan, G. P., O'Donnell, B. F., Berg, S. & Morzorati, S. L. (2010). GABAergic modulation of the 40 Hz auditory steady-state response in a rat model of schizophrenia. *Int J Neuropsychopharmacol* **13**, 487-97.
Vohs, J. L., Chambers, R. A., O'Donnell, B. F., Krishnan, G. P. & Morzorati, S. L. (2012). Auditory steady state responses in a schizophrenia rat model probed by excitatory/inhibitory receptor manipulation. *Int J Psychophysiol* **86**, 136-42.
Volk, D. W., Matsubara, T., Li, S., Sengupta, E. J., Georgiev, D., Minabe, Y., Sampson, A., Hashimoto, T. & Lewis, D. A. (2012). Deficits in transcriptional regulators of cortical parvalbumin neurons in schizophrenia. *Am J Psychiatry* **169**, 1082-91.
Vrba, J. & Robinson, S. E. (2001). Signal processing in magnetoencephalography. *Methods* **25**, 249-271.
Walton, E., Turner, J., Gollub, R. L., Manoach, D. S., Yendiki, A., Ho, B. C., Sponheim, S. R., Calhoun, V. D. & Ehrlich, S. (2013). Cumulative genetic risk and prefrontal activity in patients with schizophrenia. *Schizophr Bull* **39**, 703-11.
Wang, X., Lu, T., Snider, R. K. & Liang, L. (2005). Sustained firing in auditory cortex evoked by preferred stimuli. *Nature* **435**, 341-6.
Ward, L. M. (2003). Synchronous neural oscillations and cognitive processes. *Trends in Cognitive Sciences* **7**, 553-559.
Weber, H., Scholz, C. J., Domschke, K., Baumann, C., Klauke, B., Jacob, C. P., Maier, W., Fritze, J., Bandelow, B., Zwanzger, P. M., Lang, T., Fehm, L., Ströhle, A., Hamm, A., Gerlach, A. L., Alpers, G. W., Kircher, T., Wittchen, H. U., Arolt, V., Pauli, P., Deckert, J. & Reif, A. (2012). Gender differences in associations of glutamate decarboxylase 1 gene (GAD1) variants with panic disorder. *PLoS One* **7**, e37651.
Weickert, C. S., Fung, S. J., Catts, V. S., Schofield, P. R., Allen, K. M., Moore, L. T., Newell, K. A., Pellen, D., Huang, X. F., Catts, S. V. & Weickert, T. W. (2013). Molecular evidence of N-methyl-D-aspartate receptor hypofunction in schizophrenia. *Mol Psychiatry* **18**, 1185-92.
Whalley, H. C., Papmeyer, M., Sprooten, E., Romaniuk, L., Blackwood, D. H., Glahn, D. C., Hall, J., Lawrie, S. M., Sussmann, J. & McIntosh, A. M. (2012). The influence of polygenic risk for bipolar disorder on neural activation assessed using fMRI. *Transl Psychiatry* **2**, e130.
Whittington, M. A., Cunningham, M. O., LeBeau, F. E. N., Racca, C. & Traub, R. D. (2011). Multiple Origins of the Cortical Gamma Rhythm. *Developmental Neurobiology* **71**, 92-106.
Whittington, M. A., Stanford, I. M., Colling, S. B., Jefferys, J. G. & Traub, R. D. (1997). Spatiotemporal patterns of gamma frequency oscillations tetanically induced in the rat hippocampal slice. *J Physiol* **502 (Pt 3)**, 591-607.
Whittington, M. A., Traub, R. D. & Jefferys, J. G. (1995). Synchronized oscillations in interneuron networks driven by metabotropic glutamate receptor activation. *Nature* **373**, 612-5.

Whittington, M. A., Traub, R. D., Kopell, N., Ermentrout, B. & Buhl, E. H. (2000). Inhibition-based rhythms: experimental and mathematical observations on network dynamics. *Int J Psychophysiol* **38**, 315-36.
Williams, S. & Boksa, P. (2010). Gamma oscillations and schizophrenia. *J Psychiatry Neurosci* **35**, 75-7.
Winer & JA (1992). The functional architecture of the medial geniculate body and the primary auditory cortex. In *The mammalian auditory pathway: neuroanatomy* (ed. P. A. Webster DB, Fay RR.). Springer-Verlag: New York.
Wood, J., Kim, Y. & Moghaddam, B. (2012). Disruption of Prefrontal Cortex Large Scale Neuronal Activity by Different Classes of Psychotomimetic Drugs. *Journal of Neuroscience* **32**, 3022-3031.
Woods, S. W. (2003). Chlorpromazine equivalent doses for the newer atypical antipsychotics. *J Clin Psychiatry* **64**, 663-7.
Wu, M. C., Kraft, P., Epstein, M. P., Taylor, D. M., Chanock, S. J., Hunter, D. J. & Lin, X. (2010). Powerful SNP-set analysis for case-control genome-wide association studies. *Am J Hum Genet* **86**, 929-42.
Wu, M. C., Lee, S., Cai, T., Li, Y., Boehnke, M. & Lin, X. (2011). Rare-variant association testing for sequencing data with the sequence kernel association test. *Am J Hum Genet* **89**, 82-93.
Wynn, J. K., Light, G. A., Breitmeyer, B., Nuechterlein, K. H. & Green, M. F. (2005). Event-related gamma activity in schizophrenia patients during a visual backward-masking task. *Am J Psychiatry* **162**, 2330-6.
Xing, D. J., Yeh, C. I., Burns, S. & Shapley, R. M. (2012). Laminar analysis of visually evoked activity in the primary visual cortex. *Proceedings of the National Academy of Sciences of the United States of America* **109**, 13871-13876.
Xu, X., Roby, K. D. & Callaway, E. M. (2010). Immunochemical characterization of inhibitory mouse cortical neurons: three chemically distinct classes of inhibitory cells. *J Comp Neurol* **518**, 389-404.
Yoon, J. H., Maddock, R. J., Rokem, A., Silver, M. A., Minzenberg, M. J., Ragland, J. D. & Carter, C. S. (2010). GABA concentration is reduced in visual cortex in schizophrenia and correlates with orientation-specific surround suppression. *J Neurosci* **30**, 3777-81.
Young, R. C., Biggs, J. T., Ziegler, V. E. & Meyer, D. A. (1978). A rating scale for mania: reliability, validity and sensitivity. *Br J Psychiatry* **133**, 429-35.
Zhang, Y., Brady, M. & Smith, S. (2001). Segmentation of brain MR images through a hidden Markov random field model and the expectation-maximization algorithm. *IEEE Trans Med Imaging* **20**, 45-57.